

## POSTERS – Life Sciences

---

### P-01

#### **THE MOLECULAR BASIS OF CRYSTALLIZATION OF ISOXANTHOPTERIN CRYSTALS**

Belal Alhozeel, Keshet Shavit, Amir Sagi, Benjamin Palmer

*Department of Chemistry, Ben-Gurion University of Negev, Rahat, Israel*

### P-02

#### **SPECTRAL IMAGING OF BREAST CANCER BIOPSIES FOR MULTIPLEX BIOMARKERS DETECTION**

Maya Almagor, Yuval Garini, Roni Baron

*Biomedical Engineering, Technion-Israel Institute of Technology, Haifa, Israel*

### P-03

#### **RNA RELATED NUCLEAR PROCESSES MODULATE THE ASSEMBLY OF CYTOPLASMIC RNA GRANULES**

Mor Angel, Eden Fleshler, Mohammad Khaled Atrash, Noa Kinor, Yaron Shav-Tal

*The Mina & Everard Godman Faculty of Life Sciences & Institute of Nanotechnology, Bar-Ilan University, Ramat-Gan, Israel*

### P-04

#### **VISUALIZING MEMBRANE INTERACTIONS USING IN-CELL CRYO-ELECTRON TOMOGRAPHY**

Lior Aram<sup>1</sup>, Diede de Haan<sup>1</sup>, Neta Varsano<sup>2</sup>, Katya Rechav<sup>2</sup>, Eyal Shimoni<sup>2</sup>, Nadav Elad<sup>2</sup>, Assaf Gal<sup>1</sup>

<sup>1</sup>*Department of Plant and Environmental Sciences, Weizmann Institute of Science, Rehovot, Israel*

<sup>2</sup>*Department of Chemical Research Support, Weizmann Institute of Science, Rehovot, Israel*

### P-05

#### **MIGRATING AND PROLIFERATING STUDIES OF MESENCHYMAL STEM CELLS USING MACHINE-LEARNING PROCESSING OF PHASE-CONTRAST IMAGES**

Nambi Natchiyar Balakrishnan, Levi A Gheber

*Biotechnology Engineering, Ben-Gurion University of the Negev, Beer-Sheva, Israel*

### P-06

#### **UNRAVELING THE MOLECULAR MECHANISM UNDERLYING URIC ACID CRYSTAL FORMATION IN MEDAKA LEUCOPHORE CELLS**

Yuval Barzilay<sup>1</sup>, Rachel Lynn-Deis<sup>1</sup>, Zohar Eyal<sup>1</sup>, Tali Lerer – Goldshtein<sup>1</sup>, Anna Gorelick-ascetazi<sup>1</sup>, Iddo Pinkas<sup>2</sup>, Ziv Porat<sup>3</sup>, Neta Versano<sup>4</sup>, Smadar Zaidman<sup>4</sup>, Nili Dezarella<sup>4</sup>, Dvir Gur<sup>1</sup>

<sup>1</sup>*Department of Molecular Genetics, Weizmann Institute of Science, Rehovot, Israel*

<sup>2</sup>*Department of Chemical Research Support, Weizmann Institute of Science, Rehovot, Israel*

<sup>3</sup>*Department of Life Sciences Core Facilities, Weizmann Institute of Science, Rehovot, Israel*

<sup>4</sup>*Department of Chemical Research Support, EM unit, Weizmann Institute of Science, Rehovot, Israel*

### P-07

#### **CRYO-EM INVESTIGATIONS OF HOLOCOCOLITH CALCITE INTRACELLULAR FORMATION**

Oz Ben-Joseph<sup>1</sup>, Lior Aram<sup>1</sup>, Diede de Haan<sup>1</sup>, Katya Rechav<sup>2</sup>, Assaf Gal<sup>1</sup>

<sup>1</sup>*Department of Plant and Environmental Sciences, Weizmann Institute of Science, Rehovot, Israel*

<sup>2</sup>*Department of Chemical Research Support, Weizmann Institute of Science, Rehovot, Israel*



## P-08

### THE INTERPLAY BETWEEN pH and COLLAGEN ORGANIZATION IN THE TUMOR MICROENVIRONMENT: AN IN VITRO STUDY

**Orit Bronner**<sup>1</sup>, Einat Nativ-Roth<sup>2</sup>, Daniel Sevilla Sanchez<sup>2</sup>, Michal Zaiden<sup>1</sup>, Lior Cohen<sup>1</sup>, Netta Vidavsky<sup>1,2</sup>

<sup>1</sup>Chemical Engineering, Ben-Gurion University, Beer Sheva, Israel

<sup>2</sup>Ilse Katz Institute for Nanoscale Science & Technology, Ben-Gurion University, Beer Sheva, Israel

## P-09

### NATURAL EVOLUTION OF SILK HIERARCHICAL STRUCTURES: REVEALING THE MULTI-LENGTH SCALES ASSEMBLY BY COMBINATION OF MICROSCOPY TECHNIQUES

**Ori Brookstein**<sup>1</sup>, Dror Eliaz<sup>1</sup>, Eyal Shimoni<sup>2</sup>, Ulyana Shimanovich<sup>1</sup>

<sup>1</sup>Weizmann Institute of Science, Rehovot, Israel

<sup>1</sup>Molecular Chemistry and Material Science, Weizmann Institute of Science, Rehovot, Israel

<sup>2</sup>Chemical Research Support, Weizmann Institute of Science, Rehovot, Israel

## P-10

### MICROCALCIFICATIONS CAN TRIGGER OR SUPPRESS BREAST PRECANCER MALIGNANCY POTENTIAL AS A FUNCTION OF MINERAL TYPE IN A 3D TUMOR MODEL

**Amit Cohen**<sup>1</sup>, Lotem Gotnayer<sup>1</sup>, Dina Aranovich<sup>1</sup>, Netta Vidavsky<sup>1,2</sup>

<sup>1</sup>Chemical Engineering, Ben-Gurion University of the Negev, Beer Sheva, Israel

<sup>2</sup>Ilse Katz Institute for Nanoscale Science & Technology, Ben-Gurion University of the Negev, Beer Sheva, Israel

## P-11

### EXOCYTOSIS OF THE SILICIFIED CELL WALL OF DIATOMS INVOLVES EXTENSIVE MEMBRANE DISINTEGRATION

**Diede de Haan**<sup>1</sup>, Lior Aram<sup>1</sup>, Hadas Peled-Zehavi<sup>2</sup>, Yoseph Addadi<sup>3</sup>, Oz Ben-Joseph<sup>1</sup>, Ron Rotkopf<sup>3</sup>, Nadav Elad<sup>4</sup>, Katya Rechav<sup>4</sup>, Assaf Gal<sup>1</sup>

<sup>1</sup>Department of Plant and Environmental Sciences, Weizmann Institute of Science, Rehovot, Israel

<sup>2</sup>Department of Biomolecular Sciences, Weizmann Institute of Science, Rehovot, Israel

<sup>3</sup>Life Science Core Facilities, Weizmann Institute of Science, Rehovot, Israel

<sup>4</sup>Department of Chemical Research Support, Weizmann Institute of Science, Rehovot, Israel

## P-12

### ELUCIDATE THE ROLE OF VPS4 ISOFORMS IN CYTOKINETIC ABSCISSION

**Inbar Dvilansky**, Yarin Altaras, Dikla Nachmias, Natalie Elia

Life science, Ben Gurion University of the Negev, Beer Sheva, Israel

## P-13

### FRACTAL DIMENSION AND FRACTIONAL CONCAVITY MEASUREMENTS OF GROWTH CONE CONTOURS OF OPTIC AXONS IN SITU

Tamira Elul<sup>1</sup>, Valerie Lew<sup>1</sup>, Sukayneh Khetani<sup>1</sup>, **William Woodward**<sup>2</sup>

<sup>1</sup>College of Osteopathic Medicine, Touro University California, Vallejo, California, USA

<sup>2</sup>College of Osteopathic Medicine, Touro University Nevada, Henderson, Nevada, USA



## P-14

### **STRUCTURAL AND ANTI-MICROBIAL STUDIES OF RIBOSOME-BINDING 16-MEMBER RING MACROLIDES AGAINST STAPHYLOCOCCUS AUREUS**

Aliza Fedorenko<sup>1</sup>, Andre Rivalta<sup>1</sup>, Disha-Gajanan Hiregange<sup>1</sup>, Anat Bashan<sup>1</sup>, Jennifer J. Schmidt<sup>2</sup>, David H. Sherman<sup>2</sup>, Ada Yonath<sup>1</sup>

<sup>1</sup>Chemical and Structural Biology, Weizmann Institute of Science, Rehovot, Israel

<sup>2</sup>Medicinal Chemistry, Chemistry, Microbiology and Immunology, University of Michigan, Ann Arbor, Michigan, USA

## P-15

### **SEM CHARACTERIZATION OF NON-CaP MINERAL PARTICLES FOR BREAST PRECANCER PROGNOSIS**

Sahar Gal<sup>1</sup>, Netta Vidavsky<sup>1,2</sup>

<sup>1</sup>Department of Chemical Engineering, Ben Gurion University of the Negev, Be'er Sheva, Israel

<sup>2</sup>Ilse Katz Institute for Nanoscale Science & Technology, Ben Gurion University of the Negev, Be'er Sheva, Israel

## P-16

### **MORPHOLOGICAL QUANTIFICATION OF LEISHMANIA PARASITE LIFE CYCLE STAGES USING IMAGING FLOW CYTOMETRY**

Uzi Hadad<sup>1</sup>, Nofar Baron<sup>2</sup>, Michal Shapira<sup>2</sup>

<sup>1</sup>Ilse Katz Institute for Nanoscale Science and Technology, Ben-Gurion University of the Negev, Beer Sheva, Israel

<sup>2</sup>Department of Life Sciences, Ben-Gurion University of the Negev, Beer Sheva, Israel

## P-17

### **LABEL FREE IMAGING OF CHOLESTEROL CRYSTALS AND MACROPHAGES AS A MODEL SYSTEM FOR ATHEROSCLEROSIS**

Antonia Kaestner<sup>1,2</sup>, Yoseph Addadi<sup>3</sup>, Neta Varsano<sup>4</sup>, Ori Avinoam<sup>2</sup>, Lia Addadi<sup>1</sup>

<sup>1</sup>Chemical and Structural Biology, Weizmann Institute of Science, Rehovot, Israel

<sup>2</sup>Biomolecular Sciences, Weizmann Institute of Science, Rehovot, Israel

<sup>3</sup>Life Sciences Core Facilities, Weizmann Institute of Science, Rehovot, Israel

<sup>4</sup>Electron Microscopy Unit, Weizmann Institute of Science, Rehovot, Israel

## P-18

### **DETERMINING THE COMPOSITION OF THE ESCRT-III FILAMENT IN CYTOKINESIS ABSCISSION OF MAMMALIAN CELLS**

Nikita Kamenetsky, Natalie Elia

Life sciences, Ben-Gurion University of the Negev, Beer-Sheba, Israel

## P-19

### **SNAPSHOTS OF MITOCHONDRIAL FISSION THROUGH THE LENSE OF CRYO-SCANNING TRANSMISSION ELECTRON TOMOGRAPHY (CSTET)**

Peter Kirchweger<sup>1,2</sup>, Sharon Wolf<sup>3</sup>, Deborah Fass<sup>2</sup>, Michael Elbaum<sup>1</sup>

<sup>1</sup>Department of Chemical and Biological Physics, Weizmann Institute of Science, Rehovot, Israel

<sup>2</sup>Department of Chemical and Structural Biology, Weizmann Institute of Science, Rehovot, Israel

<sup>3</sup>Department of Chemical Research Support, Weizmann Institute of Science, Rehovot, Israel

**P-20****ROBUSTNESS OF THE CANONICAL MITOCHONDRIAL FUSION MACHINERY PROMOTES NEBENKERN FORMATION IN DROSOPHILA SPERMATIDS.**

Alina Kolpakova, Shmuel Pietrokovski, Eli Arama

*Department of Molecular Genetics, Weizmann Institute of Science, Rehovot, Israel***P-21****FIB-SEM IMAGING REVEALS IN-SITU FORMATION OF THE SILICA CELL WALL OF ALGAE**

Zipora Lansky

*Plant and Environmental Science, Weizmann Institute of Science, Rehovot, Israel***P-22****MAPPING OF PHASE SEPARATION OF SUPRAMOLECULAR PROTEIN ASSEMBLIES BY LIVE CELL HOLOTOMOGRAPHY MICROSCOPY**

Orlando Marin, Arina Dalaloyan, Michael Elbaum

*Biological and Chemical Physics, Weizmann Institute of Science, Rehovot, Israel***P-23****Asgard ESCRT-III and VPS4 reveal conserved chromatin binding properties of the ESCRT machinery**Dikla Nachmias<sup>1</sup>, Melnikov Melnikov<sup>1</sup>, Alvah Zorea<sup>1</sup>, Maya Sharon<sup>1</sup>, Reut Yemini<sup>1</sup>, Yasmin De-picchoto<sup>1</sup>, Ioannis Tsirkas<sup>1</sup>, Amir Aharoni<sup>1</sup>, Bela Frohn<sup>2</sup>, Petra Schwillie<sup>2</sup>, Raz Zarivach<sup>1</sup>, Itzhak Mizrahi<sup>1</sup>, Natalie Elia<sup>1</sup><sup>1</sup>*Department of Life Sciences, Ben-Gurion University of the Negev, Beer-Sheva, Israel*<sup>2</sup>*Department of Cellular and Molecular Biophysics, Max-Planck Institute of Biochemistry, Martinsried, Germany***P-24****THE EFFECT OF LAMIN A ON THE COHERENT DYNAMICS OF THE CHROMATIN IN LIVING CELLS**

Wajdi Nicola, Yuval Garini

*Bio-medical Engineering, Technion-Israel Institute of Technology, Haifa, Israel***P-25****STRUCTURAL STUDIES ON THE S. AUREUS ERMB METHYLTRANSFERASE MUTANT RIBOSOME IN COMPLEX WITH SOLITHROMYCIN**Andre' Rivalta<sup>1</sup>, Aliza Fedorenko<sup>1</sup>, Yehuda Halfon<sup>1</sup>, Disha-Gajanan Hiregange<sup>1</sup>, Ella Zimmerman<sup>1</sup>, Anat Bashan<sup>1</sup>, M.N. Frances Yap<sup>2</sup>, Ada Yonath<sup>1</sup><sup>1</sup>*Chemical and Structural Biology, Weizmann Institute of Science, Rehovot, Israel*<sup>2</sup>*Feinberg School of Medicine, Northwestern University, Chicago, Illinois, USA*



## P-26

### **THE EFFECT OF LOOP8 ON SPINDLE LOCALIZATION AND BI-DIRECTIONALITY OF S. CEREVISIAE KINESIN-5 CIN8**

**Mayan Sadan**<sup>1</sup>, Himanshu Pandey<sup>1,2</sup>, Sudhir Kumar Singh<sup>1</sup>, Mary Popov<sup>1</sup>, Meenakshi Singh<sup>1</sup>, Geula Davidov<sup>3</sup>, Sayaka Inagaki<sup>4</sup>, Jawdat Al-Bassam<sup>5</sup>, Raz Zarivach<sup>2,3</sup>, Steven S Rosenfeld<sup>4</sup>, Larisa Gheber<sup>1,2</sup>

<sup>1</sup>Department of Chemistry, Ben-Gurion University of the Negev, Beer-Sheva, Israel

<sup>2</sup>Ilse Katz Institute for Nanoscale Science and Technology, Ben-Gurion University of the Negev, Beer-Sheva, Israel

<sup>3</sup>Department of Life Sciences and the National Institute for Biotechnology in the Negev, Ben-Gurion University of the Negev, Beer-Sheva, Israel

<sup>4</sup>Department of Cancer Biology, Mayo Clinic, Jacksonville, FL, USA

<sup>5</sup>Department of Molecular and Cellular Biology, University of California, Davis, CA, USA

## P-27

### **BIOMINERAL FORMATION BY THE FRESHWATER GREEN ALGA PHACOTUS LENTICULARIS**

**Noy Shaked**<sup>1</sup>, Sophia Barinova<sup>4</sup>, Sefi Addadi<sup>2</sup>, Katya Rechav<sup>3</sup>, Steve Weiner<sup>1</sup>, Lia Addadi<sup>1</sup>

<sup>1</sup>Department of Chemical and Structural Biology, Weizmann Institute of Science, Rehovot, Israel

<sup>2</sup>Department of life sciences core facilities, Weizmann Institute of Science, Rehovot, Israel

<sup>3</sup>Chemical research support unit, Weizmann Institute of Science, Rehovot, Israel

<sup>4</sup>Institute of Evolution, University of Haifa, Haifa, Israel

## P-28

### **IMPROVING CRYO-ELECTRON TOMOGRAPHY DATA QUALITY AND THROUGHPUT BY STREAMLINING THE WORKFLOW**

**Marit Smeets**, Katherine Lau

Life Sciences, Delmic B.V., Delft, Zuid-Holland, Netherlands

## P-29

### **SPEC-NET: NUCLEAR SEGMENTATION FROM H&E BIOPSY WITH SPECTRAL IMAGING SCREENING**

**Adam Soker**, Yuval Garini

Bio-medical Engineering, Technion, Haifa, Israel, Israel

## P-30

### **THE ROLE OF THE NON-MOTOR N-TERMINAL REGION IN REGULATION OF FUNCTION OF THE BI-DIRECTIONAL KINESIN-5 CIN8**

**Neta Yanir**, Himanshu Pandey, Sudhir Kumar Singh, Alina Goldstein-Levitin, Leah Gheber

Department of Chemistry, Ben-Gurion University of the Negev, Beer-Sheva, Israel



## POSTERS – Materials Science

---

### P-31

#### MEASUREMENT-BASED CONTROL OF THE ELECTRON-PHOTON COUPLING COHERENCE

Hadar Aharon, Ofer Kfir

*School of Electrical Engineering, Fleischman Faculty of Engineering, Tel Aviv University, Tel Aviv 69978, Israel*

### P-32

#### IN-SITU INTERINSIC SELF-HEALING OF LOW-TOXIC Cs<sub>2</sub>ZnX<sub>4</sub> (X= Cl, Br) METAL HALIDE NANOPARTICLES

Ben Aizenshtein, Lioz Etgar

*Chemistry, Institute of Chemistry, The Center for Nanoscience and Nanotechnology, Casali Center for Applied Chemistry, The Hebrew University of Jerusalem, Jerusalem, Israel*

### P-33

#### MODULATION OF BIOGENIC CRYSTAL MORPHOGENESIS IS ACHIEVED THROUGH TRANSITION FROM REACTION-LIMITED TO TRANSPORT-LIMITED GROWTH

Emanuel Avrahami

*Department of Plant and Environmental Sciences, Weizmann Institute of Science, Rehovot, Israel*

### P-34

#### SPATIALLY CONTROLLED ATOMIC LAYER DEPOSITION WITHIN POLYMER TEMPLATES FOR MULTI-MATERIAL NANORODS AND NANOWIRES FABRICATION

Rotem Azoulay, Tamar Segal Peretz

*Chemical Engineering, Technion-Israel Institute of Technology, Haifa, Israel*

### P-35

#### PROBING MAGNETIC PHASE TRANSITIONS VIA SPIN TORQUE DRIVEN SKYRMION RESONANCE

Nirel Bernstein<sup>1</sup>, Benjamin Assouline<sup>1</sup>, Hang Li<sup>2</sup>, Igor Rozhansky<sup>1</sup>, Wenhong Wang<sup>2</sup>, Amir Capua<sup>1</sup>

<sup>1</sup>*Applied Physics, The Hebrew University of Jerusalem, Jerusalem, Israel*

<sup>2</sup>*Beijing National Laboratory for Condensed Matter Physics, Chinese Academy of Sciences, Beijing, China*

### P-36

#### EXPLORING SURFACE PHENOMENA WITH TEM AND STEM

Roei Broneshter<sup>1</sup>, Yaron Kauffmann<sup>1</sup>, Klaus Van Benthem<sup>2</sup>, Wayne D. Kaplan<sup>1</sup>

<sup>1</sup>*Material Science and engineering, Technion, Haifa, Israel*

<sup>2</sup>*Material Science and Engineering, University of California, Davis, California, USA*

### P-37

#### ADVANCED TOOLS FOR DISCRIMINATING PHASES WITH SIMILAR CRYSTAL STRUCTURE BY EBSD

Keith Dicks<sup>1</sup>, Michael Hjelmstad<sup>2</sup>, Pat Trimby<sup>1</sup>, Klaus Mehnert<sup>3</sup>, Aimo Winkelmann<sup>3</sup>

<sup>1</sup>*Applications, Oxford Instruments NanoAnalysis, High Wycombe, Buckinghamshire HP12 3SE, UK*

<sup>2</sup>*Applications, Oxford Instruments America Inc., Pleasanton, California, USA*

<sup>3</sup>*Development, ST Development GmbH, Paderborn, Germany*

## P-38

### CHIRAL GUIDED GROWTH OF CRYSTALS-ON-CRYSTALS: PREDICTABLE MORPHOLOGIES WITH LOCAL FUNCTIONALIZATION

Ofir Eisenberg<sup>1</sup>, Qiang Wen<sup>1</sup>, Maria Chiara di Gregorio<sup>1</sup>, Linda J. W. Shimon<sup>2</sup>, Lothar Houben<sup>2</sup>, Ifat Kaplan-Ashiri<sup>2</sup>, Tali Dadosh<sup>2</sup>, Yoseph Addadi<sup>3</sup>, Michal Lahav<sup>1</sup>, Milko E. van der Boom<sup>1</sup>

<sup>1</sup>Molecular Chemistry and Materials Science, Weizmann Institute of Science, Rehovot, Israel

<sup>2</sup>Chemical Research Support, Weizmann Institute of Science, Rehovot, Israel

<sup>3</sup>Life Science Core Facilities, Weizmann Institute of Science, Rehovot, Israel

## P-39

### IN-SITU AND EX-SITU INVESTIGATION OF PHASE TRANSFORMATIONS IN THE Fe<sub>4</sub>Co<sub>2.1</sub>Ni<sub>2.1</sub>Cr<sub>0.8</sub>Al<sub>0.8</sub>Ti<sub>0.2</sub> HIGH ENTROPY ALLOY

Ron Fishov<sup>1</sup>, Guy Hillel<sup>1</sup>, Susanna Syniakina<sup>1</sup>, Yaniv Zriker<sup>2</sup>, Ofer Omesi<sup>2</sup>, Yoav Snir<sup>2</sup>, Louisa Meshi<sup>1</sup>

<sup>1</sup>Department of Materials Engineering, Ben Gurion University of the Negev, Beer Sheva, Israel

<sup>2</sup>Materials science and engineering, Nuclear Research Center Negev, Beer Sheva, Israel

## P-40

### THE EFFECT OF ZN-CONTAINING MICROCALCIFICATIONS ON THE MALIGNANCY OF THYROID NODULES

Lotem Gotnayer<sup>1</sup>, Dina Aranovich<sup>1</sup>, Merav Fraenkel<sup>2,3</sup>, Uri Yoel<sup>2,3</sup>, Netta Vidavsky<sup>1,4</sup>

<sup>1</sup>Department of Chemical Engineering, Ben-Gurion University of the Negev, Beer Sheva, Israel

<sup>2</sup>Faculty of Health Sciences, Ben-Gurion University of the Negev, Beer Sheva, Israel

<sup>3</sup>Endocrinology, Soroka University Medical Center, Beer Sheva, Israel

<sup>4</sup>Ilse Katz Institute for Nanoscale Science & Technology, Ben-Gurion University of the Negev, Beer Sheva, Israel

## P-41

### SYSTEMATIC STUDY OF THE ANTI-PHASE BOUNDARIES FORMATION IN B<sub>2</sub> Fe<sub>x</sub>Al<sub>1-x</sub> ALLOYS USING ex-situ AND in-situ TRANSMISSION ELECTRON MICROSCOPY

Guy Hillel<sup>1</sup>, Itzhak Edry<sup>2</sup>, Malki Pinkas<sup>2</sup>, Louisa Meshi<sup>1</sup>

<sup>1</sup>Department of Materials Engineering, Ben-Gurion University of the Negev, Beer-Sheva, Israel

<sup>2</sup>NRCN, Beer-Sheva, Israel

## P-42

### TWO-STEP SINTERING OF MG-DOPED ALUMINA

Asaf Kazmirsky, Rachel Marder, Wayne D. Kaplan

Department of Materials Science and Engineering, Technion – Israel Institute of Technology, Haifa, Israel

## P-43

### MICROSCOPE-INTEGRATED SPECTROSCOPIC ELLIPSOMETER FOR FAST AND IN-SITU OPTICAL INVESTIGATION OF MICRON-SCALE MATERIALS AND STRUCTURES

Ralfy Kenaz<sup>1</sup>, Saptarshi Ghosh<sup>1</sup>, Pradheesh Ramachandran<sup>1</sup>, Kenji Watanabe<sup>2</sup>, Takashi Taniguchi<sup>3</sup>, Hadar Steinberg<sup>1</sup>, Ronen Rapaport<sup>1</sup>

<sup>1</sup>Racah Institute of Physics, The Hebrew University of Jerusalem, Jerusalem, Israel

<sup>2</sup>Research Center for Functional Materials, National Institute for Materials Science, Tsukuba, Japan

<sup>3</sup>International Center for Materials Nanoarchitectonics, National Institute for Materials Science, Tsukuba, Japan



## P-44

### **BRILLIANT WHITENESS IN SHRIMP FROM ULTRA-THIN LAYERS OF BIREFRINGENT NANOSPHERES**

Tali Lemcoff<sup>1</sup>, Lotem Alus<sup>2,3</sup>, Johannes S. Haataja<sup>4,5</sup>, Avital Wagner<sup>1</sup>, Gan Zhang<sup>1,9</sup>, Mariela J. Pavan<sup>6</sup>,  
Ventaka J. Yallapragada<sup>7</sup>, Silvia Vignolini<sup>4</sup>, Dan Oron<sup>2</sup>, Lukas Schertel<sup>4,8</sup>, Benjamin A. Palmer<sup>1</sup>

<sup>1</sup>Department of Chemistry, Ben-Gurion University of the Negev, Be'er Sheva, Israel

<sup>2</sup>Department of Molecular Chemistry and Materials Science, Weizmann Institute of Science, Rehovot, Israel

<sup>3</sup>Department of Chemical and Structural Biology, Weizmann Institute of Science, Rehovot, Israel

<sup>4</sup>Yusuf Hamied Department of Chemistry, University of Cambridge, Cambridge, UK

<sup>5</sup>Department of Applied Physics, Aalto University School of Science, Espoo, Finland

<sup>6</sup>Ilse Katz Institute for Nanoscale Science & Technology, Ben-Gurion University of the Negev, Beer-Sheva, Israel

<sup>7</sup>Department of Physics, Indian Institute of Technology Kanpur, Uttar Pradesh, Kanpur, India

<sup>8</sup>Department of Physics, University of Fribourg, Fribourg, Switzerland

<sup>9</sup>Current Address: College of Chemistry and Chemical Engineering, Lanzhou University, Lanzhou, China

## P-45

### **CATHODOLUMINESCENCE SEM OF CsPbBr<sub>3</sub> PEROVSKITE NANOCRYSTAL SUPERLATTICES**

Shai Levy<sup>1</sup>, Orr Be'er<sup>1</sup>, Noam Veber<sup>1</sup>, Yehonadav Bekenstein<sup>1,2</sup>

<sup>1</sup>Materials Science and Engineering, Technion-Israel Institute of Technology, Haifa, Israel

<sup>2</sup>Solid-State Institute, Technion-Israel Institute of Technology, Haifa, Israel

## P-46

### **SIZE EFFECT ON STRENGTH OF EQUILIBRATED COPPER NANOPARTICLES FABRICATED BY SOLID-STATE DEWETTING**

Zhao Liang<sup>1</sup>, Nishchal Thapa Magar<sup>2</sup>, Raj Koju<sup>2</sup>, Yuri Mishin<sup>2</sup>, Eugen Rabkin<sup>1</sup>

<sup>1</sup>Department of Materials Science and Engineering, Technion-Israel Institute of Technology, Haifa, Israel

<sup>2</sup>Department of Physics and Astronomy, George Mason University, Fairfax, Virginia, USA

## P-47

### **REGULATING GRANULE STARCH HYDROLYSIS TO MAKE POROUS STARCH**

Hongxiang Liu<sup>1,2</sup>

<sup>1</sup>Faculty of Biotechnology and Food Engineering, Technion – Israel Institute of Technology, Haifa, Israel

<sup>2</sup>Biotechnology and Food Engineering Program, Guangdong Technion – Israel Institute of Technology, Shantou, China

## P-48

### **Cr/AlCoFeNi DIFFUSION COUPLE FOR MAPPING MICROSTRUCTURAL CHANGES**

Yuval Malinker<sup>1</sup>, Einat Nativ-Roth<sup>2</sup>, Guy Hillel<sup>1</sup>, Susanna Sinyakina<sup>1</sup>, Louisa Meshi<sup>1</sup>

<sup>1</sup>Department of Materials Engineering, Ben Gurion University of the Negev, Beer Sheva, Israel

<sup>2</sup>Ilse Katz Institute for nanoscale science and technology, Ben Gurion University of the Negev, Beer Sheva, Israel

**P-49****MEASURING THE SOLUBILITY LIMIT OF DOPANTS BY FULLY STANDARDIZED WAVELENGTH DISPERSIVE SPECTROSCOPY**

Rachel Marder, Wayne D. Kaplan

*Materials Science and Engineering, Technion- Israel Institute of Technology, Haifa, Israel***P-50****CALCIUM AND ELONGATED GRAINS IN ALUMINA**

Iman Naamneh, Rachel Marder, Wayne Kaplan

*Materials Science and Engineering, Technion – Israel Institute of Technology, Haifa, Israel***P-51****THE INFLUENCE OF ADDITIVES ON THE CRYSTALLIZATION OF CALCIUM PHOSPHATE IN PHYSIOLOGICAL CONDITIONS**Yarden Nahmias<sup>1</sup>, Netta Vidavsky<sup>1,2</sup><sup>1</sup>*Chemical Engineering, Ben-Gurion University of the Negev, Beer Sheva, Israel*<sup>2</sup>*Ilse Katz Institute for Nanoscale Science & Technology, Ben-Gurion University of the Negev, Beer Sheva, Israel***P-52****DIRECTING THE MORPHOLOGY , PACKING, AND PROPERTIES OF CHIRAL METAL-ORGANIC FRAMEWORKS BY CATION EXCHANGE**Hadar Nasi<sup>1</sup>, Maria Chiara di Gregorio<sup>1</sup>, Qiang Wen<sup>1</sup>, Linda J. W. Shimon<sup>2</sup>, Ifat Kaplan-Ashiri<sup>2</sup>, Tatyana Bendikov<sup>2</sup>, Gregory Leitus<sup>2</sup>, Miri Kazes<sup>1</sup>, Dan Oron<sup>1</sup>, Michal Lahav<sup>1</sup>, Milko E. van der Boom<sup>1</sup><sup>1</sup>*Molecular Chemistry and Material Science, Weizmann Institute of Science, Rehovot, Israel*<sup>2</sup>*Department of Chemical Research Support, Weizmann Institute, Rehovot, Israel***P-53****NANOSTRUCTURAL CHARACTERIZATION OF COMPLEXES OF DNA WITH A DIBLOCK-COPOLYMER OF POSITIVELY-CHARGED AND NEUTRAL BLOCKS, AND THEIR STABILITY IN THE PRESENCE OF BLOOD SERUM ALBUMIN**Sapir Rappoport<sup>1</sup>, Varvara Chrysostomou<sup>2</sup>, Stergios Pispas<sup>2</sup>, Yeshayahu Talmon<sup>1</sup><sup>1</sup>*Department of Chemical Engineering and the Russell Berrie Nanotechnology Institute (RBNI), Technion – Israel Institute of Technology, Haifa, Israel*<sup>2</sup>*Theoretical and Physical Chemistry Institute, National Hellenic Research Foundation, Athens, Greece***P-54****OPTICAL CHARACTERIZATION OF LEAD HALIDE PEROVSKITES HETEROSTRUCTURE INTERFACE WITH CATHODOLUMINESCENCE SPECTROSCOPY**

Betty Shamaev, Yehonadav Bekenstein

*Materials Science and Engineering, Technion – Israel Institute of Technology, Haifa, Israel*



## P-55

### THE EFFECT OF SALTS ON THE NANOAGGREGATION OF SLES IN AQUEOUS SOLUTIONS OBSERVED BY CRYO-TEM

Sapir Simon<sup>1</sup>, Werner Kunz<sup>2</sup>, Thomas Zemb<sup>3</sup>, Yeshayahu Talmon<sup>1</sup>

<sup>1</sup>Department of Chemical Engineering and the Russell Berrie Nanotechnology Institute (RBNI), Technion – Israel Institute of Technology, Haifa, Israel

<sup>2</sup>Institute of Physical and Theoretical Chemistry, University of Regensburg, Regensburg, Germany

<sup>3</sup>Institute for Separation Chemistry IcsM, University of Montpellier, Marcoule, France

## P-56

### A CATION EFFECT ON SELF-HEALING IN APb3 PEROVSKITE THIN POLYCRYSTALLINE FILMS

Pallavi Singh<sup>1</sup>, Yahel Soffer<sup>1</sup>, Davide Raffaele Ceratti<sup>2</sup>, Michael Elbaum<sup>1</sup>, Dan Oron<sup>1</sup>, Gary Hodes<sup>1</sup>, David Cahen<sup>1</sup>

<sup>1</sup>Weizmann Institute of Science, Rehovot, Israel

<sup>2</sup>CNRS UMR 9006-IPVF Institut Photovoltaïque d'Ile-de-France, Paris, France

## P-57

### CERAMIC–METAL INTERFACE: THE INFLUENCE OF TITANIUM ON THE MICROSTRUCTURE OF VACUUM BRAZED ALUMINA-ALUMINUM ALLOY

Stalin Sundara Dhas, Kalaichelvan K.

Department of Ceramic Technology, ACT campus, Anna University, Chennai, Tamil Nadu, India

## P-58

### ON THE DEVELOPMENT AND ATOMIC STRUCTURE OF ZnO CRYSTALS GROWN IN POLYMERS FROM VAPOR PHASE PRECURSORS

Inbal Weisbord<sup>1</sup>, Maya Barzilay<sup>1</sup>, Alexei Kuzmin<sup>2</sup>, Andris Anspoks<sup>2</sup>, Edmund Welter<sup>3</sup>, Tamar Segal-Peretz<sup>1</sup>

<sup>1</sup>Chemical Engineering, Technion – Israel Institute of Technology, Haifa, Israel

<sup>2</sup>Institute of Solid State Physics, University of Latvia, Riga, Latvia

<sup>3</sup>Deutsches Elektronen-Synchrotron, (DESY), Hamburg, Germany

## P-59

### HIERARCHICAL SELF-ASSEMBLY INVOLVING CLASSICAL AND NONCLASSICAL STEPS IN ORGANIC CRYSTAL GROWTH

Idan Biran<sup>1</sup>, Shaked Rosenne<sup>1</sup>, Haim Weissman<sup>1</sup>, Yael Tsarfati<sup>1</sup>, Lothar Houben<sup>2</sup>, Boris Rybtchinski<sup>1</sup>

<sup>1</sup>Molecular Chemistry and Material Science, Weizmann Institute of Science, Rehovot, Israel

<sup>2</sup>Chemical Research Support, Weizmann Institute of Science, Rehovot, Israel

## P-60

### VISUALIZING THE EFFECT OF ELECTRIC FIELDS ON FOULING FORMATION USING CONFOCAL MICROSCOPY

Elina Yachnin<sup>1</sup>, David Jassby<sup>2</sup>, Tamar Segal-Peretz<sup>3</sup>, Guy Z. Ramon<sup>1</sup>

<sup>1</sup>Department of Civil and Environmental Engineering, Technion – Israel Institute of Technology, Haifa, Israel

<sup>2</sup>Department of Civil and Environmental Engineering, University of California, Los Angeles, California, USA

<sup>3</sup>Department of Chemical Engineering, Technion – Israel Institute of Technology, Haifa, Israel



## P-61

### THE EFFECT OF CALCIUM OXALATE CRYSTAL PHASE, MORPHOLOGY, AND AGGREGATION ON PROTEIN ADSORPTION AND CANCER CELL ATTACHMENT

Gabriel Yazbek Grobman<sup>1</sup>, Dina Aranovich<sup>1</sup>, Netta Vidavsky<sup>1,2</sup>

<sup>1</sup>Department of Chemical Engineering, Ben-Gurion University of the Negev, Beer Sheva, Israel

<sup>2</sup>Ilse Katz Institute for Nanoscale Science & Technology, Ben-Gurion University of the Negev, Beer Sheva, Israel

## P-72 (last minute submission)

### RATIONAL DESIGN AND FABRICATION OF BLOCK COPOLYMER TEMPLATED HAFNIUM OXIDE NANOSTRUCTURE

Ruoke Cai, Tamar Segal-peretz

Department of Chemical Engineering, Technion - Israel Institute of Technology, Haifa, Israel



## POSTERS – Instrumentation & Methodology Development

---

### P-62

#### CRYOGENIC SCANNING ELECTRON MICROSCOPY AS AN EFFECTIVE TOOL FOR NANOSTRUCTURAL STUDY OF BIOLOGICAL SYSTEMS

Irina Davidovich<sup>1</sup>, Ariel Koren<sup>2</sup>, Carina Levin<sup>2</sup>, Yeshayahu Talmon<sup>1</sup>

<sup>1</sup>Department of Chemical Engineering and the Russell Berrie Nanotechnology Institute (RBNI), Technion-Israel Institute of Technology, Haifa, Israel

<sup>2</sup>Pediatric Hematology Unit, Emek Medical Center in Afula, Afula, Israel

### P-63

#### COUNTING NANOPARTICLES IN GENERAL AND VIRUSES IN PARTICULAR ONE AT A TIME

Paz Drori<sup>1</sup>, Odelia Mouhadeb<sup>2</sup>, Gabriel Moya<sup>3</sup>, Yair Razvag<sup>1</sup>, Ron Alcalai<sup>2</sup>, Philipp Klocke<sup>3</sup>, Thorben Cordes<sup>3</sup>, Eran Zahavy<sup>2</sup>, Eitan Lerner<sup>1</sup>

<sup>1</sup> Department of Biological Chemistry, The Hebrew University of Jerusalem, Jerusalem, Israel

<sup>2</sup>Department of Biochemistry and Molecular Genetics, Israel Institute for Biological Research, Ness Ziona, Israel

<sup>3</sup>Physical and Synthetic Biology, Ludwig-Maximilians-Universität München, München, Germany

### P-64

#### MOLECULAR MOTORS ON MICROTUBULE TRACKS CREATED WITH NANO FOUNTAIN PEN

Orna Fridman<sup>1</sup>, Himanshu Pandey<sup>2</sup>, Larisa Gheber<sup>2</sup>, Levi A. Gheber<sup>1</sup>

<sup>1</sup>Avram and Stella Goldstein-Goren Department of Biotechnology Engineering, Ben-Gurion University, Beer-Sheva, Israel

<sup>2</sup>Department of Chemistry, Ben-Gurion University, Beer-Sheva, Israel

### P-65

#### TIME-GATED FLUORESCENCE LIFETIME IMAGING IN THE NEAR INFRARED REGIME; A COMPREHENSIVE STUDY TOWARD IN VIVO IMAGING

Meital Harel, Uri Arbiv, Rinat Ankri

Physics, Ariel University, Ariel, Israel

### P-66

#### SCANNING NANO-STRUCTURE ELECTRON MICROSCOPY FOR DECODING THE STRUCTURAL EVOLUTION OF META-STABLE MATERIALS

Yevgeny Rakita<sup>1,2,3</sup>, James L. Hart<sup>3</sup>, Partha P. Das<sup>4</sup>, Sina Shahrezaei<sup>5</sup>, Daniel L. Foley<sup>3</sup>, Suveen N. Mathaudhu<sup>5</sup>, Stavros Nicolopoulos<sup>4</sup>, Mitra L. Taheri<sup>3</sup>, Simon J. L. Billinge<sup>2</sup>

<sup>1</sup>Materials Engineering, Ben Gurion University, Beer Sheva, Israel

<sup>2</sup>Department of Applied Physics and Applied Mathematics, Columbia University, New York, NY, USA

<sup>3</sup>Department of Materials Science and Engineering, Johns Hopkins University, Baltimore, MD, USA

<sup>4</sup>SPRL, NanoMEGAS, Brussels, Belgium

<sup>5</sup>Department of Mechanical Engineering, University of California, Riverside, Riverside, CA, USA

## P-67

### FRET-SENSITIZED ACCEPTOR EMISSION LOCALIZATION (FRET<sub>sael</sub>) – NANOMETER ACCURACY LOCALIZATION OF BIOMOLECULAR INTERACTIONS USING FLIM-FRET LASER SCANNING CONFOCAL MICROSCOPY

Yair Razvag, Paz Drori, Eitan Lerner

*Chemical Biology, The Hebrew University, Jerusalem, Israel*

## P-68

### SHAPING OF ELECTRON BEAMS USING SCULPTED THIN FILMS

Dolev Roitman, Ady Arie

*Electrical Engineering, Tel Aviv University, Tel Aviv, Israel*

## P-69

### THE LABORATORY FOR SENSING NANOMATERIALS & CONTROLLED RELEASE TECHNOLOGIES

Gracia Safdie

*Pharmacy, The Hebrew University of Jerusalem, Jerusalem, Israel*

## P-70

### DEEP THREE-PHOTON IMAGING OF AN ADULT ZEBRAFISH BRAIN

David Sinefeld<sup>1,2</sup>, Dawnis M. Chow<sup>3</sup>, Kristine E. Kolkman<sup>3</sup>, Dimitre G. Ouzounov<sup>2</sup>, Najva Akbari<sup>2</sup>, Rose Tatarsky<sup>3</sup>, Andrew Bass<sup>3</sup>, Chris Xu<sup>2</sup>, Joseph R. Fetcho<sup>3</sup>

<sup>1</sup>*Electro-Optical Engineering and Applied Physics Dept., Jerusalem College of Technology, Jerusalem, Israel*

<sup>2</sup>*Department of Applied and Engineering Physics, Cornell University, Ithaca, New York, USA*

<sup>3</sup>*Department of Neurobiology and Behavior, Cornell University, Ithaca, New York, USA*

## P-71

### REAL-TIME STUDY OF SURFACE-GUIDED NANOWIRE GROWTH BY IN SITU SCANNING ELECTRON MICROSCOPY

XiaoMeng Sui<sup>1</sup>, Amnon Rothman<sup>2</sup>, Kristýna Bukvišová<sup>3,4</sup>, Noya Ruth Itzhak<sup>2</sup>, Ifat Kaplan-Ashiri<sup>1</sup>, Anna Eden Kossoy<sup>1</sup>, Libor Novák<sup>5</sup>, Tomáš Šikola<sup>3,4</sup>, Miroslav Kolíbal<sup>3,4</sup>, Ernesto Joselevich<sup>2</sup>

<sup>1</sup>*Department of Chemical Research Support, Weizmann Institute of Science, Rehovot, Israel*

<sup>2</sup>*Department of Molecular Chemistry and Materials Science, Weizmann Institute of Science, Rehovot, Israel*

<sup>3</sup>*Institute of Physical Engineering, Brno University of Technology, Brno, Czech Republic*

<sup>4</sup>*CEITEC BUT, Brno University of Technology, Brno, Czech Republic*

<sup>5</sup>*Thermo Fisher Scientific, Brno, Czech Republic*

P-01

## THE MOLECULAR BASIS OF CRYSTALLIZATION OF ISOXANTHOPTERIN CRYSTALS

Belal Alhozeel<sup>1</sup>, Keshet Shavit<sup>1</sup>, Amir Sagi<sup>1</sup>, Benjamin Palmer<sup>1</sup>

*Department of Chemistry, Ben-Gurion University of Negev, Rahat, Israel*

Highly reflective molecular crystals are used in many animal coloration and visual systems. Organisms exquisitely control the shape and assembly of these crystals to generate a large variety of different optical effects. However, almost nothing is known about the genes and proteins which control crystallization. Crystals of isoxanthopterin are found in reflective structures in the eyes of decapod crustaceans [1, 2]. Recent studies have shown that such crystals grow inside specialized cells called iridophores, inside a special organelle [3] [2]. We seek to elucidate the biological control mechanisms underlying crystallization. To do so, we performed a combined transcriptomic/proteomic study on a model species of freshwater prawn *Machrobrachium rosenbergii*.

In *M. rosenbergii*, we perform genetic mining of RNAseq libraries constructed at specific time points during embryo development that correlate with the emergence of crystals during ontogeny formation (Fig. 1). Crystals (indicated by the presence of birefringence in polarized micrographs), emerge after 10 days of embryogenesis in the iridophore cells (Fig. 1). In the larval organism, these crystals are used as a camouflage reflector to conceal the animal from view [2]. Candidate transcripts that are upregulated during crystal formation will then be silenced by CRISPR in early-stage embryos to ascertain the function of the related genes to the crystallization process. This strategy utilizes a recent proof-of-concept CRISPR protocol published on *M. rosenbergii* embryos [4]. Resulting phenotypic changes in the crystal morphology will be elucidated by cryo-SEM imaging in comparison with wild-type developing animals. This transcriptomic approach is supported by extraction of structural proteins directly from the mature crystal-forming organelles. This proteomic approach will further resolve the list of possible gene candidates utilized for CRISPR editing. Preliminary results show a 13 possible of proteins candidates within the crystal organelle that are intrinsically associated with the crystal. We are currently using the CRISPR system and ds-RNA injections to examine the role of those proteins and other selected genes to the crystal formation.



Fig. 1. Optical micrographs of *M. rosenbergii* embryos during development 6 distinct time points were investigated via RNA extraction in correlation with crystal emergence starting from day 9 post-fertilization (No eye) to day 16 (fully developed eyeshine) post-fertilization.

### References

1. Palmer, B.A., et al., Optically functional isoxanthopterin crystals in the mirrored eyes of decapod crustaceans. *Proc Natl Acad Sci U S A*, 2018. 115(10): p. 2299-2304.
2. Shavit, K., et al., A tunable reflector enabling crustaceans to see but not be seen. *Science*, 2023. 379(6633): p. 695-700.



3. Wagner, A., et al., Macromolecular sheets direct the morphology and orientation of plate-like biogenic guanine crystals. *Nat Commun*, 2023. 14(1): p. 589.
4. Jonathan Molcho, A.S., On genome editing in embryos and cells of the freshwater prawn *Macrobrachium rosenbergii*. *Aquaculture*, 2022. 558.

P-02

## SPECTRAL IMAGING OF BREAST CANCER BIOPSIES FOR MULTIPLEX BIOMARKERS DETECTION

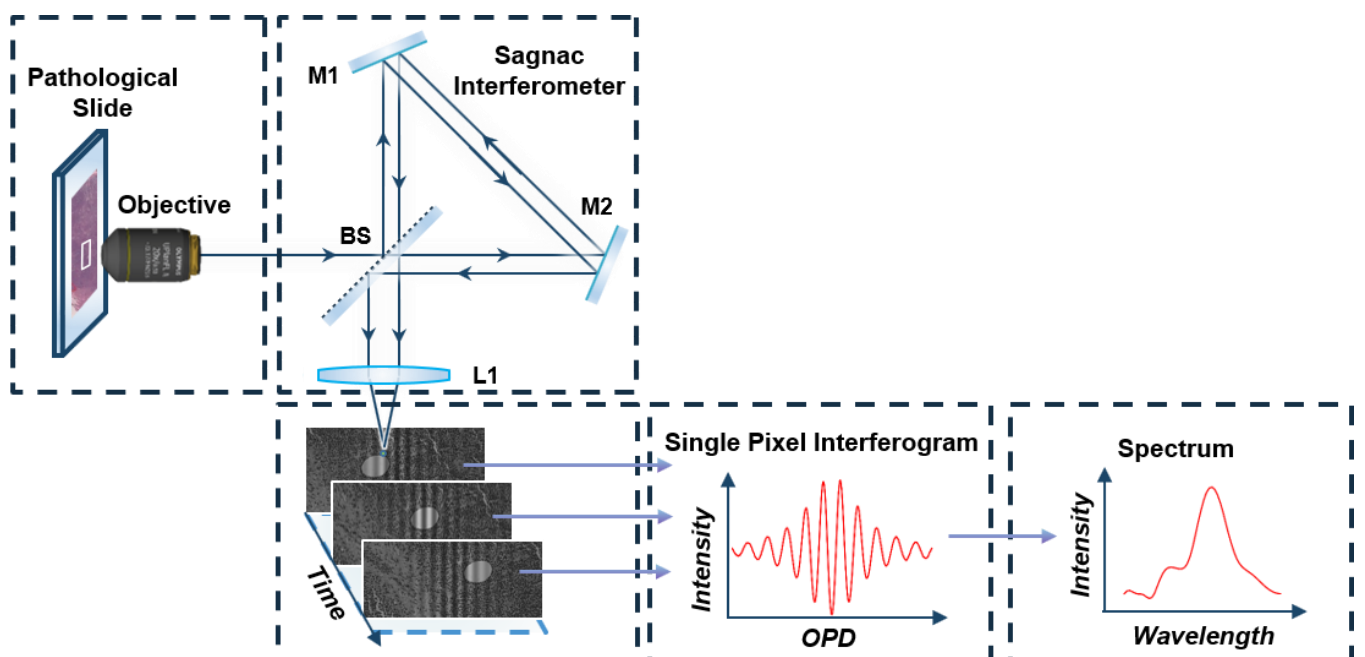
Maya Almagor<sup>1</sup>, Yuval Garini<sup>1</sup>, Roni Baron<sup>1</sup>

*Biomedical Engineering, Technion-Israel Institute of Technology, Haifa, Israel*

Precision medicine has revolutionized modern approaches to cancer treatment. Personalized drugs are effective only for a fraction of patients, which requires screening of biopsies so that the appropriate drugs can be prescribed to patients. One of the most common approaches for the characterization of biopsies utilizes the labeling of biomarkers by fluorescent molecules that are then imaged under a microscope. The accuracy of the clinical diagnosis increases as more data is collected, emphasizing the need for an efficient and practical method to detect multiple biomarkers. Due to optical and biological limitations, labeling and imaging of multiplex samples presents a challenge. Current methods measure fluorochromes sequentially, often leading to time-consuming and noisy measurements.

Here we present a novel method for efficient identification of multiple biomarkers by using a novel spectral imaging optical system on breast cancer biopsies. Imaging was performed using a Fourier spectroscopy system which is based on a Sagnac interferometer creating an optical path difference (OPD) between beams that merge and interfere on the detector, generating an interferogram. The signal collected is Fourier-transformed allowing the retrieval of a spectrum for each pixel scanned.

We performed an immunohistochemistry protocol for staining and detecting multiple protein-based biomarkers. The stained biopsies were then spectrally imaged, using an optimized optical filter. This allowed for the generation of a spectral signature of the sample which provided the basis for the calculation of molecular profiles for each cell in the imaged tissue. These results can be used as a clinical tool by providing pathologists with the cancer profiles so that the most suitable medicine can be assigned for treatment. While we studied breast cancer biomarkers, our approach can be adapted to other types of solid tumor cancers.



**P-03**

## **RNA RELATED NUCLEAR PROCESSES MODULATE THE ASSEMBLY OF CYTOPLASMIC RNA GRANULES**

**Mor Angel<sup>1</sup>, Eden Fleshler<sup>1</sup>, Mohammad Khaled Atrash<sup>1</sup>, Noa Kinor<sup>1</sup>, Yaron Shav-Tal<sup>1</sup>**

*The Mina & Everard Godman Faculty of Life Sciences & Institute of Nanotechnology,  
Bar-Ilan University, Ramat-Gan, Israel*

Stress granules (SGs) are cytoplasmic assemblies, formed under various stress conditions as a consequence of translation arrest. SGs contain RNA binding proteins, ribosomal subunits and mRNAs. It is well known that mRNAs contribute to SG formation, however, the connection between SG assembly and nuclear processes which involve mRNAs is not well established. Here, we examine the effects of transcription, splicing and nuclear export inhibition on the assembly of SGs. Specifically, we demonstrate that inhibiting splicing by targeting SF3B1, or using specific splicing inhibitors reduces the formation of canonical SGs. We also find that the splicing inhibitor madrasin promotes the assembly of RNA granules, and that splicing inhibitors have an effect not only on SGs, but also on other RNA granules such as P bodies (PBs). Strikingly, inhibiting mRNA export from the nucleus to the cytoplasm suppresses SG assembly, yet does not affect PB formation. We further investigated the effect of adding synthetic mRNAs to the cytoplasm, and found that an abundance of cytoplasmic mRNA, without applying additional stress, can directly lead to SG formation. We show that the assembly of these granules requires the activation of stress-associated protein synthesis pathways. Finally, we demonstrate that adding an excess of mRNA to cells that do not have active splicing, promotes SG formation under stress conditions, emphasizing the importance of the abundance of newly transcribed mRNA in the assembly of SGs.

**P-04**

## VISUALIZING MEMBRANE INTERACTIONS USING IN-CELL CRYO-ELECTRON TOMOGRAPHY

**Lior Aram<sup>1</sup>**, Diede de Haan<sup>1</sup>, Neta Varsano<sup>2</sup>, Katya Rechav<sup>2</sup>, Eyal Shimoni<sup>2</sup>, Nadav Elad<sup>2</sup>, Assaf Gal<sup>1</sup>

<sup>1</sup>*Department of Plant and Environmental Sciences, Weizmann Institute of Science, Rehovot, Israel*

<sup>2</sup>*Department of Chemical Research Support, Weizmann Institute of Science, Rehovot, Israel*

The silica cell wall formation in diatoms, a widespread group of unicellular microalgae, is a spectacular example of biological control over mineral formation. Diatom silicification occurs intracellularly in a membrane-bound organelle responsible for silica precipitation and morphogenesis. Despite many years of research, the inorganic-organic interactions that drive silica formation inside this organelle are unclear. This is due mainly to the limitations of traditional TEM techniques in elucidating the structural motifs of this organelle. Here we collected cryo-electron tomography datasets of cryo-FIB milled lamellae from diatom cells at various stages during cell wall formation. We visualize the mineral formation process in-situ with nanometer-scale resolution and reconstruct a timeline of mineral formation inside the cell. Our observations show that the silicification occurs in a highly confined lumen, bordered by the organelle membranes, which are in very close proximity to the plasma membrane. The plasma and organelle membranes interact via membrane contact sites, possibly facilitating continuous transport of lipids from the plasma membrane to the growing organelle, and building blocks for mineralization. These membrane-membrane interactions are manifested in the curvature of the distal organelle membrane, which molds the silica. Our findings reveal a new mechanism that regulates silica growth and shaping through membrane crosstalk.

**P-05**

## **MIGRATING AND PROLIFERATING STUDIES OF MESENCHYMAL STEM CELLS USING MACHINE-LEARNING PROCESSING OF PHASE-CONTRAST IMAGES**

**Nambi Natchiyar Balakrishnan<sup>1</sup>, Levi A Gheber<sup>1</sup>**

*Biotechnology Engineering, Ben-Gurion University of the Negev, Beer-Sheva, Israel*

Mesenchymal stem cells (MSCs) are multipotent cells with the ability to self-renew and differentiate into a number of cell types. Since the precise cues leading to MSCs' differentiation into various lineages are not well understood, following the cells' dynamics in a non-invasive and non-disrupting manner is imperative. Thus, we are following MSCs in their native form using Phase-Contrast microscopy. Subsequently, using Machine Learning, we are extracting quantitative proliferation (density) curves. Additionally, using movies of crawling MSCs, we are using Optic Flow approaches to extract velocities and angles of locomotion of the cells. The velocities as a function of cell density curves are universal for non-differentiating cells, however, may change along a differentiation pathway that the cells may take. This may aid in identification of the differentiation onset, in a continuous and non-invasive way.



P-06

## UNRAVELING THE MOLECULAR MECHANISM UNDERLYING URIC ACID CRYSTAL FORMATION IN MEDAKA LEUCOPHORE CELLS

**Yuval Barzilay**<sup>1</sup>, Rachel Lynn-Deis<sup>1</sup>, Zohar Eyal<sup>1</sup>, Tali Lerer - Goldshtein<sup>1</sup>, Anna Gorelick-ascetazi<sup>1</sup>, Iddo Pinkas<sup>2</sup>, Ziv Porat<sup>3</sup>, Neta Versano<sup>4</sup>, Smadar Zaidman<sup>4</sup>, Nili Dezorella<sup>4</sup>, Dvir Gur<sup>1</sup>

<sup>1</sup>*Department of Molecular Genetics, Weizmann Institute of Science, Rehovot, Israel*

<sup>2</sup>*Department of Chemical Research Support, Weizmann Institute of Science, Rehovot, Israel*

<sup>3</sup>*Department of Life Sciences Core Facilities, Weizmann Institute of Science, Rehovot, Israel*

<sup>4</sup>*Department of Chemical Research Support, EM unit, Weizmann Institute of Science, Rehovot, Israel*

In nature, colors can arise through the absorption of light by pigment molecules or the interaction of light with nanoscale crystalline materials, known as structural colors. Structural colors are prevalent in the animal kingdom from unicellular to multicellular organisms, serving a diverse range of optical functions such as vision, camouflage, and astonishing coloration in marine animals and chameleons. Leucophores are specialized cells containing uric acid (UA) crystals that can synthesize, transport, and accumulate large amounts of insoluble UA within organelles called leucosomes. Although these crystal-forming cells have been identified for some time, their underlying intracellular molecular processes during crystal formation remain poorly understood. Pathological UA crystallization can lead to severe illnesses such as gout and kidney stones. In this study, we used a combination of cutting-edge microscopy and spectroscopy techniques to investigate leucosome morphogenesis and molecular identity. We employed fluorescence-activated single-cell sorting (FACS) to isolate leucophores based on their unique optical properties and utilized various microscopy approaches to image leucosomes during different developmental stages. Micro-Raman spectroscopy was used to analyze the molecular content of the leucosomes, revealing them to be composed of anhydrous UA crystals. Our findings shed new light on the molecular mechanisms governing the controlled formation of molecular crystals and may contribute to the development of new biomaterials while enhancing our understanding of uncontrolled pathological UA crystallization in human diseases.

**P-07**

## **CRYO-EM INVESTIGATIONS OF HOLOCOCOLITH CALCITE INTRACELLULAR FORMATION**

**Oz Ben-Joseph<sup>1</sup>, Lior Aram<sup>1</sup>, Diede de Haan<sup>1</sup>, Katya Rechav<sup>2</sup>, Assaf Gal<sup>1</sup>**

<sup>1</sup>*Department of Plant and Environmental Sciences, Weizmann Institute of Science, Rehovot, Israel*

<sup>2</sup>*Department of Chemical Research Support, Weizmann Institute of Science, Rehovot, Israel*

Organisms can execute tight control over crystal morphology using a cellular toolkit that is not well understood. A prominent example of biological control over crystal morphology is the calcite crystals of coccolith scales covering the cell surface of marine algae. Interestingly, crystal morphology fundamentally differs in coccoliths produced by the same species` diploid and haploid life-cycle phases, called heterococcoliths and holococcoliths. While calcite crystals of heterococcoliths are highly complex and species-specific, holococcolith crystals are simple rhombohedra, the most common morphology of calcite. In this study, we focus on the growth environment of the simple holococcolith crystals utilizing cryo electron-tomography of FIB-SEM lamella. However, preparing lamellae that contain the vesicle of interest is challenging due to the small ratio of vesicle to cell volume. To overcome this challenge, thin cell layers are sequentially removed by the FIB and the exposed surface is imaged using the SEM. Once the crystal-forming vesicle is identified at the exposed cell surface, a lamella containing the region of interest is prepared. Our results indicate that rhombohedral crystals nucleate and grow intracellularly within voluminous vesicles while experiencing an unconfined, isotropic environment. In addition, solution chemistry parameters within the vesicle are evaluated. Comparing these findings with the known heterococcolith formation environment suggests that confinement of the crystallization process is a critical factor in shaping biomineral morphology.



P-08

## THE INTERPLAY BETWEEN pH and COLLAGEN ORGANIZATION IN THE TUMOR MICROENVIRONMENT: AN *IN VITRO* STUDY

Orit Bronner<sup>1</sup>, Einat Nativ-Roth<sup>2</sup>, Daniel Sevilla Sanchez<sup>2</sup>, Michal Zaiden<sup>1</sup>, Lior Cohen<sup>1</sup>, Netta Vidavsky<sup>1,2</sup>

<sup>1</sup>*Chemical Engineering, Ben-Gurion University, Beer Sheva, Israel*

<sup>2</sup>*Ilse Katz Institute for Nanoscale Science & Technology, Ben-Gurion University, Beer Sheva, Israel*

Dynamic abnormal extracellular matrix (ECM) processes are a hallmark of many diseases, including cancer. These processes can manifest as altered physical and biomechanical properties of the ECM, shifts in its composition, and changes in the spatial arrangement. Studies have shown that specific ECM properties are closely linked to the malignancy of cancerous tumors and cell migration. One fundamental property associated with cancer progression is the organization of collagen fibers. Linear, rigid collagen fibers can enhance cell migration, while curly and anisotropic fibers inhibit it. However, the relationship between ECM and cancer is complex, and it is challenging to determine whether specific ECM properties trigger cancer or whether the disease leads to abnormal ECM dynamics. The collagen structure in the tumor microenvironment can be linked to pre-malignant processes induced by cancer cells. A prominent process that characterizes a tumor microenvironment is a decrease in pH due to the anaerobic metabolism of the cancer cells. Since collagen contains ionizable residues, changes in pH can affect electrostatic interactions between collagen fibers and alter the fibers' organization. In this study, we investigate the influence of pH on the organization of collagen fibers *in vitro*. As a model for the tumor microenvironment, we use type I collagen hydrogel matrices with and without breast precancer multicellular spheroids. Initially, the collagen has a neutral pH, which changes with time due to incubation with buffer solutions or cellular activity. We characterized pH changes in the matrix over time using a pH microelectrode and confocal microscopy imaging of a fluorescent pH indicator. We show that the collagen matrix's exposure to pH resembling those of the tumor microenvironment leads to changes in structural and rheological parameters. Using Cryo Scanning Electron Microscopy (Cryo-SEM) of high-pressure frozen and freeze fractured collagen hydrogels, we observe that decreasing the collagen matrix pH to values detected in cancer resulted in shorter and disorganized fibrils. Conversely, the fibrils were longer, helical, and organized spatially when the pH increased. We employed advanced image processing to support these findings quantitatively. Switching the acidic buffer to a basic buffer resulted in long and linear fibers, indicating that the collagen structure could be restored. The structure reversibility observed in neutral collagen that became acidic and neutral again can potentially be tailored to promote healing. Additionally, rheological measurements demonstrate that the collagen's mechanical properties change under altered pH conditions. However, using Fourier Transform InfraRed Spectroscopy (FTIR), we found that the collagen secondary structure remained unaffected by pH changes, providing insights into pathological conditions. By comparing these results with Cryo-SEM imaging of the spheroids and collagen model, we evaluate the impact of acidity on collagen fibers' organization in proximity to the solid tumors and contribute to a better understanding of the ECM's complex dynamics and structural changes during cancer.



P-09

## NATURAL EVOLUTION OF SILK HIERARCHICAL STRUCTURES: REVEALING THE MULTI-LENGTH SCALES ASSEMBLY BY COMBINATION OF MICROSCOPY TECHNIQUES

**Ori Brookstein**, Dror Eliaz<sup>1</sup>, Eyal Shimoni<sup>2</sup>, Ulyana Shimanovich<sup>1</sup>

<sup>1</sup>*Molecular Chemistry and Material Science, Weizmann Institute of Science, Rehovot, Israel*

<sup>2</sup>*Chemical Research Support, Weizmann Institute of Science, Rehovot, Israel*

Silk fibers are a natural brilliant material design, having a highly-ordered hierarchical structure which gives it its extraordinary mechanical properties, combining high strength, extensibility, and toughness. Although it has been extensively studied, the self-assembly and structural transition stages that take place during the natural formation of silk multi-scale structure are still poorly understood. Generally, silk fibrillation is accompanied by the protein's transition from a soluble Random-coil state into a solidified Beta-sheet-rich conformation under acting shear forces, elongational flow, changes in metal ions composition, and pH. However, silk natural formation involves more complex and dynamic events that allow the highly unstable silk feedstock to be kept as the fluid inside the silk gland and upon the need to adopt the ordered structure of the final fiber.

Our research combines different advanced microscopy techniques to reveal the key events, at different length scale, of the silk protein's self-assembly and fiber's formation inside the silk gland. The results shed light on the multi-step process of silk protein transition in-vivo. The evolution process starts from the protein's colloidal "storage" state. It continues through the assembly of several macromolecular structures, phase separations, and transition events, which end up as bundles of nano-fibrils that form the final fiber.



P-10

## MICROCALCIFICATIONS CAN TRIGGER OR SUPPRESS BREAST PRECANCER MALIGNANCY POTENTIAL AS A FUNCTION OF MINERAL TYPE IN A 3D TUMOR MODEL

Amit Cohen<sup>1</sup>, Lotem Gotnayer<sup>1</sup>, Dina Aranovich<sup>1</sup>, Netta Vidavsky<sup>1,2</sup>

<sup>1</sup>*Chemical Engineering, Ben-Gurion University of the Negev, Beer Sheva, Israel*

<sup>2</sup>*Ilse Katz Institute for Nanoscale Science & Technology, Ben-Gurion University of the Negev, Beer Sheva, Israel*

Most early breast precancer lesions contain microcalcifications (MCs), calcium-containing pathological minerals that form in the breast and appear in more than 90% of precancer cases. The most common type of MCs is calcium phosphate crystals, mainly carbonated apatite, associated with either benign or malignant lesions. A less common type of MCs is calcium oxalate dihydrate (COD), which is almost always found in benign lesions. *In vitro* studies show that the crystal properties of apatite MCs can affect breast cancer progression. We developed a 3D tumor model of multicellular spheroids of human precancer cells containing synthetic MC analogs to link the crystal phase and properties of MCs with the progression of breast precancer to invasive cancer. Our methodology includes imaging techniques such as micro-computerized tomography, Scanning Electron Microscopy (SEM), and light microscopy to characterize the sizes, morphology, and distribution of mineral particles embedded within the multicellular spheroids. We show that apatite crystals induce precancer cell proliferation and human epidermal growth factor receptor 2 (Her2) overexpression. This tumor-triggering effect increases when the carbonate fraction in the MCs decreases. COD crystals, in contrast, reduce Her2 expression compared to control spheroids with no added MC analogs. This finding suggests that COD is not randomly located only in benign lesions but may be actively contributing to suppressing precancer progression in its surroundings. Our model provides an easy-to-manipulate platform to better understand the interactions between breast precancer cells and MCs that will potentially provide new directions for precancer prognosis and treatment.



P-11

## EXOCYTOSIS OF THE SILICIFIED CELL WALL OF DIATOMS INVOLVES EXTENSIVE MEMBRANE DISINTEGRATION

Diede de Haan<sup>1</sup>, Lior Aram<sup>1</sup>, Hadas Peled-Zehavi<sup>2</sup>, Yoseph Addadi<sup>3</sup>, Oz Ben-Joseph<sup>1</sup>,  
Ron Rotkopf<sup>3</sup>, Nadav Elad<sup>4</sup>, Katya Rechav<sup>4</sup>, Assaf Gal<sup>1</sup>

<sup>1</sup>*Department of Plant and Environmental Sciences, Weizmann Institute of Science, Rehovot, Israel*

<sup>2</sup>*Department of Biomolecular Sciences, Weizmann Institute of Science, Rehovot, Israel*

<sup>3</sup>*Life Science Core Facilities, Weizmann Institute of Science, Rehovot, Israel*

<sup>4</sup>*Department of Chemical Research Support, Weizmann Institute of Science, Rehovot, Israel*

Exocytosis is a fundamental process for cellular metabolism, communication, and growth. During exocytosis, a vesicle fuses with the plasma membrane to deliver its contents to the extracellular space. In classical exocytosis, where the secretory vesicles are much smaller than the cell, membrane homeostasis is maintained by recycling excess membrane back into the cell. An extreme case of exocytosis is the extrusion of silica cell wall elements by eukaryotic microalgae called diatoms. After formation in a membrane-bound silica deposition vesicle (SDV), the large and rigid silica element is exocytosed. During this process, the cell needs to deal with a nominal doubling of its plasma membrane. We studied membrane dynamics during cell wall exocytosis in two diatom species, using live-cell confocal microscopy, transmission electron microscopy and cryo-electron tomography. Our results show that silica is precipitated in a highly confined lumen bound by the SDV membrane, which is tethered to the plasma membrane via membrane contact sites. During exocytosis, the distal SDV membrane and the plasma membrane gradually detach from the mineral and disintegrate in the extracellular space, without any noticeable endocytic retrieval or extracellular repurposing. Within the cell, there is no evidence for the formation of a new plasma membrane, thus the proximal SDV membrane becomes the new barrier between the cell and its environment and assumes the role of a new plasma membrane. Our findings reveal a unique exocytosis mechanism used by these organisms to cope with the geometrical and physical challenges of exocytosis.<sup>1</sup>

1. de Haan, D, Aram, L, Peled-Zehavi, H, Addadi, Y, Ben-Joseph, O, Rotkopf, R, Elad, N, Rechav, K and Gal, A. 2023. Exocytosis of the silicified cell wall of diatoms involves extensive membrane disintegration. *Nature Communications*. 14:480.

**P-12****ELUCIDATE THE ROLE OF VPS4 ISOFORMS IN CYTOKINETIC ABSCISSION****Inbar Dvilansky<sup>1</sup>, Yarin Altaras<sup>1</sup>, Dikla Nachmias<sup>1</sup>, Natalie Elia<sup>1</sup>***Life science, Ben Gurion University of the Negev, Beer Sheva, Israel*

The AAA-ATPase, VPS4, is part of the ESCRT machinery that drives membrane constriction and fission in numerous processes in cells. The ESCRT complex is comprised of over 20 proteins in mammalian cells that are divided into 5 sub-families, ESCRT 0-III and VPS4. VPS4 is the most evolutionary conserved and is indispensable for the fission reaction. Notably, mammalian cells encode for two VPS4 isoforms – VPS4A and VPS4B, but the role of each isoform is unknown. Here, we set to characterize the role of VPS4 isoforms in ESCRT mediated membrane fission, employing the well documented ESCRT mediated cytokinetic abscission as a model.

To this end, we generated CRISPR/cas9 knock out cell lines of VPS4A, VPS4B and VTA1, a cofactor that stabilizes the hexameric, active form of VPS4. Our results show that depletion of VPS4A causes a considerably more severe delay in abscission compared to VPS4B depletion. STORM imaging revealed that lack of VPS4A leads to over-accumulation of the ESCRT-III protein IST1, at early abscission stages, suggesting a role for VPS4A in early abscission stages that precedes the fission reaction itself. Unexpectedly, a VPS4A mutant locked in the monomeric, inactive, state was able to partially rescue the abscission delay in VPS4A KO cells, and interacted with known abscission checkpoint proteins. Moreover, depletion of VTA1, shifted endogenous VPS4A proteins to their monomeric resulting in accelerated abscission. Collectively, our data highlight a role for monomeric VPS4A in regulating the abscission checkpoint, which is independent from its ATP hydrolysis activity.

**P-13**

## **FRACTAL DIMENSION AND FRACTIONAL CONCAVITY MEASUREMENTS OF GROWTH CONE CONTOURS OF OPTIC AXONS IN SITU**

Tamira Elul<sup>1</sup>, Valerie Lew<sup>1</sup>, Sukayneh Khetani<sup>1</sup>, **William Woodward<sup>2</sup>**

<sup>1</sup>*College of Osteopathic Medicine, Touro University California, Vallejo, California, USA*

<sup>2</sup>*College of Osteopathic Medicine, Touro University Nevada, Henderson, Nevada, USA*

Establishment of neuronal connectivity during development requires that axons extend along specific paths to reach their target tissues in the developing fetal brain. Growth cones located at the tips of axons are responsible for much of the extension and navigation of these growing axons. Non muscle Myosin IIB is one essential cellular factor that can modify the shape and motility of growth cones through modulating actin cytoskeletal dynamics. In this study, we used morphometrics to determine whether two novel shape parameters not previously applied to growth cone contours (fractal dimension and fractional concavity) could differentiate between GFP-expressing control and Myosin II inhibitor (Blebbistatin) exposed growth cones of optic axons in the optic tract of whole mount brains from *Xenopus laevis* tadpoles. Our results show that fractal dimension mean was not while fractional concavity mean were significantly different between control and experimental growth cones. However, variability in fractal dimension did differentiate between control and experimental growth cones. These results advance our understanding of growth cone morphology and introduce new morphometric parameters that can potentially assess the impacts of specific perturbations on growth cone contour complexity.



P-14

**STRUCTURAL AND ANTI-MICROBIAL STUDIES OF RIBOSOME-BINDING 16-MEMBER RING MACROLIDES AGAINST STAPHYLOCOCCUS AUREUS**

Aliza Fedorenko<sup>1</sup>, Andre Rivalta<sup>1</sup>, Disha-Gajanan Hiregange<sup>1</sup>, Anat Bashan<sup>1</sup>, Jennifer J. Schmidt<sup>2</sup>, David H. Sherman<sup>2</sup>, Ada Yonath<sup>1</sup>

<sup>1</sup>*Chemical and Structural Biology, Weizmann Institute of Science, Rehovot, Israel*

<sup>2</sup>*Medicinal Chemistry, Chemistry, Microbiology and Immunology, University of Michigan, Ann Arbor, Michigan, USA*

The increasing emergence of bacterial resistance to antibiotics, and a dwindling pipeline for new antibiotic discovery, threaten a regression to the pre-antibiotic era. One way to combat this problem is to perform chemical derivatization to the current drugs by rational drug design, which requires deep structural knowledge of the target in complex with proposed next-generation compounds. The antimicrobial activity of the 16-member ring macrolides M-4365 G2, Juvenimicin A3, and 5-O-desosaminy-tylonolide, originally discovered in the 70's and 80's, showed promise but have remained underexplored. To expand rational design efforts, we determined the cryo-EM structures of three promising 16-member ring macrolides in complex with the ribosome of *Staphylococcus aureus*, an aggressive Gram-positive pathogen. We determined the IC<sub>50</sub> values of these compounds with *S. aureus* and compared their activity and structure to other macrolides currently in clinical use. Our structural results indicate that the differences in activity between the three derivatives do not result from differences in binding, as first hypothesized, but may result from differences in the interactions between the antibiotics and the nascent peptide chain. Other observed differences in activity between these compounds and the clinically relevant drugs, such as erythromycin and tylosin, can be attributed to structural elements other than the derivatizations, such as a specific covalent bond between the antibiotic and the ribosome, or the lack of additional sugar groups. These provide insights for directed antibiotic engineering.

## SEM CHARACTERIZATION OF NON-CaP MINERAL PARTICLES FOR BREAST PRECANCER PROGNOSIS

Sahar Gal<sup>1</sup>, Netta Vidavsky<sup>1,2</sup>

<sup>1</sup>*Department of Chemical Engineering, Ben Gurion University of the Negev, Be'er Sheva, Israel*

<sup>2</sup>*Ilse Katz Institute for Nanoscale Science & Technology, Ben Gurion University of the Negev, Be'er Sheva, Israel*

Ductal Carcinoma in Situ (DCIS) is a non-invasive precancer stage of breast cancer, and only ~35% of DCIS cases develop into invasive cancer[1]. However, it is currently impossible to predict the progression of DCIS, possibly leading to unnecessary treatments. Microcalcifications (MCs) are calcium deposits in the breast, a common finding in DCIS mammography[2]. MCs are either calcium phosphate (CaP) or, less commonly, non-CaP crystals, such as calcium oxalates and calcite. The MC crystal phase is correlated with malignancy, and while CaP crystals are associated with either benign or malignant lesions, non-CaP MCs are commonly found in benign lesions[1,2]. Hence, the crystal properties of CaP MCs were the focus of many studies, which show that the CaP crystal morphology, particle size, structure, and chemical composition correlate with malignancy and may have a diagnostic or prognostic value[2]. Recent in vitro work from our group shows that non-CaP MCs consisting of calcium oxalate dihydrate (COD) might suppress precancer cell malignancy potential, suggesting that COD presence in precancer lesions may be correlated with better DCIS prognosis.

Here, we report on a retrospective study of clinical samples collected from DCIS patients more than five years ago, for which the overall clinical state, including illness progression, is known. We study breast MCs embedded within tissue sections using microscopy and vibrational spectroscopy, focusing on non-CaP crystals. To investigate links between the MC crystal properties and precancer prognosis, we use SEM and EDS to obtain the MC morphologies, particle sizes, and elemental composition, Raman mapping to determine the MC phases, and light microscopy for a histopathological overview of the sections.

We analyzed 81 individual MCs obtained from three patients with different illness outcomes. Individual MCs can be either from tumorous or normal tissue regions for the same patient. The non-CaP MCs varied in particle sizes, ranging from hundreds of nanometers to tens of micrometers. We identified morphologies such as punctulate, faceted, spherical, and spongy particles. Furthermore, some MCs were in the form of aggregates with either homogenous or heterogeneous sub-morphologies. In the developed DCIS cases, we mostly identified small homogeneous aggregates, less than 10  $\mu\text{m}$  in diameter, consisting of spherical sub-morphologies. In both tumorous and benign regions for all illness outcomes, Raman spectroscopy showed calcite, which is currently not correlated with prognosis.

Because individual non-CaP MCs are often smaller than one micrometer and are dispersed in the tissue, in future work, we will locate them in the tissue using XRF mapping and measure their Ca K-edge  $\mu$ -XANES to detect their structures to be correlated with DCIS prognosis. By retrospectively integrating medical information with the MC features, this study will potentially shed light on the role of the less common breast microcalcifications non-CaP crystals and provide a better insight into the DCIS prognosis based on their features.

[1]Gosling, S., et al. (2022). A multi-modal exploration of heterogeneous physico-chemical properties of DCIS breast microcalcifications. *Analyst*,147(8).

[2]Kunitake, J. A. M. R., et al. (2023). Biomineralogical signatures of breast microcalcifications. *Science Advances*,9(8).

**P-16**

## **MORPHOLOGICAL QUANTIFICATION OF LEISHMANIA PARASITE LIFE CYCLE STAGES USING IMAGING FLOW CYTOMETRY**

**Uzi Hadad<sup>1</sup>, Nofar Baron<sup>2</sup>, Michal Shapira<sup>2</sup>**

*<sup>1</sup>Ilse Katz Institute for Nanoscale Science and Technology, Ben-Gurion University of the Negev, Beer Sheva, Israel*

*<sup>2</sup>Department of Life Sciences, Ben-Gurion University of the Negev, Beer Sheva, Israel*

Leishmaniasis is a parasitic disease that is found in parts of the tropics, subtropics, and southern Europe. Leishmaniasis is caused by infection with Leishmania parasites that are transmitted to humans by the bite of phlebotomine sand flies. The parasites cycle between sand-fly vectors and mammalian hosts adapting to different environments. These life cycle events are accompanied by distinct morphological changes that involve differences in size and dimensions including the flagellum length.

Imaging flow cytometry (IFC) is a high throughput widefield microscopy-based method that capture fluorescence and brightfield images of particles (e.g. cells) in suspension, providing the morphological information. We developed an IFC method to analyze changes in shape and flagellum length of Leishmania parasites. We used this method to provide information on the changes that Leishmania cells are presenting following CRISPR-Cas9 mediated hemizygous deletion in the Eukaryotic translation initiation factor 4E2 (LeishIF4E2). We found that cells that lack one copy of LeishIF4E2 (LeishIF4E2 +/-) are smaller, round, and equipped with a very short flagellum.

Our quantitative method can be expanded to other parasites thus providing researchers with an efficient and simple tool to analyze morphological changes, without the need to label the cells.



P-17

## LABEL FREE IMAGING OF CHOLESTEROL CRYSTALS AND MACROPHAGES AS A MODEL SYSTEM FOR ATHEROSCLEROSIS

Antonia Kaestner<sup>1,2</sup>, Yoseph Addadi<sup>3</sup>, Neta Varsano<sup>4</sup>, Ori Avinoam<sup>2</sup>, Lia Addadi<sup>1</sup>

<sup>1</sup>*Chemical and Structural Biology, Weizmann Institute of Science, Rehovot, Israel*

<sup>2</sup>*Biomolecular Sciences, Weizmann Institute of Science, Rehovot, Israel*

<sup>3</sup>*Life Sciences Core Facilities, Weizmann Institute of Science, Rehovot, Israel*

<sup>4</sup>*Electron Microscopy Unit, Weizmann Institute of Science, Rehovot, Israel*

Atherosclerosis is a pathology characterized by the build-up of plaques from an accumulation of cholesterol-rich lipoproteins and later cholesterol crystals inside the arterial walls, and is the cause of most cardiovascular diseases. A key player in the atherosclerotic lesions are macrophages. The macrophage tasks in the body include the identification, uptake and disposal of harmful bodies. Within the plaques, their recruitment is triggered by the excess presence of cholesterol-rich lipoproteins. There is however also evidence that crystalline cholesterol is a target for the macrophages [1].

Understanding the cholesterol crystal interaction with other plaque components is important due to their activation of an inflammatory immune response, the possible crystal-induced rupture of cell membranes and plaque rupture, which may cause obstruction of arteries [1].

Previous research showed that macrophages have the capacity for uptake of cholesterol crystals [1], and mainly focused on understanding the immune response triggered by the cholesterol crystals. Meanwhile, our focus is to observe the crystal phagocytosis events, possibly followed by crystal dissolution. To gain a better understanding of the mechanism of crystal uptake and subsequent processing, we incubate macrophages of the J774A.1 cell line with synthetic cholesterol crystals. We utilize three label free imaging techniques: confocal reflection microscopy, a refraction-based microscopy technique (NanoLive) and scanning electron microscopy under cryogenic conditions (cryo-SEM). Labeling the crystals is undesirable because it may alter the recognition, uptake and dissolution of the crystals by the macrophages. Imaging in the NanoLive allowed live 3D observation of the uptake process. Starting at around 45min after co-incubating cells and cholesterol crystals, phagocytosis events of clusters of crystals occur. Each uptake process takes around 10 to 15 minutes, and some cells will phagocytose multiple sets of crystals. The cholesterol crystals can be identified extra- and intracellularly both visually and based on the NanoLive detection of differences in the refractive index of the crystals (~ 1.6), relative to the cytoplasm (~1.3-1.4). Using confocal reflection microscopy with a 488 or 514nm laser, cholesterol crystals can also be confirmed both inside and outside the cells.

Cryo-SEM images performed on freeze-fractured surfaces show abundant intracellular cholesterol crystals. Unambiguously identifying instances of dissolution is difficult, although the increased presence of what appear to be lipid droplets near or directly attached to clusters of cholesterol crystals, may be a good indication of crystal processing by the macrophages.

Combining the information collected with the different imaging technologies provides a detailed observation of the process in space and time with high fidelity and minimal influence on the biological process.

[1] Duewell, P., Kono, H., Rayner, K. J., Sirois, C. M., Vladimer, G., Bauernfeind, F. G., Abela, G. S., Franchi, L., Nüez, G., Schnurr, M., Espevik, T., Lien, E., Fitzgerald, K. A., Rock, K. L., Moore, K. J., Wright, S. D., Hornung, V., & Latz, E. (2010). NLRP3 inflammasomes are required for atherogenesis and activated by cholesterol crystals. *Nature*, 464(7293), 1357–1361. <https://doi.org/10.1038/nature08938>

**P-18**

## **DETERMINING THE COMPOSITION OF THE ESCRT-III FILAMENT IN CYTOKINESIS ABSCISSION OF MAMMALIAN CELLS**

**Nikita Kamenetsky<sup>1</sup>, Natalie Elia<sup>1</sup>**

*Life sciences, Ben-Gurion University of the Negev, Beer-Sheba, Israel*

The ESCRT machinery (ESCRT 0, I, II, III and the AAA ATPase VPS4) participates in membrane constriction and fission in a variety of processes in cells. Cytosolic ESCRT-III proteins and VPS4, the driving force for membrane fission, assemble into cortical filaments to induce membrane constriction and severing. One of the ESCRT mediated processes is abscission of the intercellular bridge connecting two daughter cells at the end of cytokinesis, which constitutes the last step of cell division.

Over 10 different ESCRT-III proteins were identified in the mammalian genome (named CHMP 1-7 and IST1), but the specific role of ESCRT-III subunits in constriction and fission have not been defined. In vitro studies suggest that the ESCRT-III components CHMP2A was designated as one of the components required for the final fission event. To test the effect of CHMP2A on ESCRT mediated membrane remodeling in cells, we generated CHMP2A knock-out HeLa cells. Live-cell imaging experiments performed in CHMP2A KO cells revealed that abscission is severely delayed in the absence of CHMP2A. Surprisingly, in contrast to other essential abscission components, all the cells eventually completed abscission suggesting that CHMP2A is not essential for the final fission event. SIM imaging of the core ESCRT-III components CHMP4B and IST1 revealed defected in the spatiotemporal organization of the filament during the process. Surprisingly, labeling both proteins in the same cell revealed that while these proteins co-localize in normal cells, their organization pattern is spatially separated in CHMP2A KO cells, suggesting that the polymerization process itself is affected by CHMP2A depletion. Together, these results suggest a role for CHMP2A in filament polymerization rather than in the final fission process itself.



P-19

## SNAPSHOTS OF MITOCHONDRIAL FISSION THROUGH THE LENSE OF CRYO-SCANNING TRANSMISSION ELECTRON TOMOGRAPHY (CSTET)

Peter Kirchweger<sup>1,2</sup>, Sharon Wolf<sup>3</sup>, Deborah Fass<sup>2</sup>, Michael Elbaum<sup>1</sup>

<sup>1</sup>*Department of Chemical and Biological Physics, Weizmann Institute of Science, Rehovot, Israel*

<sup>2</sup>*Department of Chemical and Structural Biology, Weizmann Institute of Science, Rehovot, Israel*

<sup>3</sup>*Department of Chemical Research Support, Weizmann Institute of Science, Rehovot, Israel*

Cryo-Scanning Transmission Electron Tomography (CSTET) allows imaging of areas in a cell up to 1  $\mu\text{m}$  in thickness (Wolf, Houben, and Elbaum 2014; Wolf et al. 2017), values unreached by cryo-ET. Thus, CSTET enables the visualization of intact mitochondria and their surrounding environment in native cells without sectioning or milling.

We developed deconvolved dual-axis CSTET (ddCSTET, Waugh et al. 2020; Kirchweger et al. 2022). Deconvolution successfully removes the “salt-and-pepper” noise, and by combining dual-axis tomography with deconvolution, the missing wedge is reduced and accounted for, which results in near-isotropic resolution.

We applied ddCSTET to image stalled fission intermediates of mitochondria. A set of proteins play a significant role in fission. These include the mitochondrial fission factor (Mff), an outer mitochondrial membrane (OMM) protein that recruits dynamin-related protein 1 (Drp1), a cytosolic GTPase, which performs the final fission step. Cells lacking Mff (Mff<sup>-/-</sup>) generate mitochondrial constrictions under fission-inducing conditions, but, as expected, successful fission is reduced. We first image Mff<sup>-/-</sup> cells under normal and fission-inducing conditions by fluorescence microscopy. While the diameter of the WT mitochondria appears to be more equal, the MFF<sup>-/-</sup> mutant displays different morphologies. These include “beads-on-the-string” and mitochondria with increased thickness, up to several  $\mu\text{m}$  in diameter. We then characterized them by ddCSTET. DdCSTET of those different mitochondrial morphologies displays different health states of the mitochondria, as judged by the appearance of the cristae. We show 3D CSTET volumes of the “beads-on-the-string” morphology, of a “garbage can”, i.e., a mitochondrial blob with several  $\mu\text{m}$  in diameter, and a 3D volume of a 10  $\mu\text{m}$  long mitochondria. This shows that the cell tries to segregate the healthy section of a mitochondria from the unhealthy section. Additionally, we show contacts between mitochondria and their surrounding organelles and the cytoskeleton participating in the fission process.

As a summary, ddCSTET provides insight into the whole “cellular theater”.

Kirchweger, Peter, Debakshi Mullick, Prabhu Prasad Swain, Sharon G. Wolf, and Michael Elbaum. 2022. “Bridging the Light-Electron Resolution Gap with Correlative Cryo-SRRF and Dual-Axis Cryo-STEM Tomography.” *BioRxiv*.  
Waugh, Barnali, Sharon G. Wolf, Deborah Fass, Eric Branlund, Zvi Kam, John W. Sedat, and Michael Elbaum. 2020. “Three-Dimensional Deconvolution Processing for STEM Cryotomography.” *Proceedings of the National Academy of Sciences of the United States of America* 117 (44): 27374–80.

Wolf, Sharon Grayer, Lothar Houben, and Michael Elbaum. 2014. “Cryo-Scanning Transmission Electron Tomography of Vitrified Cells.” *Nature Methods* 11 (4): 423–28.

Wolf, Sharon Grayer, Yael Mutsafi, Tali Dadosh, Tal Ilani, Zipora Lansky, Ben Horowitz, Sarah Rubin, Michael Elbaum, and Deborah Fass. 2017. “3D Visualization of Mitochondrial Solid-Phase Calcium Stores in Whole Cells.” *ELife* 6 (November).



P-20

## ROBUSTNESS OF THE CANONICAL MITOCHONDRIAL FUSION MACHINERY PROMOTES NEBENKERN FORMATION IN DROSOPHILA SPERMATIDS.

Alina Kolpakova<sup>1</sup>, Shmuel Pietrokovski<sup>1</sup>, Eli Arama<sup>1</sup>

*Department of Molecular Genetics, Weizmann Institute of Science, Rehovot, Israel*

Mitochondria are the bioenergetics powerhouses and biosynthetic centers of the cell. The mitochondria are constantly changing shape and subcellular distribution according to function, energy and metabolic demands of the cell. Mitochondrial morphology usually ranges from small spheres and short tubules to elongated tubules and reticular networks. These changes are mainly controlled by the balance between two opposing mechanisms of membrane dynamics, fusion and fission, which when perturbed, can lead to severe pathologies.

Perhaps the most dramatic morphological changes and structural organizations of the mitochondria occur during spermatogenesis. In *Drosophila* spermatids, individual mitochondria aggregate near the newly formed haploid nucleus and subsequently coalesce and fuse into a giant sphere called Nebenkern. The Nebenkern is composed of two giant mitochondria wrapped around each other and arranged in an onion-like spherical segments of layers upon layers. During subsequent spermatid elongation stages, the Nebenkern is transformed from a 6.7  $\mu\text{m}$  sphere to two, 1.8 mm long, cylindrical mitochondrial derivatives extending alongside the axoneme. Although detailed ultrastructural description of Nebenkern formation was already reported five decades ago, the molecular mechanisms underlying the formation of this extraordinary organelle remains largely obscure.

To further characterize the genetic components, involved in Nebenkern formation, we utilized several advanced microscopy techniques such as live imaging, electron microscopy and expansion microscopy. We show that already during the second meiosis division, mitochondria start fusing to elongated tubular organelles, which continue fusing and collapsing to form the spherical Nebenkern, achieved by the robust and lasting action of the canonical fusion machinery. We demonstrate that the testis-specific mitochondrial fusion protein, Fzo, and the more generally expressed mitochondrial fusion protein, Marf, function similarly in promoting spherical mitochondrial fusion.

Finally, using a candidate screen through a compiled list of mitochondrial and cytoskeletal genes, we identified additional components involved in Nebenkern formation.

**P-21**

## **FIB-SEM IMAGING REVEALS IN-SITU FORMATION OF THE SILICA CELL WALL OF ALGAE**

**Zipora Lansky<sup>1</sup>**

*Plant and Environmental Science, Weizmann Institute of Science, Rehovot, Israel*

The intricate geometrical patterns in the silica cell wall of unicellular algae have long sparked curiosity as to their process of formation. These cells take up silicic acid from the ocean and precipitate it in a controlled manner to form a cell wall patterned with pores and ridges that are species specific. Here we visualize in 3D the in-situ cell wall formation of the diatom *Stephanopyxis turris*. We imaged whole cells using a slice-and-view approach with a focused ion beam SEM (FIB-SEM), both in fixed cells and at cryo conditions. Our data reveal that the hexagonal pore pattern of the mature valve is created by silica precipitating into radial rods which are then connected by bridges to form pores. These results of radial rods being the initial step of silica cell wall formation was observed in studies of very different diatom species, and may suggest an underlying principle of silica precipitation in diatoms.



P-22

## MAPPING OF PHASE SEPARATION OF SUPRAMOLECULAR PROTEIN ASSEMBLIES BY LIVE CELL HOLOTOMOGRAPHY MICROSCOPY

Orlando Marin<sup>1</sup>, Arina Dalaloyan<sup>1</sup>, Michael Elbaum<sup>1</sup>

*Biological and Chemical Physics, Weizmann Institute of Science, Rehovot, Israel*

Protein condensation, phase separation, and self-assembly are different aspects of very similar phenomena. Weak but multivalent intermolecular interactions drive the growth of supramolecular protein assemblies much larger than the size of the protein unit. The physical state of such condensates may be crystalline, amorphous solid, gel, or liquid. Ferritin proves to be an ideal scaffold on which to study self-assembly. Mammalian ferritin contains 24 polypeptide subunits in a nearly-spherical shell with octagonal symmetry. The N termini are disordered and point to the exterior. Exogenous expression in cells of a hybrid ferritin with dimerizing fluorescent proteins such as Citrine resulted in self-assembly of fluorescent protein bodies<sup>1</sup>. Mutation of the hydrophobic dimerizing patch to one containing cysteine led to oxidation-sensitive self-assembly<sup>2</sup>. Addition to ferritin of intrinsically disordered domains with light-sensitive coupling, named Corelets, has helped to map phase separation within cellular compartments by means of protein condensation<sup>3</sup>. In this work we revisit these systems using a new holographic microscopy tool to map refractive index in 3D, avoiding dependence on fluorescence imaging and setting the stage for correlative electron tomography of the protein assemblies in solid or liquid phase.

Ref.:

1. Giuliano, B. et al, *Angew. Chem. Int. Ed.*, 2014, 53, 1534–1537.
2. Giuliano, B. et al, *Nano Lett.*, 2016, 16, 6231–6235.
3. Bracha, D. et al, *Cell*, 2018, 175, 1467–1480.



P-23

## ASGARD ESCRT-III AND VPS4 REVEAL CONSERVED CHROMATIN BINDING PROPERTIES OF THE ESCRT MACHINERY

Dikla Nachmias<sup>1</sup>, Melnikov Melnikov<sup>1</sup>, Alvah Zorea<sup>1</sup>, Maya Sharon<sup>1</sup>, Reut Yemini<sup>1</sup>, Yasmin De-picchoto<sup>1</sup>, Ioannis Tsirkas<sup>1</sup>, Amir Aharoni<sup>1</sup>, Bela Frohn<sup>2</sup>, Petra Schwille<sup>2</sup>, Raz Zarivach<sup>1</sup>, Itzhak Mizrahi<sup>1</sup>, Natalie Elia<sup>1</sup>

<sup>1</sup>*Department of Life Sciences, Ben-Gurion University of the Negev, Beer-Sheva, Israel*

<sup>2</sup>*Department of Cellular and Molecular Biophysics, Max-Planck Institute of Biochemistry, Martinsried, Germany*

The archaeal Asgard superphylum currently stands as the most promising prokaryotic candidate, from which eukaryotic cells emerged. This unique superphylum encodes for eukaryotic signature proteins (ESP) that could shed light on the origin of eukaryotes, but the properties and function of these proteins is largely unresolved. Here, we set to understand the function of an Asgard archaeal protein family, namely the ESCRT machinery, that is conserved across all domains of life and executes basic cellular eukaryotic functions, including membrane constriction during cell division. We find that ESCRT proteins encoded in Loki archaea, express in mammalian and yeast cells, and that the Loki ESCRT-III protein, CHMP4-7, resides in the eukaryotic nucleus in both organisms. Moreover, Loki ESCRT-III proteins associated with chromatin, recruited their AAA-ATPase VPS4 counterpart to organize in discrete foci in the mammalian nucleus, and directly bind DNA. The human ESCRT-III protein, CHMP1B, exhibited similar nuclear properties and recruited both human and Asgard VPS4s to nuclear foci, indicating interspecies interactions. Mutation analysis revealed a role for the N terminal region of ESCRT-III in mediating these phenotypes in both human and Asgard ESCRTs. These findings suggest that ESCRT proteins hold chromatin binding properties that were highly preserved through the billion years of evolution separating Asgard archaea and humans. The conserved chromatin binding properties of the ESCRT membrane remodeling machinery, reported here, may have important implications for the origin of eukaryogenesis.

**P-24**

## **THE EFFECT OF LAMIN A ON THE COHERENT DYNAMICS OF THE CHROMATIN IN LIVING CELLS**

**Wajdi Nicola<sup>1</sup>, Yuval Garini<sup>1</sup>**

*Bio-medical Engineering, Technion-Israel Institute of Technology, Haifa, Israel*

During the last decade, extensive studies highlighted the complex structure of the chromatin inside the cell nucleus. The chromatin is packed inside the small volume of the cell nucleus in an organized yet dynamic manner. The organization and dynamics of the chromatin within the nucleus of eukaryotic cells are closely related to cellular functions, such as gene regulation and mitosis. The mechanism of genome organization has been studied through various models and the identification of the nuclear structural proteins.

Recent experiments have shown that lamin A contributes significantly to reducing chromatin dynamics and directly affects the mechanical properties of the nucleus. These studies were based on tracking specific chromosome loci and single particle tracking methods. However, further experiments are needed to understand the inner life of the nucleus. In this research, we aim to study the chromatin as a bulk material and the role of lamin A in the large-scale dynamics of the chromatin.

Our measurements include mapping the whole chromatin dynamics in living cells using H2B-GFP tagged histones. We used displacement correlation spectroscopy methods, based on particle image velocimetry (PIV) techniques, in order to map the whole chromatin across the entire nuclear volume. We measured cells with modified levels of the protein lamin A to quantify the role of the protein in governing the dynamics of the chromatin at large length and time scales.

In our research we use various techniques, such as confocal microscopy and PIV analysis, to develop a theoretical model that describes the biophysical function of the proteins and the mechanisms involved in chromatin organization. Our research will contribute to better understanding of genome organization as well as the dynamic properties of the chromatin in eukaryotic cells.



P-25

## STRUCTURAL STUDIES ON THE *S. AUREUS* ERMB METHYLTRANSFERASE MUTANT RIBOSOME IN COMPLEX WITH SOLITHROMYCIN

Andre' Rivalta<sup>1</sup>, Aliza Fedorenko<sup>1</sup>, Yehuda Halfon<sup>1</sup>, Disha-Gajanan Hiregange<sup>1</sup>, Ella Zimmerman<sup>1</sup>, Anat Bashan<sup>1</sup>, M.N. Frances Yap<sup>2</sup>, Ada Yonath<sup>1</sup>

<sup>1</sup>*Chemical and Structural Biology, Weizmann Institute of Science, Rehovot, Israel*

<sup>2</sup>*Feinberg School of Medicine, Northwestern University, Chicago, Illinois, USA*

About 40% of clinically used antibiotics target ribosomes, the complex nano-machines that translate the genetic code to proteins in all living cells. However, we are witnessing an increasing number of drug-resistant pathogens, coupled with the underwhelming development of new antibiotics. Additional structural studies on antibiotic-resistant strains may provide insights onto mode of action and improve our odds in fighting against bacterial infections. A prime example of resistance mechanisms is the methylation of adenosine 2058 of the 23S ribosomal RNA by an Erm-methyltransferase, which confers resistance to several drugs, including macrolides. Here we show the cryo-EM structure of a methylated A2058 ribosome from *Staphylococcus aureus* (SA), a life-threatening Gram-positive bacterium, that forms a complex with a macrolide despite the presence of methylation.



P-26

## THE EFFECT OF LOOP8 ON SPINDLE LOCALIZATION AND BI-DIRECTIONALITY OF *S. CEREVISIAE* KINESIN-5 CIN8

Mayan Sadan<sup>1</sup>, Himanshu Pandey<sup>1,2</sup>, Sudhir Kumar Singh<sup>1</sup>, Mary Popov<sup>1</sup>, Meenakshi Singh<sup>1</sup>, Geula Davidov<sup>3</sup>, Sayaka Inagaki<sup>4</sup>, Jawdat Al-Bassam<sup>5</sup>, Raz Zarivach<sup>2,3</sup>, Steven S Rosenfeld<sup>4</sup>, Larisa Gheber<sup>1,2</sup>

<sup>1</sup>*Department of Chemistry, Ben-Gurion University of the Negev, Beer-Sheva, Israel*

<sup>2</sup>*Ilse Katz Institute for Nanoscale Science and Technology, Ben-Gurion University of the Negev, Beer-Sheva, Israel*

<sup>3</sup>*Department of Life Sciences and the National Institute for Biotechnology in the Negev, Ben-Gurion University of the Negev, Beer-Sheva, Israel*

<sup>4</sup>*Department of Cancer Biology, Mayo Clinic, Jacksonville, FL, USA*

<sup>5</sup>*Department of Molecular and Cellular Biology, University of California, Davis, CA, USA*

Precise segregation of chromosomes during mitosis is essential for maintaining genetic stability and preventing mutations that can lead to genetic diseases and cancer. Chromosome segregation is mediated by the mitotic spindle, a microtubule based bipolar structure. In each mitotic cycle, the mitotic spindle undergoes a well-defined set of morphological changes that are temporally and spatially regulated. Thus, the elucidation of unknown mechanisms and regulatory pathways will enable the identification of potential new targets for treating and preventing cancer. We use a genetically traceable eukaryote, *S. cerevisiae*, as a model to answer basic unresolved questions regarding the mechanisms and regulation of mitosis.

Kinesin-5 motor proteins are highly conserved from yeast to humans and play central roles in establishing and maintaining the mitotic spindle during cell division. These motors are homotetramers with two pairs of catalytic domains located at the opposite sides of the active complex. This architecture enables kinesin-5s to crosslink and slide apart antiparallel microtubules (MTs) of the mitotic spindle. Recent studies have demonstrated that some kinesin-5 motors, including the *Saccharomyces cerevisiae* Cin8 move bi-directionally along microtubules, switching directionality under different conditions. Cin8 carries a uniquely large insert in loop8 in its motor domain, compared to other Kinesin-5 homologues. The role of loop 8 in regulating the motile properties of Cin8 is still unknown.



P-27

## BIOMINERAL FORMATION BY THE FRESHWATER GREEN ALGA PHACOTUS LENTICULARIS

Noy Shaked<sup>1</sup>, Sophia Barinova<sup>4</sup>, Sefi Addadi<sup>2</sup>, Katya Rechav<sup>3</sup>, Steve Weiner<sup>1</sup>, Lia Addadi<sup>1</sup>

<sup>1</sup>*Department of Chemical and Structural Biology, Weizmann Institute of Science, Rehovot, Israel*

<sup>2</sup>*Department of life sciences core facilities, Weizmann Institute of Science, Rehovot, Israel*

<sup>3</sup>*Chemical research support unit, Weizmann Institute of Science, Rehovot, Israel*

<sup>4</sup>*Institute of Evolution, University of Haifa, Haifa, Israel*

Many unicellular algae produce CaCO<sub>3</sub> minerals in marine and freshwater ecosystems, and some of them are known to also form guanine crystals. One freshwater species, *Phacotus lenticularis*, is abundant in lakes and ponds. *P. lenticularis* produces a complex shell composed of aligned crystal plates of calcite. These shells constitute a significant fraction of basin sediments especially during the bloom period.

We investigate the mechanism of shell formation, and the pathway of ion transport and mineral deposition, using multimodal microscopy techniques. We enriched natural *P. lenticularis* cells and followed the different stages of shell formation using in-vivo fluorescence microscopy assays combined with cryo-SEM, which enable observation of the shell and the associated cells under fully hydrated conditions. We observed calcium trafficking into the cell, intracellular crystallization and developmental changes in the hierarchy and morphology of the shell crystals.

*P. lenticularis* in our cell cultures does not calcify, and we investigate the signals that trigger calcification both in the cell cultures and in natural environments at the onset of the bloom period.

We also observed that cell cultures grown under phosphate stress conditions, produce birefringent crystals that were identified as beta guanine. The crystals were observed inside specific vacuoles using cryo-SEM and cryo-FIB-SEM. Localization and distribution of the crystals was obtained using cryo-Soft-X-ray tomography and near edge spectroscopy.

Investigation of the two biomineralization pathways and determining if any connections between the two exist, may provide insight into the guanine and calcite crystals' function and evolutionary development in *P. lenticularis* and other unicellular organisms.

**P-28**

## **IMPROVING CRYO-ELECTRON TOMOGRAPHY DATA QUALITY AND THROUGHPUT BY STREAMLINING THE WORKFLOW**

**Marit Smeets<sup>1</sup>, Katherine Lau<sup>1</sup>**

*Life Sciences, Delmic B.V., Delft, Zuid-Holland, Netherlands*

Cryo-electron tomography (cryo-ET) is a very powerful technique that allows researchers to obtain high resolution information about macromolecular complexes in their native cellular environment. Recently the technique has gained popularity and an increasing number of researchers are implementing it in their lab.

The power of cryo-ET is undisputed but the fact that the workflow is very error-prone has limited the data output<sup>1</sup>. In the workflow, there are two main challenges: keeping the sample ice contamination-free and targeting the region of interest (ROI).

At Delmic we developed two workflow solutions called CERES and METEOR to solve these problems. The CERES Ice Defence System is based on the tools developed by Tacke et al<sup>2</sup>. and consists of multiple innovative tools that are tailored to minimize ice contamination during sample handling (Clean Station), transfer (Vitri-Lock) and FIB milling (Ice Shield). METEOR is an integrated fluorescence light microscope (FLM) that greatly enhances the ROI targeting inside the cryo-FIB/SEM while reducing the number of handling steps required<sup>3</sup>.

We show that combining these innovative tools can lead to improved cryo-ET data quality and throughput.

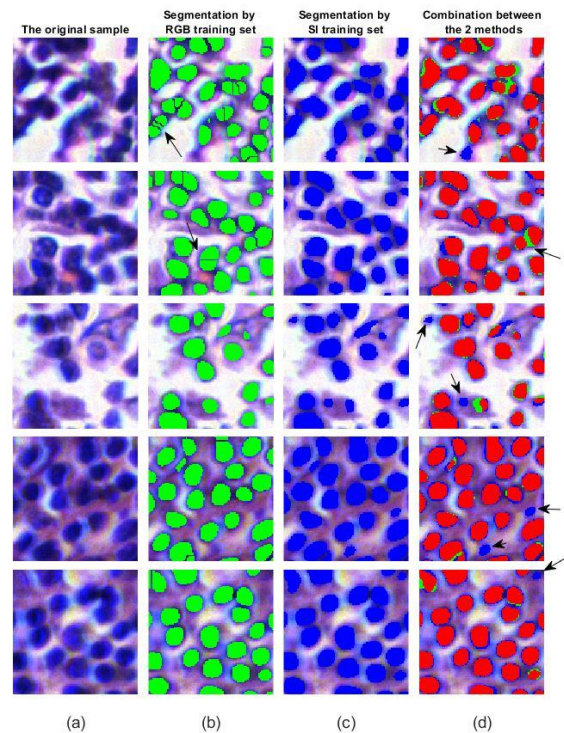
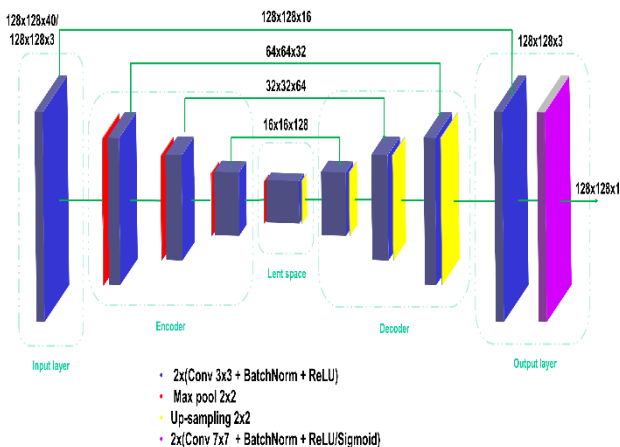
1. Lau, K., Jonker, C., Liu, J. & Smeets, M. The Undesirable Effects and Impacts of Ice Contamination Experienced in the Cryo-Electron Tomography Workflow and Available Solutions. *Micros Today* 30, 30–35 (2022).
2. Tacke, S. et al. A streamlined workflow for automated cryo focused ion beam milling. *J Struct Biol* 213, 107743 (2021).
3. Smeets, M. et al. Integrated Cryo-Correlative Microscopy for Targeted Structural Investigation In Situ. *Micros Today* 29, 20–25 (2021).

## SPEC-NET: NUCLEAR SEGEMENTATION FROM H&E BIOPSY WITH SPECTRAL IMAGING SCREENING

Adam Soker, Yuval Garini<sup>1</sup>

*Bio-medical Engineering, Technion, Haifa, Israel, Israel*

Biopsy diagnostics is a common method for analyzing cancer and other fatal diseases. In recent years, digital tools like digital imaging and Whole-Slide Imaging (WSI) have become more popular for biopsy analyzing, which allows the use of image processing and artificial intelligence (AI). One of the main tasks for these technologies is nuclei segmentation from Hematoxylin and Eosin stain (H&E). While AI has shown some success in this area, it is still not widely used in the medical community due to concerns about accuracy. In this paper, we present a novel approach for analyzing H&E stains using Spectral Imaging (SI) screening, which provides multiple intensity values for each pixel, compared to just three values for each pixel with RGB imaging. Our application is based on a U-net model with an adjusted input layer for SI size and was compared to Performance of model that was train on RGB images. Despite limitations with the quality of the data labeling, the models showed improved performance when measured by F1-score and Aggregated Jaccard Index (AJI). The study also showed by logistic regression model, that SI images had an advantage in pixel-level classification compared to RGB images.





P-30

## THE ROLE OF THE NON-MOTOR N-TERMINAL REGION IN REGULATION OF FUNCTION OF THE BI-DIRECTIONAL KINESIN-5 CIN8

Neta Yanir<sup>1</sup>, Himanshu Pandey<sup>1</sup>, Sudhir Kumar Singh<sup>1</sup>, Alina Goldstein-Levitin<sup>1</sup>, Leah Gheber<sup>1</sup>

*Department of Chemistry, Ben-Gurion University of the Negev, Beer-Sheba, Israel*

During mitosis, the bipolar kinesin-5 motor proteins perform central functions in mitotic spindle dynamics by crosslinking and sliding antiparallel microtubules (MTs) apart. Recent studies have indicated that the *Saccharomyces cerevisiae* kinesin-5 Cin8 moves bi-directionally along MTs, in minus-end and plus-end directions. The mechanism of this bi-directional motility remains unknown. In this study we examined the roles of sequences in the non-motor N-terminal region in regulating the function of bi-directional Cin8. For this purpose, we generated N-terminal deletion variants of GFP-tagged Cin8 and examined their intracellular localization. We found that in *S. cerevisiae* cells containing Cin8 variant, in which aa 39-69 were deleted (Cin8 $\Delta$ 39-69), close to 30% of the cells were monopolar with no Cin8-GFP signal, compared to wt Cin8 that exhibited only 7% of this phenotype, suggesting that the deletion of aa 39-69 within Cin8 generated less stable Cin8 variant. In addition, in monopolar cells, Cin8 $\Delta$ 39-69 and  $\Delta$ 70-75, exhibited mis localization in the nucleus and/or on nuclear MTs, compared to wt Cin8 that concentrated mainly at the poles, indicating that these variants are either defective in minus-end directed motility or exhibit reduced affinity to MTs. Consistently, these two variants exhibited lower percentage of cells with short bipolar spindles compared to wt Cin8, indicating that these variants are defective in bipolar spindle assembly. According to these results we suggest that sequences in the nonmotor N-terminal region of Cin8 regulate the intracellular localization of this motor, mainly prior to spindle assembly, which affects the functionality of Cin8 in cells.



P-31

## MEASUREMENT-BASED CONTROL OF THE ELECTRON-PHOTON COUPLING COHERENCE

Hadar Aharon<sup>1</sup>, Ofer Kfir<sup>1</sup>

*School of Electrical Engineering, Fleischman Faculty of Engineering, Tel Aviv University, Tel Aviv 69978, Israel*

Electron microscopes allow for nanometric resolution for material science, microelectronics, and research of light fields well below the wavelength of visible light. The electron-photon coupling induced by the electron beam can be used to generate a high-resolution image of samples by producing various types of emissions, thus helpful in studying the properties of materials and their interactions with electromagnetic radiation. Where the properties of luminescence from the passage of a localized electron beam are readily derived by assuming a point-particle electron, the expansion to higher dimensions depends on its quantum aspects. A pioneering experiment by Remez et al. on Smith-Purcell radiation [1], found that its wavefunction is extended spatially the electron still behaves as a point-like particle, passing along one path at a time. Here we derive an interaction model allowing for entanglement between the electron and the cathodoluminescent photons, and suggest an approach to control the quantumness of the coupling. Our model shows that the distinguishability of the electron paths in experiments thus far suppressed quantum interference, leading to radiation distribution compatible with a point-particle electron. As an experimentally viable approach for observing the quantum coupling features we suggest: (i) the use of long-lived optical modes within micro-sphere resonators, characterized by full spatial coherence, and (ii), manipulate the electron's final state such that the measurement lacks "which-path" information. This work extends the fundamental concept of electron-photon entanglement to two dimensions, thereby solving a standing question in the coupling of basic particles. This proposal and the experiment suggested here open a path to implications in the fields of quantum physics while deepen our understanding of the fundamental principles that govern the behavior of matter and energy.

[1] R. Remez, A. Karnieli, S. Trajtenberg-Mills, N. Shapira, I. Kaminer, Y. Lereah, and A. Arie, *Phys. Rev. Lett.* 123, 60401 (2019).



P-32

## IN-SITU INTERINSIC SELF-HEALING OF LOW-TOXIC Cs<sub>2</sub>ZnX<sub>4</sub> (X= Cl, Br) METAL HALIDE NANOPARTICLES

Ben Aizenshtein<sup>1</sup>, Lioz Etgar<sup>1</sup>

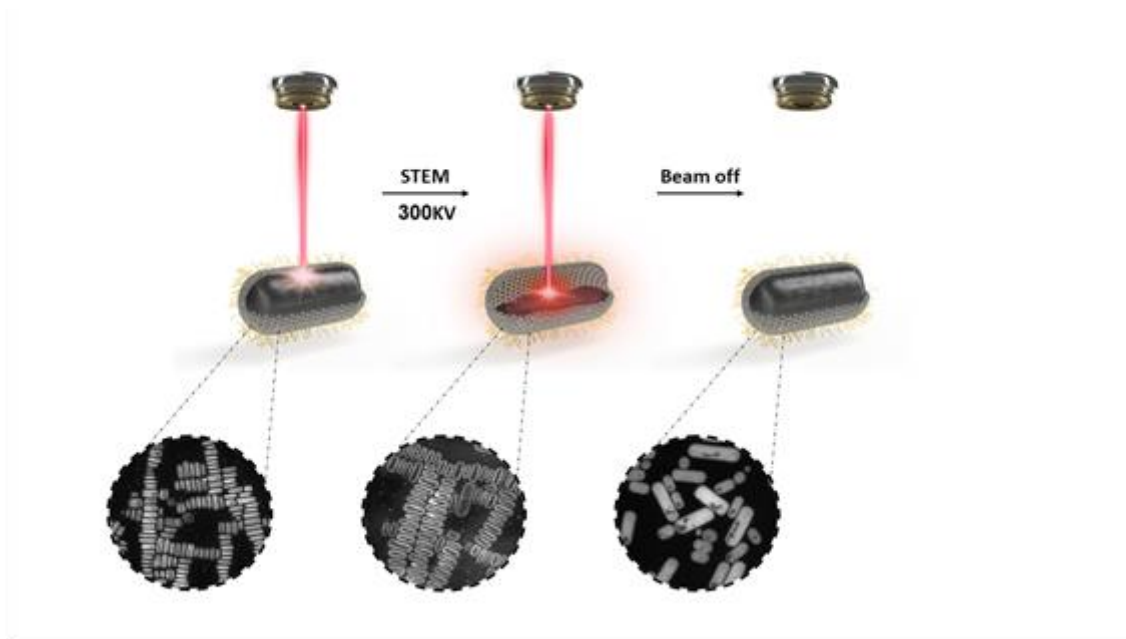
*Chemistry, Institute of Chemistry, The Center for Nanoscience and Nanotechnology,  
Casali Center for Applied Chemistry, The Hebrew University of Jerusalem, Jerusalem,  
Israel*

This study presents research on metal halide nanoparticles with the composition Cs<sub>2</sub>ZnX<sub>4</sub> (X=Cl, Br) and their unique ability for self-healing under a wide range of damages in a fast time scale of seconds without the intervention of an external additive of material. The phenomenon is divided into several parts, including the ability to create nanoshells from the original nanoparticles by an electron beam in STEM mode. The resulting nanoshells preserve the original morphology of the nanoparticles and can be obtained in different morphologies depending on the shape of the nanoparticles from which they started. These nanoshells exhibit extensive self-healing, and by closing the electron beam for a short time, it is possible to observe the complete healing of the nanoshells back to the original complete intact particles. The research also revealed another form of self-healing that manifests as dynamic and continuous self-healing where damage created in the particle in the TEM mode by the beam moves from side to side within the frame of the particle, while the areas where the damage occurred crystallize back to the original phase, structure, and composition of the particle before the damage.

We used EDS and FFT analyzes to prove that after healing, the particles return to the original structure and phase like the particles before the creation of the nanoshells. High-resolution images taken as well as EDS analyzes show that in all the different states of damage, there remains a thin crystalline layer that remains as a shell around the entire particle both in the state of local damage by the TEM and in the state of the nanoshells formed in the STEM. As a result of the electron beam hitting the particles, many inelastic interactions are created, which create local heat that stimulates atomic vibrations in the material resulting in the displacement of atoms and their diffusion within the particle. The mobilized atomic fraction inside the particle is kept throughout all the state of damage inside the particle and cannot come out because of the thin crystalline layer that remains as a container and shell that keeps the damaged material inside.

We conducted an extensive and comprehensive research in different irradiation conditions, including variation of the dose and the acceleration voltage (80,200,300 KV) to examine the effect of different irradiation intensities on the damage created and the healing processes prevented. For each defined irradiation condition, we took high-resolution videos from which we extracted trends and analytical values such as the damage growth rate for a given acceleration voltage and dose, the healing velocity, and linear adjustments between the size of the damage and the irradiation time.

In order to support the theory and make sure that the damage and healing processes are not created only as a result of an electron beam, the researchers carried out a unique experiment that included the use of an in-situ TEM heating stage holder that allows the particles to be heated while they are being eluted in EM. Minimizing the beam to a necessary minimum made it possible to isolate the effect of heating in the 50-250 °C range and to observe damage and heating processes that are identical to those observed by the electron beam.



This work concludes that these nanoparticles, which exhibit extensive healing capabilities at the atomic level, can be used for a wide variety of optoelectronic applications that require stability and healing capabilities over time.

**P-33**

## **MODULATION OF BIOGENIC CRYSTAL MORPHOGENESIS IS ACHIEVED THROUGH TRANSITION FROM REACTION-LIMITED TO TRANSPORT-LIMITED GROWTH**

**Emanuel Avrahami<sup>1</sup>**

*Department of Plant and Environmental Sciences, Weizmann Institute of Science,  
Rehovot, Israel*

Biogenic crystals exhibit a wide range of intricate morphologies that are formed with precision that is unmatched by synthetic means. Coccoliths, which are calcite multi-crystal arrays created by unicellular marine algae, form complex shapes using only stable rhombohedral facets. However, it is currently unclear how through seemingly simple crystallography species-specific architectures are constructed. To investigate this, we utilized various advanced electron microscopy techniques to observe crystal growth both in and out of the cellular environment. Our findings suggest that crystal growth can switch between space-filling and branched growth, similar to forming of snowflakes, albeit in a reproducible manner. During this process, the crystals elongate via their stable crystallographic facets and corners, but the final shape is determined by growth arrest due to transport limitation. Directional membrane-mediated fluxes are believed to control this process, regulating the switch between reaction-limited and transport-limited growth regimes. This study demonstrates how precise control over crystal morphology can be achieved by coupling crystallographic growth with a well-controlled environment.



P-34

## SPATIALLY CONTROLLED ATOMIC LAYER DEPOSITION WITHIN POLYMER TEMPLATES FOR MULTI-MATERIAL NANORODS AND NANOWIRES FABRICATION

Rotem Azoulay<sup>1</sup>, Tamar Segal Peretz<sup>1</sup>

*Chemical Engineering, Technion-Israel Institute of Technology, Haifa, Israel*

Today's nanofabrication techniques require multistep and costly processes in order to fabricate complex, multi-materials nanostructures. Performing atomic layer deposition (ALD) within polymeric templates can offer a simple solution for nanostructure fabrication. In this process, named sequential infiltration synthesis (SIS), high partial pressures and long exposures times lead to inorganic materials growth within polymers. Sequential polymer removal results in polymer-templated inorganic nanostructure. While SIS shows great potential in fabricating large variety of structures, it is currently limited to a single material growth process.

In this research, we demonstrated, for the first time, multi-material SIS process with control over the spatial location of each material and fabricate heterostructure nanorods and nanowires. We studied SIS within self-assembled block copolymer (BCP) films and electrospun polymer fibers and developed multi-material SIS, where two metal oxides are grown together in a single process, with precise control over their location within the polymer template. We used cylinder forming poly (styrene-block-methyl methacrylate) (PS-b-PMMA) films and electrospun PMMA as the polymeric template and DEZ (diethyl zinc), TMA (trimethyl aluminum) as the organometallic precursors. We achieved control over the growth location of each metal oxide by tuning the organometallic precursors diffusion time, forming heterostructures after polymer removal. A short exposure of the first precursor resulted in a limited growth only at the outer part of the polymer, while a long exposure of the second precursor enabled it to reach the full depth of the polymer besides the section which was already occupied by the first precursor. An exposure to water completed the cycle. We demonstrated this process on BCP films to achieve AlO<sub>x</sub>-ZnO nanorods arrays, and on polymer fibers to achieve AlO<sub>x</sub>-ZnO fibers. We performed structural characterization using scanning and transmission electron microscopy (SEM and TEM, respectively) to characterize the nanowires and nanorods as well as three-dimensional characterization scanning TEM (STEM) tomography and energy-dispersive X-ray spectroscopy (EDS) STEM tomography in order to probe the structure and the chemical composition in 3D. This research opens new pathways for multi-materials nano scale structure fabrication through ALD-based growth within polymers.



P-35

## PROBING MAGNETIC PHASE TRANSITIONS VIA SPIN TORQUE DRIVEN SKYRMION RESONANCE

Nirel Bernstein<sup>1</sup>, Benjamin Assouline<sup>1</sup>, Hang Li<sup>2</sup>, Igor Rozhansky<sup>1</sup>, Wenhong Wang<sup>2</sup>,  
Amir Capua<sup>1</sup>

<sup>1</sup>*Applied Physics, The Hebrew University of Jerusalem, Jerusalem, Israel*

<sup>2</sup>*Beijing National Laboratory for Condensed Matter Physics, Chinese Academy of Sciences, Beijing, China*

Magnetic Skyrmions are attractive for ultra-dense data storage applications such as the racetrack memory (RM) [1-3]. Recently, frustration in ferromagnetic (FM) crystals was predicted of being capable of providing the topological protection of the Skyrmion [4] without relying on the DMI and the effect was immediately discovered in Fe<sub>3</sub>Sn<sub>2</sub> bulk crystals [5,6]. Surprisingly, these Skyrmions survive even at room temperature and are controllable by electrical current. These advances illustrate the exceptional technological potential of the Fe<sub>3</sub>Sn<sub>2</sub> system. In this work, we study the dynamics of a bulk Fe<sub>3</sub>Sn<sub>2</sub> crystal through an optically probed spin torque driven ferromagnetic resonance (OSTFMR) technique. We excite the magnetic system by passing RF current through the crystal where the charge current converts into spin-polarized current through the spin Hall effect. From the dynamical response we identify the rotational (clock-wise or counter-clock-wise) and the translational (breathing) modes and reconstruct the phase transitions of the magnetic skyrmion texture. Using this technique, we follow the evolution of the two modes as a function of the externally applied magnetic field and map the magnetic phase transitions of the Fe<sub>3</sub>Sn<sub>2</sub> crystal. A complementary numerical micromagnetic simulations confirms our results.

### References

- [1] Y. Zhang, J. Železný, Y. Sun, J. van den Brink, and B. Yan, "**Spin Hall effect emerging from a noncollinear magnetic lattice without spin-orbit coupling**", *New Journal of Physics* **20**, 073028 (2018).
- [2] N. Nagaosa, "**Emergent electromagnetism in condensed matter**", *Proceedings of the Japan Academy, Series B* **95**, 278 (2019).
- [3] Y. He, S. Schneider, T. Helm, J. Gayles, D. Wolf, I. Soldatov, H. Borrmann, W. Schnelle, R. Schaefer, G. H. Fecher, B. Rellinghaus, and C. Felser, "**Topological Hall effect arising from the mesoscopic and microscopic non-coplanar magnetic structure in MnBi**", *Acta Materialia* **226**, 117619 (2022).
- [4] Z. Hou, W. Ren, B. Ding, G. Xu, Y. Wang, B. Yang, Q. Zhang, Y. Zhang, E. Liu, F. Xu, W. Wang, G. Wu, X. Zhang, B. Shen, and Z. Zhang, "**Observation of Various and Spontaneous Magnetic Skyrmionic Bubbles at Room Temperature in a Frustrated Kagome Magnet with Uniaxial Magnetic Anisotropy**", *Advanced Materials* **29**, 1701144 (2017).
- [5] Z. Hou, Q. Zhang, X. Zhang, G. Xu, J. Xia, B. Ding, H. Li, S. Zhang, N. M. Batra, P. M. F. J. Costa, E. Liu, G. Wu, M. Ezawa, X. Liu, Y. Zhou, X. Zhang, and W. Wang, "**Current-Induced Helicity Reversal of a Single Skyrmionic Bubble Chain in a Nanostructured Frustrated Magnet**", *Advanced Materials* **32**, 1904815 (2020).
- [6] X. Z. Yu, Y. Onose, N. Kanazawa, J. H. Park, J. H. Han, Y. Matsui, N. Nagaosa, and Y. Tokura, "**Real-space observation of a two-dimensional skyrmion crystal**", *Nature* **465**, 901 (2010).



P-36

## EXPLORING SURFACE PHENOMENA WITH TEM AND STEM

Roei Broneschter<sup>1</sup>, Yaron Kauffmann<sup>1</sup>, Klaus Van Benthem<sup>2</sup>, Wayne D. Kaplan<sup>1</sup>

<sup>1</sup>*Material Science and engineering, Technion, Haifa, Israel*

<sup>2</sup>*Material Science and Engineering, University of California, Davis, California, USA*

The surfaces of a material are planar defects with excess energy and the 2-D structure may differ from that of the bulk. Surface conducting materials can be characterized by scanning tunneling microscopy (STM) which is challenging or impossible for insulators such as most ceramic materials. To characterize ceramic surfaces, electron microscopy in a direction parallel to the surface can be used.

In this work, the atomic structure of the thermally annealed {111} surface of yttria stabilized zirconia (YSZ) was characterized by three different electron microscopy techniques implemented together. Both high resolution transmission electron microscopy (HRTEM) and scanning transmission electron microscopy (STEM) micrographs of the same region were acquired and subsequently analyzed to determine the atomic structure of the {111} surface and a reconstructed {101} surface of YSZ.

In STEM mode, micrographs of the sample were acquired using both high angle annular dark field (HAADF) and integrated differential phase contrast (iDPC) techniques. iDPC complements HAADF imaging by providing information on the position of light atoms, in this case oxygen anions. In HRTEM mode, micrographs were acquired through focal series image acquisition to ensure imaging conditions with a negative spherical aberration coefficient (Cs). Multislice image simulations and automatic matching software were used to determine objective lens defocus and relative sample thickness. This approach allows for an assessment of the accuracy of the surface characterization by TEM. The combined TEM and STEM data provided information on the 2-D structure of the {101} and {111} surfaces of YSZ.

**P-37**

## ADVANCED TOOLS FOR DISCRIMINATING PHASES WITH SIMILAR CRYSTAL STRUCTURE BY EBSD

Keith Dicks<sup>1</sup>, Michael Hjelmstad<sup>2</sup>, Pat Trimby<sup>1</sup>, Klaus Mehnert<sup>3</sup>, Aimo Winkelmann<sup>3</sup>

<sup>1</sup>*Applications, Oxford Instruments NanoAnalysis, High Wycombe, Buckinghamshire  
HP12 3SE, UK*

<sup>2</sup>*Applications, Oxford Instruments America Inc., Pleasanton, California, USA*

<sup>3</sup>*Development, ST Development GmbH, Paderborn, Germany*

Electron Back Scatter Diffraction (EBSD) is a very effective technique for discriminating between phases with different crystallographic characteristics, but is less sensitive to the subtle changes in diffraction patterns from phases with similar structures. For example, EBSD can easily separate ferrite (body centered cubic Fe, space group 229) from austenite (face centered cubic Fe, space group 225) but will struggle to separate Cu from Ni (both face centered cubic, space group 225).

The use of compositional information from energy dispersive X-ray spectrometry (EDS) can be used to assist phase discrimination. However, the X-ray signal typically comes from a much larger source volume than the EBSD pattern, making effective discrimination between small features (e.g. 5  $\mu\text{m}$ ) and across phase boundaries very challenging. In addition, some EBSD systems are not equipped with an integrated EDS capability, or there may exist geometrical limitations that prevent effective combined EBSD and EDS analyses.

Here we highlight two developments that enable more effective discrimination between phases with similar crystal structures, by EBSD alone.

### 1. Using Kikuchi band widths

Firstly, the width of individual Kikuchi bands can be used to differentiate between structures that have different sized unit cells. We outline an iterative approach that, when activated for selected phases, determines accurately the Kikuchi band widths and then applies a voting scheme to select the best fitting structure. This approach is fast (with little impact on the maximum analysis speed) and is very effective on structures that have significant (e.g. 10%) differences between their respective unit cell dimensions.

### 2. Pattern Matching

The second approach is to use newly developed pattern matching techniques. Here, the experimental EBSD pattern is indexed using standard Hough-based techniques, but the pattern is saved and is subsequently compared to simulated patterns for candidate phases using the previously determined crystallographic orientation. The phase that gives the highest cross correlation coefficient between the experimental and simulated patterns is then selected for each point. This approach allows for discrimination between structures with very similar unit cell dimensions. For both approaches, we will examine the limits of the respective techniques to separate close structures, and we will investigate the role of the EBSD pattern resolution and quality, providing examples from a range of different application fields.



P-38

## CHIRAL GUIDED GROWTH OF CRYSTALS-ON-CRYSTALS: PREDICTABLE MORPHOLOGIES WITH LOCAL FUNCTIONALIZATION

Ofir Eisenberg<sup>1</sup>, Qiang Wen<sup>1</sup>, Maria Chiara di Gregorio<sup>1</sup>, Linda J. W. Shimon<sup>2</sup>, Lothar Houben<sup>2</sup>, Ifat Kaplan-Ashiri<sup>2</sup>, Tali Dadosh<sup>2</sup>, Yoseph Addadi<sup>3</sup>, Michal Lahav<sup>1</sup>, Milko E. van der Boom<sup>1</sup>

<sup>1</sup>*Molecular Chemistry and Materials Science, Weizmann Institute of Science, Rehovot, Israel*

<sup>2</sup>*Chemical Research Support, Weizmann Institute of Science, Rehovot, Israel*

<sup>3</sup>*Life Science Core Facilities, Weizmann Institute of Science, Rehovot, Israel*

Metal-organic frameworks (MOFs) are a promising class of porous, crystalline materials with diverse potential applications. Their properties depend on their structures, including both their compositions and architectures. The intensive research of MOFs has led to an emerging family of hybrid crystals constructed by the conjugation of two or more different MOF units. Such hybrid crystals mainly consist of a core-shell structure, in which a guest MOFs is grown on a pre-synthesized host MOF, isotropically. We designed a unique co-MOF by combining two known crystal structures resulting in a dumbbell-shaped morphology. The dumbbell “weights” have been formed by epitaxial growth on the bases of the dumbbell’s “bar”, due to a common (001) facet. These unique crystals maintain their original morphologies and crystal structures in the co-MOF and their chiral nanosized channels are perfectly aligned along their long axis. Moreover, single crystal X-Ray analysis and modelling confirmed that there is chirality transfer from the “bar” to the “weights”. The two crystal structures have channel walls with different chemical properties. We were able to utilize this difference and selectively confine different chromophores to the “bar” and “weight” regions resulting in selective optical functionalization of these micro-scale objects.



P-39

## IN-SITU AND EX-SITU INVESTIGATION OF PHASE TRANSFORMATIONS IN THE $\text{Fe}_4\text{Co}_{2.1}\text{Ni}_{2.1}\text{Cr}_{0.8}\text{Al}_{0.8}\text{Ti}_{0.2}$ HIGH ENTROPY ALLOY

Ron Fishov<sup>1</sup>, Guy Hillel<sup>1</sup>, Susanna Syniakina<sup>1</sup>, Yaniv Zriker<sup>2</sup>, Ofer Omesi<sup>2</sup>, Yoav Snir<sup>2</sup>,  
Louisa Meshi<sup>1</sup>

<sup>1</sup>*Department of Materials Engineering, Ben Gurion University of the Negev, Beer Sheva, Israel*

<sup>2</sup>*Materials science and engineering, Nuclear Research Center Negev, Beer Sheva, Israel*

Fe-Ni-Co-Cr-Al-Ti system is part of the wide family of Face-Centered Cubic (FCC)-based High Entropy Alloys (HEAs) with outstanding mechanical properties [1-2, and references therein]. Although FCC-HEAs exhibit high ductility, their strength is not sufficient for many industrial applications. One of the possible ways to enhance this property is by precipitation-strengthening mechanism. In this system, either precipitates of the  $\text{Ni}_3(\text{Al,Ti})$ -type ( $\gamma'$ ) with  $L1_2$  structure (ordered FCC) or NiAl-type B2 (ordered Body Centered Cubic (BCC)) phase can form as a function of thermo-mechanical history and composition. One of the most important factors influencing the precipitation sequence and type is total (Al+Ti) amount and/or specific Al/Ti ratio [2-5]. Depending on the precipitates` type and their size - mechanical properties of the alloys vary dramatically. Therefore, precise characterization of the precipitates which form during the phase transformation and precipitation sequence is of primarily importance for future industrial implementation.

In the Fe-Ni-Co-Cr-Al-Ti system, most researchers have focused on Ni-rich alloys [4]. In our work we have concentrated on Fe-rich composition, namely  $\text{Fe}_4\text{Co}_{2.1}\text{Ni}_{2.1}\text{Cr}_{0.8}\text{Al}_{0.8}\text{Ti}_{0.2}$ . Following recrystallization and cold rolling, ex-situ heat treatments at 600-800°C (for four hours) were performed studying the phase transitions and microstructural changes. Characterization was carried out using Scanning Electron Microscopy (SEM) and Transmission Electron Microscopy (TEM). Precipitation sequence was studied by in-situ TEM, heating the sample up to 900°C. The effect of phase transformations on mechanical properties was evaluated by hardness test. Upon aging, coherent  $L1_2$ - $\text{Ni}_3(\text{Al,Ti})$  - type particles have formed. As a function of temperature, they dissolved and instead B2-NiAl - type flake-like particles precipitated. Although both precipitates` types could contribute to strengthening, the  $L1_2$  particles influenced the hardness more effectively probably due to their smaller size and more coherent interfaces with the matrix (as compared to B2).

References:

- [1] Salishchev G.A., et al. "Effect of Mn and V on structure and mechanical properties of HEAs based on CoCrFeNi system" J. Alloys Compd, 591 (2014): 11-21.
- [2] Xu, Y., et al. "Relationship between Ti/Al ratio and stress-rupture properties in nickel-based superalloy." Mat. Sci. Eng. A 544 (2012): 48-53.
- [3] Joseph, J., et al. "Computational design of thermally stable and precipitation-hardened Al-Co-Cr-Fe-Ni-Ti HEAs." J. Alloys Compd 888 (2021): 161496.
- [4] Li, Z., et al. "Improving mechanical properties of an FCC HEA by  $\gamma'$  and B2 precipitates strengthening." Mat. Char. 159 (2020): 109989.
- [5] Huang, S. "The chemical ordering and elasticity in  $\text{FeCoNiAl}_{1-x}\text{Ti}_x$  HEAs." Scr. Mater. 168 (2019): 5-9.



P-40

## THE EFFECT OF ZN-CONTAINING MICROCALCIFICATIONS ON THE MALIGNANCY OF THYROID NODULES

Lotem Gotnayer<sup>1</sup>, Dina Aranovich<sup>1</sup>, Merav Fraenkel<sup>2,3</sup>, Uri Yoel<sup>2,3</sup>, Netta Vidavsky<sup>1,4</sup>

<sup>1</sup>*Department of Chemical Engineering, Ben-Gurion University of the Negev, Beer Sheva, Israel*

<sup>2</sup>*Faculty of Health Sciences, Ben-Gurion University of the Negev, Beer Sheva, Israel*

<sup>3</sup>*Endocrinology, Soroka University Medical Center, Beer Sheva, Israel*

<sup>4</sup>*Ilse Katz Institute for Nanoscale Science & Technology, Ben-Gurion University of the Negev, Beer Sheva, Israel*

Thyroid nodules (TNs) are common neck ultrasonography (US) findings, yet only 5-10% of these nodules harbor thyroid cancer. Fine needle aspiration for cytology (FNAC) is performed when US characteristics indicate an intermediate or high suspicion of TN malignancy. Up to 30% of FNAC results can be indeterminate, necessitating repeated tests, expensive molecular testing, or diagnostic partial thyroid resection. TN diagnostic algorithms should thus be further refined without exposing patients to additional invasive procedures. As calcifications detected during thyroid US are considered a high-risk feature for malignancy, we used the remaining material following routine thyroid FNAC to isolate microcalcifications (MCs). Our subsequent analysis of these MCs revealed differences between benign and malignant TN regarding their elemental composition, morphology, and crystal phases. Specifically, we use SEM-EDS and FTIR to show that thyroid MCs are calcium phosphate crystals containing varying magnesium, sodium, iron, and zinc levels. The MCs obtained from malignant TNs were composed of sub-micrometer spherical particles, while those from benign TNs were faceted. Zinc was largely absent from MCs from benign TNs, whereas samples from malignant TNs contained zinc (7% vs. 91%, respectively, p0.001). Thus, zinc in MCs obtained from TN during routine FNAC can serve as a biomarker of TN malignancy.

P-41

## SYSTEMATIC STUDY OF THE ANTI-PHASE BOUNDARIES FORMATION IN B2 $\text{Fe}_x\text{Al}_{1-x}$ ALLOYS USING *ex-situ* AND *in-situ* TRANSMISSION ELECTRON MICROSCOPY

Guy Hillel<sup>1</sup>, Itzhak Edry<sup>2</sup>, Malki Pinkas<sup>2</sup>, Louisa Meshi<sup>1</sup>

<sup>1</sup>*Department of Materials Engineering, Ben-Gurion University of the Negev, Beer-Sheva, Israel*

<sup>2</sup>*NRCN, Beer-Sheva, Israel*

Anti-Phase Boundary (APB) is a planar crystalline defect which might appear in ordered superlattice structures, such as the B2 (ordered Body Centered Cubic (BCC)). APBs are classified into two types, based on their morphology and the way they are formed [1]: thermal (appearing due to order/disorder transformation) and shear (formed in B2 by the dissociation of super-dislocations into partials separated by APB). It was proposed that increase in density of the APBs in B2 might improve its poor ductility [2]. Having this idea in mind, major goal of this research was to engineer the material so that APBs density will be substantially high, improving the ductility without reduction in strength. Current work presents first milestone towards achieving this goal. Here, understanding of the APB formation mechanism in B2 structure was attained. To perform this task –  $\text{Fe}_x\text{Al}_{1-x}$  B2 alloys were chosen following [3] as a model of B2 matrix of the AlCoCrFeNi High Entropy Alloys (which have a potential to become new structural materials). These alloys exhibited improved properties following the appearance of APBs [4,5]. In the past,  $\text{Fe}_x\text{Al}_{1-x}$  B2 alloys were studied with regard APBs formation experimentally [6,7] and using computational methods [8] presenting nonsystematic, contradicting results.

In current research, systematic study was performed on a series of  $\text{Fe}_x\text{Al}_{1-x}$  ( $x = 0.5-0.73$ ) alloys which were cast and investigated using transmission electron microscopy (TEM). As can be seen in Figure 1a<sub>1</sub>-a<sub>5</sub>, no APBs have formed in alloys with  $x=0.5-0.67$ . Instead, varying density of dislocations was detected. Applying 2 beam conditions and trace analyses [9], two different slip systems – (001)[100] and (011)[111] were revealed. Identification of a presence of type dislocations is of high importance, since as stated earlier, they can dissociate into partials which bound APBs. APBs themselves were found only in samples having  $x \geq 0.68$ . Increasing the Fe content, over 68 at %Fe and up to 70 at %Fe elevated the density of the APBs. Yet, these boundaries have not formed cells of domains but appeared as ribbons. Furthermore, in these samples along with an increase in the number of APBs, small highly dense DO<sub>3</sub> phase (identified by means of electron diffraction) has formed [10]. Increasing the content of Fe to 73 at % has altered the APBs morphology to more orthodox cellular structure. The density of the APBs has dramatically increased, and they were commonly found in the B2 grains. Amount of DO<sub>3</sub> phase has increased with the Fe content. The presence of DO<sub>3</sub> raises a question of “an egg and the chicken”: the APBs are formed in B2 regardless DO<sub>3</sub> or formation of APBs is correlated to the B2-DO<sub>3</sub> phase transformation. Numerous quenching from high temperature has not eliminated the DO<sub>3</sub> formation. To evaluate the necessity of DO<sub>3</sub> for APB formation, *in-situ* heating in TEM was done.

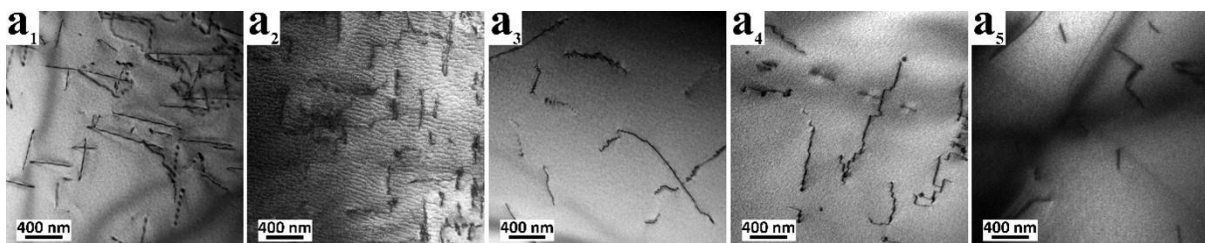




Figure 1: TEM images of the (a<sub>1</sub>) 50at%Fe, (a<sub>2</sub>) 55at%Fe, (a<sub>3</sub>) 59at%Fe, (a<sub>4</sub>) 62at%Fe, (a<sub>5</sub>) 64at%Fe samples

For this purpose, 70 at% Fe sample was heated *in-situ* in TEM from room temperature (RT) to temperature above the B2-DO<sub>3</sub> transition to a single-phase B2, i.e., above 1073K (the hold was 30 min) and then cooled down (at rate of 1°C/ms) back to RT. Figure 2a<sub>1</sub> shows APBs in the B2 matrix at RT, prior heating. The changes that accrued during the *in-situ* heating process are presented in Fig. 2a<sub>2</sub>-a<sub>5</sub>. DO<sub>3</sub> phase was found to be stable up to ~1063K, and no change in morphology of the APBs was observed until that point, see Fig. 2a<sub>2</sub>. At 1073K, decomposition of the DO<sub>3</sub> phase was documented by electron diffraction. At this temperature, growth of the existing at RT APB and formation of additional APBs was observed, see Fig. 2a<sub>3</sub>-a<sub>4</sub>. Furthermore, APBs maintained their cellular morphology during cooling, as shown in Fig. 2a<sub>5</sub>. Following this experiment, it can be concluded that APBs formation does not relate to the B2-DO<sub>3</sub> phase transition. Furthermore, taking into account that the value at which APBs have started to form was  $x=0.68$ , we estimated, using [11], the long-range order parameter at this composition as 0.53. Knowing this value – other means to achieve required degree of disorder can be proposed (such as alloying) to engineer the material. Density Functional Theory calculations performed by group of Prof. Fuks yielded results which fully agree with our observations.

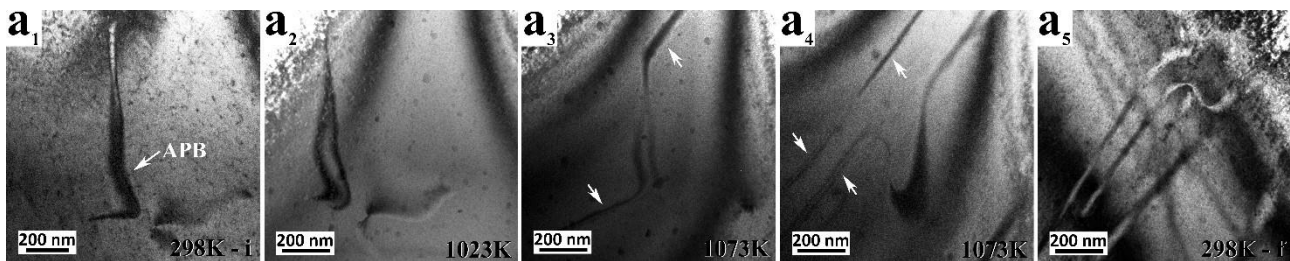


Figure 2: *in-situ* heating of the 70% at Fe sample from (a<sub>1</sub>) initial room temperature (RT) to (a<sub>2</sub>) 1023K. Image prior the decomposition of DO<sub>3</sub> phase. (a<sub>3</sub>) 1073K. APBs grow in the B2 phase, as marked by arrows. (a<sub>4</sub>) After a hold at 1073K. Density of the APBs increased. (a<sub>5</sub>) Final RT state.

- [1] Rong TS., et al. Intermetallics, 9(6) (2001)499.
- [2] Inoue A., et al. Metall Mater Trans A. 14(7) (1983)1367.
- [3] Vidal D., et al. Intermetallics, 141 (2022)107434.
- [4] Linden Y., et al. Scripta Mater. 139, (2017)49.
- [5] Meshi L., et al. Mater. Character. 148 (2019)171.
- [6] Prakash U., et al. Philosophical Magazine A. 64(4) (1991)
- [7] Kattner U.R., et al. ASM International. (1990)147.
- [8] Khachaturyan A.G. Soviet Physics JETP. 36(4) (1973).
- [9] Edington, J. W. et al. Macmillan International Higher Education. (1977) 118-130.
- [10] Popiel, E., et al. J. less-common met. 146 (1989) 127-135.
- [11] Khachaturian, A. G. Prog. Mater. Sci. 22, (1978) 1-150.

**P-42****TWO-STEP SINTERING OF Mg-DOPED ALUMINA****Asaf Kazmirsky<sup>1</sup>, Rachel Marder<sup>1</sup>, Wayne D. Kaplan<sup>1</sup>***Department of Materials Science and Engineering, Technion - Israel Institute of  
Technology, Haifa, Israel*

This work verifies the applicability of two-step sintering as a means of suppressing grain growth while preparing high-density alumina samples made by uniaxially pressing RTP (ready-to-press) powder prior to CIP (cold isostatic pressing). The first step of the process should be short at a relatively high temperature of 1500°C in order to achieve a high initial densification without significant grain growth. The second step is carried out at a lower temperature of 1250°C over an extended period of time to facilitate further densification with little to no additional grain growth. The density of the sintered samples was measured by Archimedes' method. The microstructure was observed using secondary electron scanning electron microscopy of fracture surfaces and polished cross-sections. Alumina with a relative (to the theoretical) density of 98.1% and a mean grain size of  $1.4 \pm 0.7 \mu\text{m}$  was prepared by two-step sintering. A conventional sintering process at 1500°C for 2 hours yielded a higher relative density of 99.6% and a mean grain size of  $3.0 \pm 1.5 \mu\text{m}$ .



P-43

## MICROSCOPE-INTEGRATED SPECTROSCOPIC ELLIPSOMETER FOR FAST AND IN-SITU OPTICAL INVESTIGATION OF MICRON-SCALE MATERIALS AND STRUCTURES

**Ralfy Kenaz**<sup>1</sup>, Saptarshi Ghosh<sup>1</sup>, Pradheesh Ramachandran<sup>1</sup>, Kenji Watanabe<sup>2</sup>, Takashi Taniguchi<sup>3</sup>, Hadar Steinberg<sup>1</sup>, Ronen Rapaport<sup>1</sup>

<sup>1</sup>*Racah Institute of Physics, The Hebrew University of Jerusalem, Jerusalem, Israel*

<sup>2</sup>*Research Center for Functional Materials, National Institute for Materials Science, Tsukuba, Japan*

<sup>3</sup>*International Center for Materials Nanoarchitectonics, National Institute for Materials Science, Tsukuba, Japan*

Spectroscopic ellipsometry (SE) is a widely used optical technique in both industry and research for determining the optical properties and thicknesses of thin films. The technique is based on analyzing the change in light polarization upon oblique-angle reflection from a sample. SE is well-established, non-invasive, highly accurate and sensitive; for example, capable of measuring the thicknesses of thin films with atomic-level precision. However, the effective use of SE on micro-structures is limited by low lateral resolution down to tens-of-microns only, or very slow data acquisition. As micron-scale structures are crucial and abundant in today's technology and research, these limitations significantly hinder the utilization of the powerful SE technique for future technologies.

In this work, we introduce our patented [1] Spectroscopic Micro-Ellipsometer (SME), which is a microscope-integrated ellipsometer with a lateral resolution down to 2 microns, capable of recording spectrally resolved ellipsometric data simultaneously at multiple angles of incidence in a single measurement of a few seconds, *by utilizing Fourier-plane imaging for ellipsometry* [2]. This makes SME the fastest in ellipsometric data acquisition, three orders-of-magnitude faster than the state-of-the-art high-resolution commercial ellipsometers. Most importantly, the SME can be easily integrated into generic optical microscopes as an add-on unit without disturbing their capabilities (Figs. 1a and 1b), by addition of a few standard components. *This allows transforming an imaging microscope into a sophisticated optical characterization instrument.*

In order to address a current scientific challenge in material sciences and demonstrate the unique combined accuracy and high lateral resolution of the SME, we have shown characterization of the optical properties and thicknesses of exfoliated two-dimensional material flakes which only have a few microns of lateral dimensions. As performance of van der Waals heterostructure devices is governed by the nanoscale thicknesses and homogeneity of their constituent mono- to few-layer flakes, accurate mapping of these properties with high lateral resolution becomes imperative. The SME can perform angstrom-level accurate and consistent thickness mapping on mono-, bi- and trilayers of graphene, hexagonal boron nitride (hBN) and transition metal dichalcogenide (MoS<sub>2</sub>, WS<sub>2</sub>, MoS<sub>2</sub>, WSe<sub>2</sub>) flakes [3]. Our highly sensitive system can successfully identify near-transparent monolayer hBN, a challenging proposition for other characterization tools. The optical microscope integrated ellipsometer can also map minute thickness variations over a micron-scale flake, revealing its lateral inhomogeneity (Figs. 1c-1e). *The prospect of adding standard optical elements to augment generic optical microscopes with accurate in-situ ellipsometric mapping capability presents new opportunities for investigation of exfoliated 2D materials, as well as many other micron-scale systems such as meta-materials and biological structures which previously were not conveniently addressable by spectroscopic ellipsometry.*

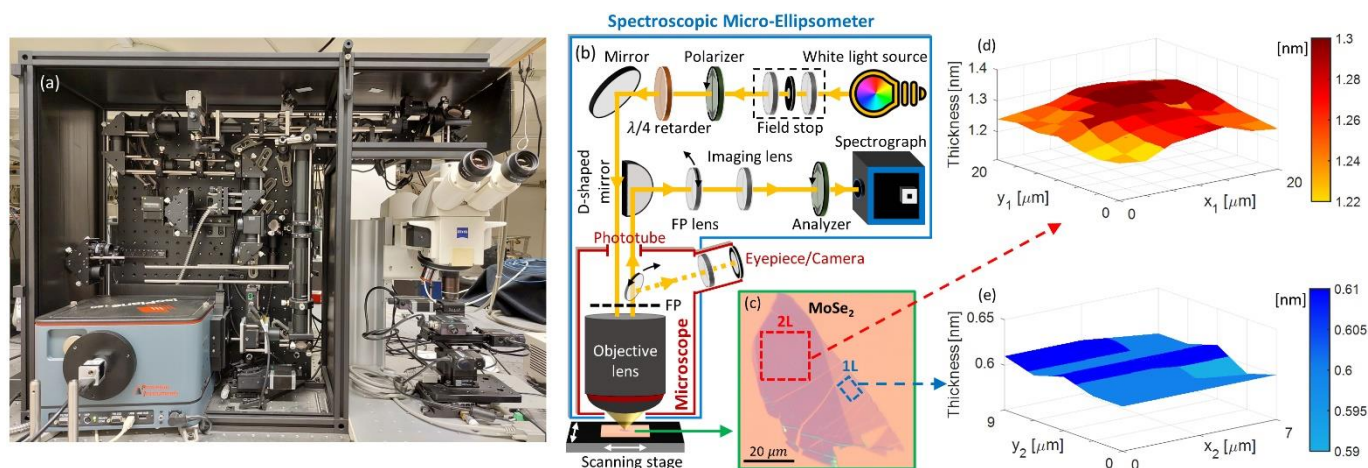


Figure 1 – (a) Current version of the Spectroscopic Micro-Ellipsometer (SME), integrated into a commercial optical microscope. (b) Schematic of the SME; FP: Fourier Plane. (c) Exfoliated MoSe<sub>2</sub> monolayer (1L) and bilayer (2L) flake with marked areas for thickness mapping by the SME. (d) Thickness map of MoSe<sub>2</sub> bilayer over an area of 20 x 20 μm<sup>2</sup>. (e) Thickness map of MoSe<sub>2</sub> monolayer over an area of 7 x 9 μm<sup>2</sup>. The SME spot size for these measurements is 5 μm.

## REFERENCES

- [1] R. Kenaz and R. Rapaport. "System and method for use in high spatial resolution ellipsometry,". US Patent No.: 11,262,293 B2, 2022.
- [2] R. Kenaz and R. Rapaport, "Mapping spectroscopic micro-ellipsometry with sub-5 microns lateral resolution and simultaneous broadband acquisition at multiple angles", Review of Scientific Instruments 94, 023908 (2023). <https://doi.org/10.1063/5.0123249>
- [3] R. Kenaz, S. Ghosh, P. Ramachandran, K. Watanabe, T. Taniguchi, H. Steinberg, and R. Rapaport. "Thickness mapping and layer number identification of exfoliated van der Waals materials by Fourier imaging micro-ellipsometry". arXiv:2211.07437, 2022. <https://doi.org/10.48550/arXiv.2211.07437>  
[Under revision in ACS Nano]



P-44

## BRILLIANT WHITENESS IN SHRIMP FROM ULTRA-THIN LAYERS OF BIREFRINGENT NANOSPHERES

Tali Lemcoff<sup>1</sup>, Lotem Alus<sup>2,3</sup>, Johannes S. Haataja<sup>4,5</sup>, Avital Wagner<sup>1</sup>, Gan Zhang<sup>1,9</sup>,  
Mariela J. Pavan<sup>6</sup>, Ventaka J. Yallapragada<sup>7</sup>, Silvia Vignolini<sup>4</sup>, Dan Oron<sup>2</sup>, Lukas  
Schertel<sup>4,8</sup>, Benjamin A. Palmer<sup>1</sup>

<sup>1</sup>*Department of Chemistry, Ben-Gurion University of the Negev, Be'er Sheva, Israel*

<sup>2</sup>*Department of Molecular Chemistry and Materials Science, Weizmann Institute of Science, Rehovot, Israel*

<sup>3</sup>*Department of Chemical and Structural Biology, Weizmann Institute of Science, Rehovot, Israel*

<sup>4</sup>*Yusuf Hamied Department of Chemistry, University of Cambridge, Cambridge, UK*

<sup>5</sup>*Department of Applied Physics, Aalto University School of Science, Espoo, Finland*

<sup>6</sup>*Ilse Katz Institute for Nanoscale Science & Technology, Ben-Gurion University of the Negev, Beer-Sheva, Israel*

<sup>7</sup>*Department of Physics, Indian Institute of Technology Kanpur, Uttar Pradesh, Kanpur, India*

<sup>8</sup>*Department of Physics, University of Fribourg, Fribourg, Switzerland*

<sup>9</sup>*Current Address: College of Chemistry and Chemical Engineering, Lanzhou University, Lanzhou, China*

White colors are produced by diffuse light propagation in disordered media. To generate whiteness, photons of all wavelengths must be scattered multiple times and lose their directional information to produce broadband, angular independent reflectance. While this is easily achieved with thick samples, it is difficult to obtain with thin layers of material. For typical nanoparticle-based scatterers, reflectance decreases above filling fractions of ~30% due to near-field coupling of adjacent scatterers. Here we show how cleaner shrimp generate one of the most efficient white colors in nature, by tuning both single particle and ensemble scattering properties(1). We used cryo-scanning electron microscopy, STEM, TEM, selected-area-electron-diffraction and Raman spectroscopy to discover the nature of the impressive white color, which provides effective signaling in an aqueous habitat. The whiteness arises from white chromatophore cells containing densely packed nanospheres composed of isoxanthopterin. The nanospheres are composed of 1-dimensionally ordered, stacked assemblies of isoxanthopterin which project radially outwards from the center of the sphere (i.e., a spherulite). Strikingly, numerical simulations reveal that extreme birefringence, which originates from the spherulitic arrangement of isoxanthopterin molecules, diminishes optical crowding effects, enabling intense scattering up to the maximal packing achievable for random spheres (~65% filling fraction). Overall, the combination of the high refractive index ( $n \approx 2.0$ ), extreme birefringence (~ 30%), and polydispersity of the nanospheres enables intense scattering from an ultra-thin layer. These results inspire the design of biologically benign replacements for artificial scatterers like titanium dioxide and highlight the importance of birefringence as a structural handle to enhance the performance of such materials.

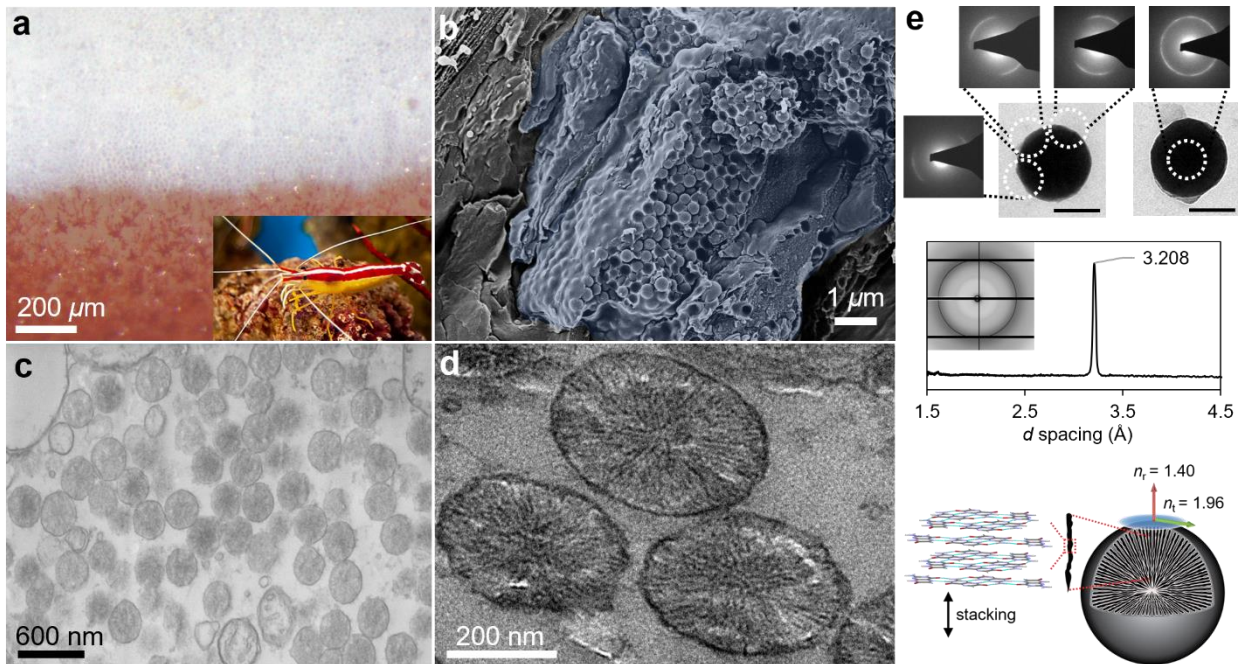


Figure 1. a) Optical image of the white stripe on the cleaner shrimp's back exhibiting the dense and dendritic white chromatophores. Insert: Image of the Pacific Cleaner Shrimp (*Lysmata amboinensis*). b) Cryo-SEM image of a white chromatophore cell under the transparent chitin cuticle. c) STEM micrograph of nanospheres within a cell in an ultrathin tissue section ( $\sim 100$  nm). d) TEM micrograph of the nanospheres in an ultrathin tissue section exhibiting the spoke-like, spherulitic structure. e) Top: TEM images and corresponding selected area electron diffraction of two particles with  $d$  spacing  $\sim 3.2$  Å. The reflection angle changes when moving along the dihedral angles of the particle indicating that the stacking axis projects away from the center of the sphere. Scale bar: 200 nm. Middle: In situ  $\mu$ -spot wide-angle X-ray scattering (WAXS) diffraction pattern from the maxilliped (obtained by radial integration of the 2D scattering pattern (inset)). Bottom: Schematic of a nanosphere showing the spherulitic arrangement of stacked isoxanthopterin molecules. Radial ( $n_r$ ) and tangential ( $n_t$ ) refractive index vectors on the nanosphere surface illustrate the birefringence produced from the spherulitic arrangement.

## References

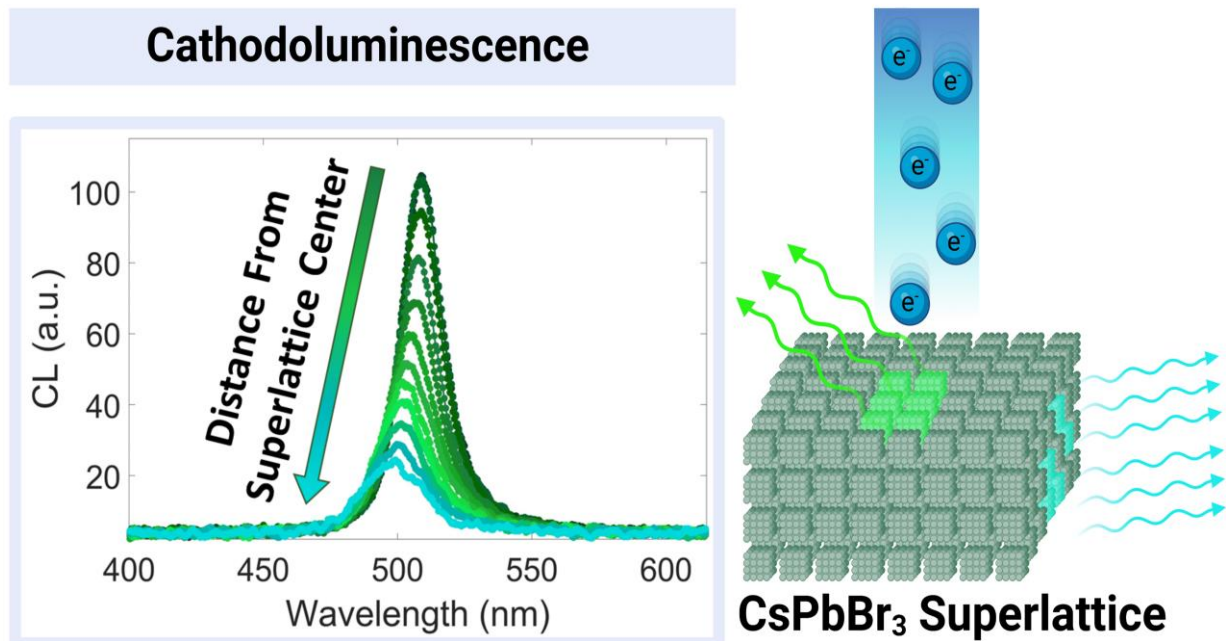
- 1) Lemcoff T., Alus L., Haataja, J.H., Wagner, A., Zhang, G., Pavan, M.J., Yallapragada, V.J., Vignolini, S., Oron, D., Schertel, L., Palmer, B.A., Brilliant whiteness in shrimp from ultra-thin layers of birefringent nanospheres. In Press. (2023)

P-45

## CATHODOLUMINESCENCE SEM OF CsPbBr<sub>3</sub> PEROVSKITE NANOCRYSTAL SUPERLATTICES

Shai Levy<sup>1</sup>, Orr Be'er<sup>1</sup>, Noam Veber<sup>1</sup>, Yehonadav Bekenstein<sup>1,2</sup><sup>1</sup>Materials Science and Engineering, Technion-Israel Institute of Technology, Haifa, Israel<sup>2</sup>Solid-State Institute, Technion-Israel Institute of Technology, Haifa, Israel

Perovskite nanocrystal superlattices (NC SLs) display optoelectronic properties which differ from individual crystals, and give rise to new ensemble collective phenomena. Structural and optical heterogeneities in the SLs lead to a reduced coupled emission, and change the collective ensemble properties. Free electrons in scanning electron microscopy (SEM) are used to probe the cathodoluminescence (CL) properties of CsPbBr<sub>3</sub> SLs with high spatial resolution. Combined CL-SEM measurements allow simultaneous characterization of structural and optical heterogeneities of the SLs. Hyperspectral CL mapping shows multipole emissive domains within a single SL. Additionally, light emission from the edges of the SLs is blue shifted by up to 65meV relative to their center. This CL shift is dependent both on the sizes of the SL and NC building blocks. Residual uniaxial compressive strains accompanying SL formation are contributors to this emission shifts.



**P-46**

## **SIZE EFFECT ON STRENGTH OF EQUILIBRATED COPPER NANOPARTICLES FABRICATED BY SOLID-STATE DEWETTING**

**Zhao Liang**<sup>1</sup>, Nishchal Thapa Magar<sup>2</sup>, Raj Koju<sup>2</sup>, Yuri Mishin<sup>2</sup>, Eugen Rabkin<sup>1</sup>

<sup>1</sup>*Department of Materials Science and Engineering, Technion-Israel Institute of  
Technology, Haifa, Israel*

<sup>2</sup>*Department of Physics and Astronomy, George Mason University, Fairfax, Virginia,  
USA*

It is now well established that mechanical properties of metal samples of nanometric dimensions are very different from those of their bulk counterparts. Strong size effect in mechanical strength has been reported for many face centered cubic (FCC) metals and alloys, yet the dislocation nucleation-controlled plasticity mechanisms are still poorly understood. In the present work, solid state dewetting technique was employed to produce defect-scarce copper nano- and microparticles of various sizes exhibiting equilibrium crystal shape. The results of in-situ microcompression tests revealed two clear size-related regimes, where large copper particles exhibit a strong size effect in strength with size exponent comparable to other FCC metals, while their smaller counterparts show weak size dependence of strength, which saturates at about 10 GPa. Our experimental results were in good quantitative agreement with the results of atomistic molecular dynamic simulations of Cu nanoparticles compression. We related the two different size effect regimes to the high probability of dislocation nucleation event at the corner of the particle facets, and increasing probability of finding crystal structure defects inside the particles with increasing particle size.

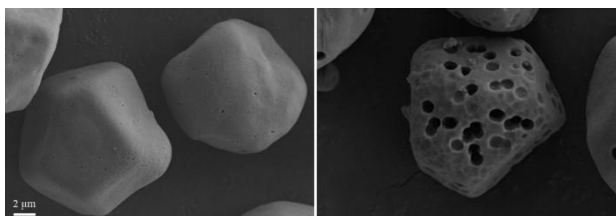
P-47

**REGULATING GRANULE STARCH HYDROLYSIS TO MAKE POROUS STARCH****Hongxiang Liu<sup>1,2</sup>**

*Faculty of Biotechnology and Food Engineering, Technion - Israel Institute of  
Technology, Haifa, Israel*  
*Biotechnology and Food Engineering Program, Guangdong Technion - Israel Institute  
of Technology, Shantou, China*

Starch is the second most abundant biological polymer, after cellulose, produced on earth. Native starch exists in the form of granules of different sizes and shapes, that depend on the botanical source. Porous starch is a modified starch that is non-toxic and economical adsorbent extensively used in food, pharmaceutical and environmental applications. It consists of abundant pores that are distributed on the granule surface and extend towards the central cavities, without changing the granular structure. Enzymolysis of raw starch granule at sub-gelatinization temperature is a good way to make porous starch. The alternating structure of amorphous and crystalline layers of starch guarantees the continuity of this hydrolysis.

In this work, we make porous starch from different botanical sources by hydrolysis with amylase. We study the structure and morphology using advanced electron microscopy methods, and additionally defined the concept of GSHU (Granule Starch Hydrolysis Units) and prove it is a useful tool to regulate double-amylase hydrolysis treated with UHP (Ultra high-pressure processing). GSHU reflects the difficulty of how granular starches are attacked by enzyme and it can be a good way to unify the degree of hydrolysis of granule starch. With UHP treatment, lower amount of enzyme (or shorter processing) is needed to reach the same porosity compared to untreated samples. The GSHU parameter can guide the selection of catalysts to achieve similar porosity.





P-48

**Cr/AlCoFeNi DIFFUSION COUPLE FOR MAPPING MICROSTRUCTURAL CHANGES****Yuval Malinker<sup>1</sup>**, Einat Nativ-Roth<sup>2</sup>, Guy Hillel<sup>1</sup>, Susanna Sinyakina<sup>1</sup>, Louisa Meshi<sup>1</sup><sup>1</sup>*Department of Materials Engineering, Ben Gurion University of the Negev, Beer Sheva, Israel*<sup>2</sup>*Ilse Katz Institute for nanoscale science and technology, Ben Gurion University of the Negev, Beer Sheva, Israel*

Novel metallurgical approach of High Entropy Alloys (HEAs) suggests using multiple elements at approximately equiatomic composition to achieve solid solutions which exhibit unique physical properties [1]. One of the most studied HEAs is AlCoCrFeNi. This system might form: Cr-Fe rich Body Centered Cubic (BCC), Al-Ni rich B2 (ordered BCC) and Fe-Co-Cr rich Face Centered Cubic (FCC) phases as a function of thermo-mechanical treatments and composition [2, for example]. To understand the effect of composition, influence of specific elements on quinary Al-Co-Cr-Fe-Ni system was studied [3-7]. It was concluded in [7] that Cr influences dramatically the microstructure and, thus, the mechanical properties of the (AlCoFeNi)<sub>1-x</sub>Cr<sub>x</sub> alloys. However, all investigations of the effect of elements on this system were performed non-linearly, i.e. by casting specific compositions. Therefore, the knowledge gathered in this way is not complete. In current research, diffusion couple approach was used to study the effect of Cr on (AlCoFeNi)<sub>1-x</sub>Cr<sub>x</sub> alloys in details. To the best of our knowledge, this approach was not used before on any HEAs. The Cr/AlCoFeNi diffusion couple was prepared using arc-melting. Microstructural study was carried out by High Resolution Scanning Electron Microscopy (HRSEM) and Transmission Electron Microscopy (TEM). Focused Ion Beam (FIB) was used to extract TEM lamellae at specific compositions. This allowed mapping the microstructure, crystallographic structures and composition of different phases forming as a function of Cr content.

## References:

- [1] Yeh, J. W., Chen, S. K., Lin, S. J., Gan, J. Y., Chin, T. S., Shun, T. T., ... & Chang, S. Y. (2004). *Advanced engineering materials*, 6(5), 299-303.
- [2] Meshi, L., Linden, Y., Munitz, A., Salhov, S., & Pinkas, M. (2019). *Materials Characterization*, 148, 171-177.
- [3] Li, C., Zhao, M., Li, J. C., & Jiang, Q. (2008). *Journal of applied physics*, 104(11), 113504.
- [4] Hillel, G., Natovitz, L., Salhov, S., Haroush, S., Pinkas, M., & Meshi, L. (2020). *Metals*, 10(10), 1275.
- [5] Jiang, H., Li, L., Wang, R., Han, K., & Wang, Q. (2021). *Acta Metallurgica Sinica (English Letters)*, 34, 1565-1573.
- [6] Wang, Y. P., Li, B. S., Ren, M. X., Yang, C., & Fu, H. Z. (2008). *Materials Science and Engineering: A*, 491(1-2), 154-158.
- [7] Shockner, R., Edry, I., Pinkas, M., & Meshi, L. (2023). *Journal of Alloys and Compounds*, 168897.



P-49

## MEASURING THE SOLUBILITY LIMIT OF DOPANTS BY FULLY STANDARDIZED WAVELENGTH DISPERSIVE SPECTROSCOPY

Rachel Marder<sup>1</sup>, Wayne D. Kaplan<sup>1</sup>

*Materials Science and Engineering, Technion- Israel Institute of Technology, Haifa, Israel*

The development and implementation of polycrystalline ceramic materials strongly depends on the ability to control the microstructure of the sintered material. Many studies have focused on the mechanism that governs and influences the evolving microstructure during densification and how such changes in the microstructure affect the properties. Specifically in alumina, the influence of impurities and dopants has been extensively studied. Changes in the grain boundary mobility were observed at impurity levels below the solubility limit, without the presence of a secondary phase or liquid phase, due to solute-drag or solute-acceleration caused by an adsorbate. To understand the role of key dopants in alumina and their influence on the microstructure, it is important to know their solubility.

In our group, a technique was developed to measure the solubility limit of dopants in a ceramic matrix using fully standardized wavelength dispersive spectroscopy (WDS). Due to the low concentration of many key dopants in fully saturated alumina, WDS is an ideal technique to measure the solubility limit, which can be as low as a few ppms. The solubility limits of key dopants, such as Mg, Ca, Si, Fe, and C in alumina at 1600°C were measured by WDS using fully saturated alumina samples quenched from 1600°C [1-6]. The technique will be presented and the results will be discussed.

- [1] L. Miller, A. Avishai, W. D. Kaplan, Solubility Limit of MgO in Al<sub>2</sub>O<sub>3</sub> at 1600°C, Journal of the American Ceramic Society, 89[1]:350-353, 2006.
- [2] R. Akiva, A. Berner, W. D. Kaplan, The Solubility Limit of CaO in  $\alpha$ -Alumina at 1600°C, Journal of the American Ceramic Society, 96[10]:3258-3264, 2013
- [3] R. Moshe, A. Berner, W.D. Kaplan, The solubility limit of SiO<sub>2</sub> in  $\alpha$ -alumina at 1600°C, Scripta Materialia, 86:40-43, 2014.
- [4] R. Moshe and W.D. Kaplan, The combined influence of Mg and Ca on microstructural evolution of alumina, Journal of the American Ceramic Society 102[8]: 4882-4887, 2019.
- [5] P. Ghosh, R. Marder, A. Berner, W.D. Kaplan, The influence of temperature on the solubility limit of Ca in alumina, Journal of the European Ceramic Society, 40[15]:5767-72, 2020.
- [6] L. Cohen, P. Gosh, A. Berner, R. Marder, W.D. Kaplan, The solubility limit of carbon in alumina at 1600°C, Microscopy and Microanalysis 29[1]:314–325, 2023.



P-50

## CALCIUM AND ELONGATED GRAINS IN ALUMINA

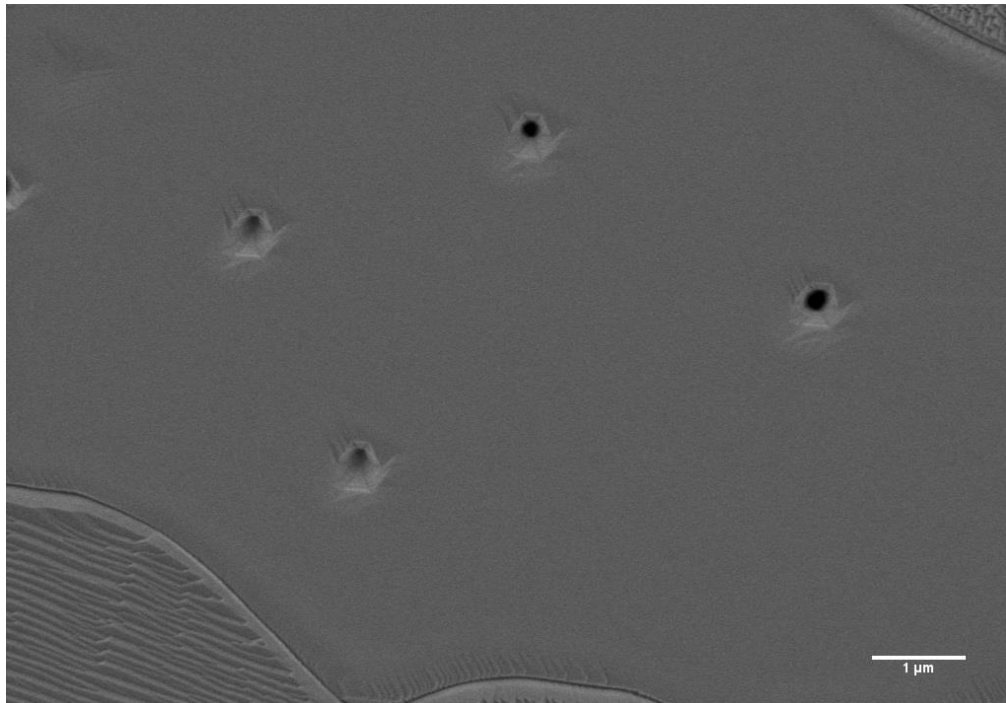
Iman Naamneh<sup>1</sup>, Rachel Marder<sup>1</sup>, Wayne Kaplan<sup>1</sup>

*Materials Science and Engineering, Technion - Israel Institute of Technology, Haifa,  
Israel*

Grain growth is an important process which occurs together with densification during sintering of polycrystalline ceramic materials. The shape of grains can influence the properties of a sintered material, and thus it is important to understand the reasons behind morphological changes during thermal processing of ceramics.

$\alpha$ -alumina is one of the most studied ceramics, in part due to its optical and mechanical properties, and thus it is often used as a model system for fundamental studies. Previous studies have clearly demonstrated that doping alumina with calcium (Ca) below the solubility limit results in accelerated and anisotropic grain growth, and as a result changes the crystal shape, where elongated plate-like alumina grains form. It is not clear if the elongated shape is due to the system approaching equilibrium, i.e. the equilibrium crystal shape of alumina due to adsorbed Ca to some crystallographic surfaces, or if this is a kinetic shape where Ca results in anisotropic grain boundary mobility.

In on-going this study, undoped and Ca-doped alumina was sintered to obtain a dense microstructure. Combined electron microscopy techniques were used to correlate the crystallographic shape of elongated grains in Ca-doped alumina, compared to the shape of equilibrated pores occluded in the alumina grains.





P-51

## THE INFLUENCE OF ADDITIVES ON THE CRYSTALLIZATION OF CALCIUM PHOSPHATE IN PHYSIOLOGICAL CONDITIONS

Yarden Nahmias<sup>1</sup>, Netta Vidavsky<sup>1,2</sup>

<sup>1</sup>*Chemical Engineering, Ben-Gurion University of the Negev, Beer Sheva, Israel*

<sup>2</sup>*Ilse Katz Institute for Nanoscale Science & Technology, Ben-Gurion University of the Negev, Beer Sheva, Israel*

Hydroxyapatite (HA) crystals are the inorganic component of physiological minerals such as bones and teeth. They are a significant component of pathological calcifications, mineral deposits that form in soft tissues. HA crystals can form in renal and cardiovascular disorders, inflammation, and cancer. In breast and thyroid cancers, microscopic HA particles called microcalcifications (MCs) are associated with higher malignancy and poorer prognosis. While physiological mineralization is a highly regulated process yielding crystals with consistent characteristics, pathological minerals are often heterogeneous in composition, crystal phase, and morphology. Most studies report that in tumors, HA crystallization occurs in the extracellular environment. Blood plasma is such extracellular fluid that is supersaturated with respect to HA. Hence, a solution mimicking the blood plasma can serve as a platform to manipulate and inhibit HA crystallization in the context of cancer. We utilize a simulated body fluid (SBF) solution specifically modified to resemble the inorganic ion concentrations, pH, ionic strength, and temperature of blood plasma. We use anionic additives rich in carboxyl acid groups, such as polyacrylic acid (PAA) and polyaspartic acid (PAsp), to inhibit HA precipitation in SBF. We were able to inhibit more than 88% of HA crystallization using PAA, depending on its concentration (100; 200 mg/mL) and molecular weight (8000; 100,000 g/mol), with inhibition increasing with molecular weight and concentration. We show that PAsp can inhibit and promote HA formation in a concentration-dependent manner, as high PAsp concentration inhibits HA formation while low concentration promotes it. Those additives not only inhibit the formation of HA but also affect the resulting crystal phase by stabilizing amorphous calcium phosphate (ACP), an unstable precursor for HA formation. Furthermore, significant HA inhibition (40%) occurs through the stabilization of ACP. The effects of various additives on the crystallization process and behavior within the SBF solution are investigated using optical microscopy, while the morphological influence of the additives is analyzed using scanning electron microscopy. In the future, we will explore these additives in an in vitro 3D tumor model for their ability to inhibit MC formation and potentially suppress malignancy. We aim to contribute to developing new approaches for inhibiting pathological mineralization and ultimately improving patient outcomes in breast and other cancers.



P-52

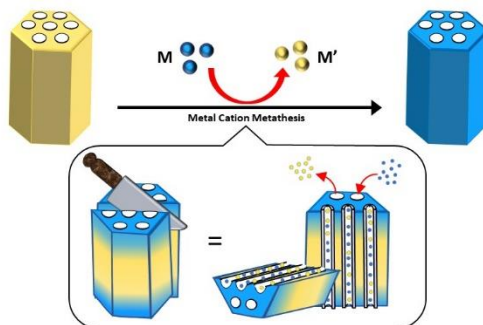
## DIRECTING THE MORPHOLOGY, PACKING, AND PROPERTIES OF CHIRAL METAL-ORGANIC FRAMEWORKS BY CATION EXCHANGE

Hadar Nasi<sup>1</sup>, Maria Chiara di Gregorio<sup>1</sup>, Qiang Wen<sup>1</sup>, Linda J. W. Shimon<sup>2</sup>, Ifat Kaplan-Ashiri<sup>2</sup>, Tatyana Bendikov<sup>2</sup>, Gregory Leitus<sup>2</sup>, Miri Kazes<sup>1</sup>, Dan Oron<sup>1</sup>, Michal Lahav<sup>1</sup>, Milko E. van der Boom<sup>1</sup>

<sup>1</sup>*Molecular Chemistry and Material Science, Weizmann Institute of Science, Rehovot, Israel*

<sup>2</sup>*Department of Chemical Research Support, Weizmann Institute, Rehovot, Israel*

Predicting crystal morphology, packing and composition is with great interest in material science. Metal-organic frameworks (MOFs) are well studied and explore materials due to their use for many applications.<sup>[1-3]</sup> Here we show that metal-organic frameworks, based on tetrahedral pyridyl ligands, can be used as a morphological and structural template to form a series of isostructural crystals having different metal cations and properties. The primary manganese-based crystals are characterized by an uncommon space group (*P622*). The packing includes two different chiral channels that can mediate the cation exchange, as indicated by energy-dispersive X-ray spectroscopy on microtome-sectioned crystals. The observed cation exchange is in excellent agreement with the Irving-Williams series<sup>[4]</sup> associated with the relative stability of the resulting coordination nodes (MnFeCoNiCuZn). The crystals maintain their morphology, allowing a quantitative comparison of their optical and magnetic properties at both the ensemble and single-crystal level.



### References

- (1) Chen, Z.; Kirlikovali, K. O.; Li, P.; Farha, O. K. *Acc. Chem. Res.* **2022**, *55*, 579–591.
- (2) Rosi, N. L.; Eckert, J.; Eddaoudi, M.; Vodak, D. T.; Kim, J.; O’Keeffe, M.; Yaghi, O. M. *Science*. **2003**, *300*, 1127–1129.
- (3) Cook, T. R.; Zheng, Y. R.; Stang, P. J. *Chem. Rev.* **2013**, *113*, 734–77.
- (4) R. F. See, R. A. Kruse, W. M. Strub, *Inorg. Chem.* **1998**, *37*, 5369–5375.

P-53

## NANOSTRUCTURAL CHARACTERIZATION OF COMPLEXES OF DNA WITH A DIBLOCK-COPOLYMER OF POSITIVELY-CHARGED AND NEUTRAL BLOCKS, AND THEIR STABILITY IN THE PRESENCE OF BLOOD SERUM ALBUMIN

Sapir Rappoport<sup>1</sup>, Varvara Chrysostomou<sup>2</sup>, Stergios Pispas<sup>2</sup>, Yeshayahu Talmon<sup>1</sup>

<sup>1</sup>*Department of Chemical Engineering and the Russell Berrie Nanotechnology Institute (RBNI), Technion – Israel Institute of Technology, Haifa, Israel*

<sup>2</sup>*Theoretical and Physical Chemistry Institute, National Hellenic Research Foundation, Athens, Greece*

Quaternized poly(2-(dimethylamino ethyl methacrylate)-b-poly(oligo(ethyleneglycol) methyl ether methacrylate) (QPDMAEMA-b-POEGMA) is a copolymer of a positively charged block and a non-ionic hydrophilic block. The positively charged block, QPDMAEMA, can electrostatically interact with oppositely charged polymers such as DNA, to form complexes, also known as polyplexes. These complexes are stable in aqueous solution due to the hydrophilic block, POEGMA, which provides colloidal stability and biocompatibility. Polyplexes can be used as non-viral vectors in gene therapy. The polyplexes are essential for delivering genetic material into cells because they protect the genetic material from degradation before reaching the target cells, thus increasing the transfection efficiency. In-vitro study of these polyplexes at charge ratio of 2 and 4, showed transfection efficiency of almost 50%. However, currently used polyplexes show a low transfection efficiency in-vivo, probably because the polyplexes are exposed to blood proteins, such as serum albumin, which cause their dissociation.

We used cryogenic transmission electron microscopy (cryo-TEM) and small-angle x-ray scattering (SAXS) to study the inner structure of QPDMAEMA-b-POEGMA and DNA complexes at different charge ratios. The results show that lamellar and hexagonal structures are formed depending on the charge ratio. Studies showed that hexagonal complexes have higher transfection efficiency than lamellar complexes. Such hexagonal complexes are shown in Figure 1. The complexes were also examined after exposing them to bovine serum albumin (BSA). We found that BSA does not affect the complexes for seven days. That stability is essential for better design and formulation of vectors for gene therapy.

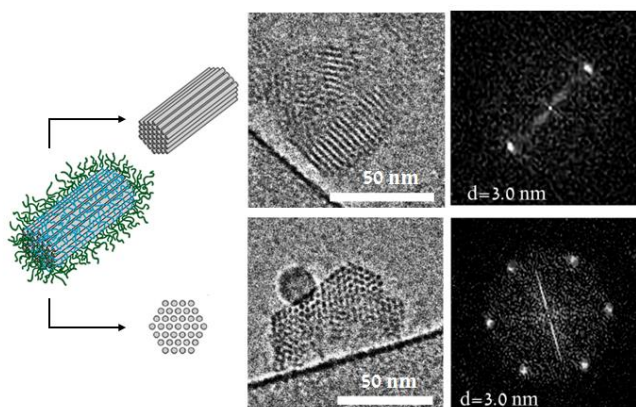


Figure 1. Different projections of a hexagonal structure of QPDMAEMA-b-POEGMA and DNA complexes at CR of 10 in cryo-TEM micrographs (left). The spacing is 3 nm, as shown in the Fourier transforms on the right.

**P-54**

## **OPTICAL CHARACTERIZATION OF LEAD HALIDE PEROVSKITES HETEROSTRUCTURE INTERFACE WITH CATHODOLUMINESCENCE SPECTROSCOPY**

**Betty Shamaev<sup>1</sup>, Yehonadav Bekenstein<sup>1</sup>**

*Materials Science and Engineering, Technion - Israel Institute of Technology, Haifa,  
Israel*

Heterostructures and interfaces are crucial in determining the local electronic material properties in semiconducting devices. Halide perovskites are less explored semiconductors that have raised interest due to their unique optoelectronic properties with promising suitability for photovoltaics, lasing, and detection applications.

In this work, we explore the interfaces of CsPbBr<sub>3</sub> with competing phases - Cs<sub>4</sub>PbBr<sub>6</sub> and CsPb<sub>2</sub>Br<sub>5</sub> grown from the vapor phase on Si substrate.

Although these phases are similar in composition, they vary in microstructures and electronic properties. Cathodoluminescence spectroscopy (CL) and time-resolved cathodoluminescence (TRCL) are high-energy electron microscopy techniques that provide a powerful way to characterize optical properties. This research used a CL DELMIC SPARC installed in SEM (FEI Quanta 650) with an ultra-fast beam blaster, providing a few nm spatial resolution and around 50ps time resolution. These properties enable distinguishing between such phases, mapping the material interface, and correlating microstructure with dynamic properties of the emitted light.

Using those methods, we detect an enhancement of CL emission at the perovskite interface. In a similar setup, we detect defects and analyze their effects on optical properties, enabling an advanced understanding of material properties and engineering. Our vision is to develop and engineer perovskite heterostructures with controlled properties for ultra-fast light emission.



P-55

## THE EFFECT OF SALTS ON THE NANOAGGREGATION OF SLES IN AQUEOUS SOLUTIONS OBSERVED BY CRYO-TEM

Sapir Simon<sup>1</sup>, Werner Kunz<sup>2</sup>, Thomas Zemb<sup>3</sup>, Yeshayahu Talmon<sup>1</sup>

<sup>1</sup>*Department of Chemical Engineering and the Russell Berrie Nanotechnology Institute (RBNI), Technion – Israel Institute of Technology, Haifa, Israel*

<sup>2</sup>*Institute of Physical and Theoretical Chemistry, University of Regensburg, Regensburg, Germany*

<sup>3</sup>*Institute for Separation Chemistry Icsm, University of Montpellier, Marcoule, France*

Sodium lauryl ether sulfate (SLES) is an amphiphilic molecule widely used as an anionic surfactant in soaps, personal care, and cosmetic products. Minor components, like salts or fragrance molecules, are usually added to the industrial formulations of SLES-based products, and significantly affect their nanostructure and properties. SLES in aqueous solutions, with the addition of minor components, self-assemble into different nanoaggregates, such as nanometric spheroidal micelles, threadlike micelles, branched networks, and vesicles (Figure 1), depending on the concentrations of SLES and the additive. Direct imaging of SLES with commonly used salt additives can explain the nanostructural modifications affecting the macroscopic properties of the solution. This could serve as a basis for optimized formulation design of SLES-based products.

We use cryogenic transmission electron microscopy (cryo-TEM) direct imaging to study the effect of different salts on the nanostructure of SLES aqueous solutions, at different salt-to-surfactant molar ratios ( $X$ ). We conduct rheological measurements to predict nanostructural changes, as the viscosity is strongly affected by the self-aggregated nanostructure of the system. In our study, we show the correlation between the rheological properties and the nanostructural changes of SLES with varying salt concentrations. Moreover, we present the formation of different nanostructures when different types of salts (LiCl, NaCl, KCl, and CsCl). We also demonstrate how the specimen preparation process affects the imaged nanostructures through artifact formation.

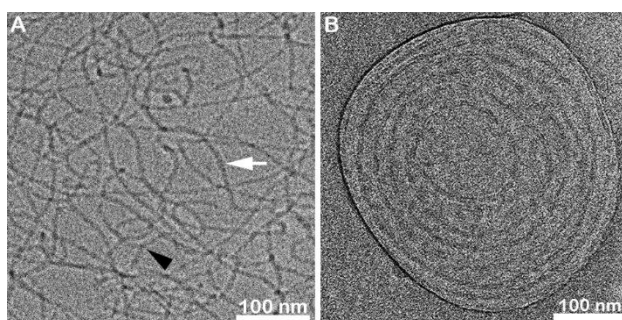


Figure 1. Cryo-TEM micrographs demonstrating the different nanostructures of 5 wt.% SLES with a salt-to-surfactant molar ratio,  $X$ , that gives the maximum zero-shear viscosity, with NaCl and KCl; (A) With NaCl, at  $X=10$ , showing networks of elongated threadlike micelles (white arrow) with several branching points (black arrowhead). (B) with KCl, at  $X=3.5$ , showing concentric multi-layered vesicle-like structures.



P-56

## A CATION EFFECT ON SELF-HEALING IN APbI<sub>3</sub> PEROVSKITE THIN POLYCRYSTALLINE FILMS

Pallavi Singh<sup>1</sup>, Yahel Soffer<sup>1</sup>, Davide Raffaele Ceratti<sup>2</sup>, Michael Elbaum<sup>1</sup>, Dan Oron<sup>1</sup>, Gary Hodes<sup>1</sup>, David Cahen<sup>1</sup>

<sup>1</sup>Weizmann Institute of Science, Rehovot, Israel

<sup>2</sup>CNRS UMR 9006-IPVF Institut Photovoltaïque d'Ile-de-France, Paris, France

In terms of sustainable use, Halide Perovskite (HaP) semiconductors have a strong advantage over other classes of (opto)electronic materials, as they can self-heal from damage autonomously.<sup>1-4</sup> Using “1-Photon fluorescence recovery after photobleaching” (FRAP) technique, we show for the first time self-healing (SH) in encapsulated Pb iodide perovskite (APbI<sub>3</sub>) polycrystalline thin films (the form used in devices for PV, LED, radiation detection). We showed the electronically inactive A cation significantly affects the kinetics of SH. We excite and damage the material with 488 nm supra-bandgap laser pulses of different power densities to inflict different extents of damage and measure the PL to compare SH in 4 types of photoactive APbI<sub>3</sub> encapsulated perovskite thin films, viz., 1. Tetragonal MAPbI<sub>3</sub>; 2. Tetragonal 20% Guanidinium-substituted MAPbI<sub>3</sub>; 3. High-temperature cubic  $\alpha$ -FAPbI<sub>3</sub> and 4. Low-temperature orthorhombic  $\gamma$ -CsPbI<sub>3</sub>. We compared the healing kinetics and extent of healing of numerous spots that were damaged by the laser pulses, over given periods of time. Among them,  $\gamma$ -CsPbI<sub>3</sub> healed fastest and completely from close to 100% damage, in less than 1.5 hrs, followed by complete healing of the HT photoactive  $\alpha$ -FAPbI<sub>3</sub> phase in 3 hrs; 20% Guanidinium substituted MAPbI<sub>3</sub> took 6 hrs, whereas, MAPbI<sub>3</sub> showed the slowest healing kinetics and only 30% PL recovery occurs from >95% photo-damage after 9 hrs. Compared to MAPbI<sub>3</sub>, all other perovskite films, substituted with either bulkier organic cations with lower dipole moments (and with additional options for H-bonds) or smaller inorganic cations, can be viewed as strained due to monovalent cation size mismatch (as per tolerance factor). Remarkably all these recovered completely in a period equivalent to one night cycle, i.e., highly relevant for solar cells. This study will help in the selection of better functional materials for autonomously sustainable optoelectronics. The more reversible the photo-damage (without external intervention), the more sustainable is the material, and, with it, the device that is based on its function.

### References:

1. ACS Energy Lett. 2023, 8, 2447–2455.
2. Adv. Mater. 2018, 30, 1706273.
3. Adv. Funct. Mater. 2022, 32, 2113354.
4. Mater. Horiz. 2021, 8, 1570–1586.



P-57

## CERAMIC–METAL INTERFACE: THE INFLUENCE OF TITANIUM ON THE MICROSTRUCTURE OF VACUUM BRAZED ALUMINA-ALUMINUM ALLOY

Stalin Sundara Dhas<sup>1</sup>, Kalaichelvan K.<sup>1</sup>

*Department of Ceramic Technology, ACT campus, Anna University, Chennai, Tamil Nadu, India*

The influence of titanium (Ti) active metal element on grain growth in enhancing the wetting behaviour and adhesion of the alumina (Al<sub>2</sub>O<sub>3</sub>) substrate and its effect on the aid of residual stress in vacuum brazed Al<sub>2</sub>O<sub>3</sub>/Aluminum alloy joints were evaluated. Physical vapour deposition (PVD) of the titanium of 5 μm thickness coated over the surface of Al<sub>2</sub>O<sub>3</sub> as additive manufacturing (AM) vacuum brazed with aluminum alloy at 630 °C holding for 5 minutes using eutectic Al4047 filler alloy in a vacuum condition ranging from 10<sup>-3</sup> to 10<sup>-5</sup> torr. The effect of titanium on interfacial joint microstructure with respect to the brazing temperature and brazing time was investigated by scanning electron microscopy with energy dispersive spectrometry and the X-ray diffraction technique was used to identify the reaction compound formation, and also to measure the relief of residual stress at the interface. The typical interfacial structure of ceramic-metal joint: ceramic Al<sub>2</sub>O<sub>3</sub>/(Ti-O-Al)/Ti/(Ti-Al-Cu-Fe)/(Al-Si-Fe) intermetallic/(Al-Si-Cu-Fe)/Aluminum alloy substrate. The interfacial characterization of titanium-doped alumina exhibits titanium adsorption to the grain surface. The titanium-rich reaction phase adjoining Al<sub>2</sub>O<sub>3</sub> becomes gradually discontinuous from continuity as the brazing time extends. The brazed interface response to residual stress was assessed by measuring the d-spacings using the X-ray diffraction method. The evaluated tensile residual stress on the interface is -3.4 MPa. The brazed Al<sub>2</sub>O<sub>3</sub> with titanium coating resulted in a significant increase in relieving the residual stress formed due to the thermal expansion coefficient mismatch. Achieving a highly reliable metal-ceramic joint is dependent on both enhancing the wettability of the Al<sub>2</sub>O<sub>3</sub> faying surface through the titanium-rich intermetallic compound formation in a controlled atmosphere and also by the relief of residual stress at the interface.

### References

1. Brandon, David G., and Wayne D. Kaplan, (1997). *Joining processes: an introduction* (1<sup>st</sup> ed.). Wiley.
2. S. Stalin, K. Kalaichelvan. (2023). Ceramic–metal interface: In-situ microstructural characterization aid vacuum brazing additive manufacturing technology. In R. K. Ajay Kumar (Ed.), *Advances in Additive Manufacturing - Artificial Intelligence, Nature-Inspired, and Bio-manufacturing* (pp. 235-251). Elsevier. DOI: <https://doi.org/10.1016/B978-0-323-91834-3.00001-6>.



P-58

## ON THE DEVELOPMENT AND ATOMIC STRUCTURE OF ZnO CRYSTALS GROWN IN POLYMERS FROM VAPOR PHASE PRECURSORS

Inbal Weisbord<sup>1</sup>, Maya Barzilay<sup>1</sup>, Alexei Kuzmin<sup>2</sup>, Andris Anspoks<sup>2</sup>, Edmund Welter<sup>3</sup>,  
Tamar Segal-Peretz<sup>1</sup>

<sup>1</sup>*Chemical Engineering, Technion - Israel Institute of Technology, Haifa, Israel*

<sup>2</sup>*Institute of Solid State Physics, University of Latvia, Riga, Latvia*

<sup>3</sup>*Deutsches Elektronen-Synchrotron, (DESY), Hamburg, Germany*

Sequential infiltration synthesis (SIS), an ALD-derived method for growth of inorganic materials inside polymeric structures, is an emerging technique for hybrid materials and inorganic nanostructure fabrication which can be utilized in a wide array of applications. In this work, we study the development of ZnO crystalline particles within SU-8, polymethacrolein (PMCHO), and polymethyl methacrylate (PMMA) at the atomic scale. We probe the growth throughout diethyl zinc (DEZ)/H<sub>2</sub>O SIS cycles, as well as after polymer removal. The crystalline ZnO structure is deciphered by combining two powerful methods: extended x-ray absorption fine structure (EXAFS) and high-resolution scanning transmission electron microscopy (HR-STEM). Synchrotron-based EXAFS provides large-scale statistical information on the crystals' long-range order and predicts their Wurtzite structure. HR-STEM of the hybrid polymer-ZnO films corroborates the predicted structure and allows for precise analysis of crystal size, orientation, and existing defects, as well as the dispersion of the particles inside each polymer. Significantly, the polymer matrix allows us to probe the growth, cycle-by-cycle, providing insights to ZnO atomic growth mechanism inside different polymers and extending our understanding of SIS. In addition, the methodology developed for such high-resolution imaging of hybrid films will allow future studies of additional hybrid systems.

P-59

## HIERARCHICAL SELF-ASSEMBLY INVOLVING CLASSICAL AND NONCLASSICAL STEPS IN ORGANIC CRYSTAL GROWTH

Idan Biran<sup>1</sup>, Shaked Rosenne<sup>1</sup>, **Dr. Haim Weissman<sup>1</sup>**, Yael Tsarfati<sup>1</sup>, Lothar Houben<sup>2</sup>,  
Boris Rybtchinski<sup>1</sup>

<sup>1</sup>*Molecular Chemistry and Material Science, Weizmann Institute of Science, Rehovot, Israel*

<sup>2</sup>*Chemical Research Support, Weizmann Institute of Science, Rehovot, Israel*

Organic crystal nucleation and growth are complex processes that often do not fit into the scope of the existing crystallization theories. We investigated a crystal growth mechanism of an organic dye, perylene diimide, using high-resolution cryogenic transmission electron microscopy and optical spectroscopy. We were able to demonstrate that the evolution of order in our system had a high level of complexity and involved both classical and nonclassical steps. The crystallization mechanism included a series of supramolecular transformations, where each step defined the next one. The crystal growth started from a molecular self-assembly into  $\pi$ -stacks that eventually underwent intermolecular ordering that optimized interactions within the stacks. The latter transformed at the larger scale, by stack interactions, which formed crystalline domains. Finally, the formed faceted crystals gradually grew through oriented attachment of other crystal, and attachment of residual monomeric molecules from solution (Figure 1).

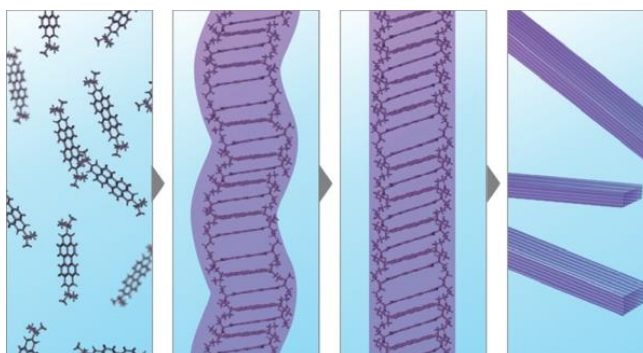


**Fig.1** An illustration of order evolution during the crystallization of perylene diimide.

Our findings present a detailed insight into organic crystal growth and reveal that both classical and nonclassical mechanisms can operate within a crystallization process.<sup>1</sup> However, classical/nonclassical dichotomy provides only a partial insight into the crystallization mechanism, which may be described as a sequence of supramolecular events, traversing a vast size scale from the optimization of intermolecular interactions to the oriented attachment of crystals. In summary, our work revealed the inherent nature of supramolecular transformations occurring in organic crystallization, thus advancing conceptually our understanding of order evolution in organic matter.

1. Biran, I.; Rosenne, S.; Weissman, H.; Tsarfati, Y.; Houben, L.; Rybtchinski, B. *Cryst. Growth Des.* **2022**, *22* (11), 6647–6655.

P-60

## VISUALIZING THE EFFECT OF ELECTRIC FIELDS ON FOULING FORMATION USING CONFOCAL MICROSCOPY

Elina Yachnin<sup>1</sup>, David Jassby<sup>2</sup>, Tamar Segal-Peretz<sup>3</sup>, Guy Z. Ramon<sup>1</sup>

<sup>1</sup>*Department of Civil and Environmental Engineering, Technion – Israel Institute of Technology, Haifa, Israel*

<sup>2</sup>*Department of Civil and Environmental Engineering, University of California, Los Angeles, California, USA*

<sup>3</sup>*Department of Chemical Engineering, Technion - Israel Institute of Technology, Haifa, Israel*

The accumulation of organic and inorganic substances on functional equipment, often referred to as fouling, is a common and severe problem in various processes, such as water treatment membranes and heat exchangers. The formation of a fouled layer leads to reduced performance, increased energy consumption, increased chemical waste, and increased operational costs. Fouling mitigation using electric fields is a promising method<sup>1,2</sup>; however, an understanding of the exact dynamics and scalant-surface interactions is still lacking. It is hypothesized that electric fields mitigate heterogeneous scaling formation through the disruption of the ion stoichiometry required for nucleation, via counter-ion repulsion within the electric double layer (EDL) formed near a charged surface. This study aims to understand the effect of electric field application on fouling formation and removal using in-situ direct observation confocal microscopy. For that purpose, a designated flow cell was designed. The novelty of this flow cell is that it enables to perform microscopic process experiments, such as water filtration through a membrane or heat exchange process, under applied electric field. The flow cell was mounted on a confocal microscope, and the spatial and temporal accumulation of deposit on the functional surface was monitored during the experiment. Dyes and microparticles with fluorescent labels were used as model foulants, simulating salts and colloids forming foulants found in water, used for membrane filtration and heat exchange processes. Copper foil and electrically conductive membranes were used as model surfaces. As electric field was applied, the foulant distribution at the surface and at different distances from it was imaged (Fig. 1); higher concentration of foulant near a surface will result in increased fouling. Analysis of these images showed that electric field affects the dye distribution near the surface in agreement with the charge of the dye and surface polarity, leading to potential use of electric field as foulant removing method. For the microparticles, a tradeoff between the applied electric field and process parameters was observed. This led to irreversible deposition at the tested conditions.

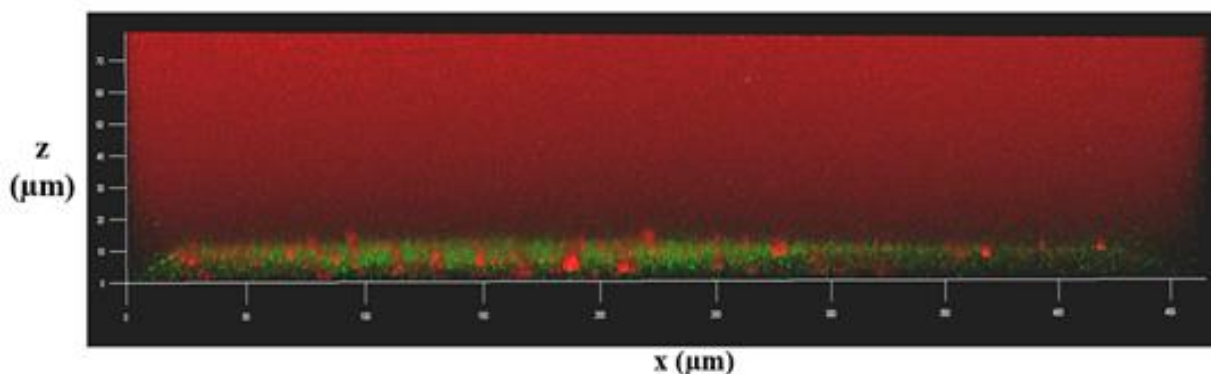


Fig. 1: Confocal image of a positively charged fluorescent dye (red) near a negatively charged surface (green)



References:

- [1] Duan Wenyan, Dudchenko Alexander, Mende Elizabeth, Flyer Celeste, Zhu Xiaobo, Jassby David, Electrochemical Mineral Scale Prevention and Removal on Electrically Conducting Carbon Nanotube – Polyamide Reverse Osmosis Membranes (2014) *Environ. Sci.: Processes Impacts*, 16(6), 1300-1308
- [2] Rao Unnati, Iddya Arpita, Jung Bongyeon, Khor Chia Miang, Hendren Zachary, Turchi Craig, Cath Tzahi, Hoek Eric M. V., Ramon Guy Z., Jassby David, Mineral Scale Prevention on Electrically Conducting Membrane Distillation Membranes Using Induced Electrophoretic Mixing (2020), *Environ. Sci. Technol.*, 54(6), 3678-3690



P-61

## THE EFFECT OF CALCIUM OXALATE CRYSTAL PHASE, MORPHOLOGY, AND AGGREGATION ON PROTEIN ADSORPTION AND CANCER CELL ATTACHMENT

Gabriel Yazbek Grobman<sup>1</sup>, Dina Aranovich<sup>1</sup>, Netta Vidavsky<sup>1,2</sup>

<sup>1</sup>*Department of Chemical Engineering, Ben-Gurion University of the Negev, Beer Sheva, Israel*

<sup>2</sup>*Ilse Katz Institute for Nanoscale Science & Technology, Ben-Gurion University of the Negev, Beer Sheva, Israel*

Calcium oxalates (CaOx) are pathological biominerals observed in kidney stones and breast and thyroid cancer. In breast cancer microcalcifications, CaOx crystals are exclusively associated with benign lesions. However, calcium phosphates are found in both malignant and benign lesions and trigger cancerous behavior in breast epithelial cells *in vitro* according to their crystal properties. Based on recent results from our lab showing that calcium oxalate dihydrate (COD) crystals can suppress breast cancer progression *in vitro*, we hypothesize that this positive effect will also vary as a function of COD crystal properties.

Here, we focus on the two physiologically relevant calcium oxalate hydrates, COD and calcium oxalate monohydrate (COM). We study the influence of COD and COM with different crystal properties, including morphology, particle size, and surface area on crystal aggregation, protein adsorption, and crystal-cell interactions. We synthesized five different COD morphologies: Thin-bipyramid, thick-bipyramid, dumbbell-like, rod-like, and spherical, by crystallization from solutions, varying the supersaturation, stirring speed, modifier addition, and time of crystallization. The crystal phases were characterized by Fourier transform infrared spectroscopy (FTIR) and X-ray diffraction (XRD), and the crystal morphology and particle sizes by scanning electron microscopy (SEM). Furthermore, we used light microscopy to monitor crystal aggregation. The crystal aggregation rate of COD with all five morphologies was more significant in a biological-like environment (cell culture media) than in phosphate buffer saline (PBS), most likely due to the presence of biological macromolecules that adsorb to the crystal surfaces. Additionally, the thick-bipyramid morphology is prone to form bigger aggregates than the other four COD morphologies, while dumbbell-like morphology forms the greatest number of aggregates. Our ongoing work includes an assessment of model protein adsorption and cell attachment to COD and COM crystals, normalized to their surface area, to determine the role of the CaOx hydration state and morphology on the crystal interactions with biological materials.



P-72 (last minute submission)

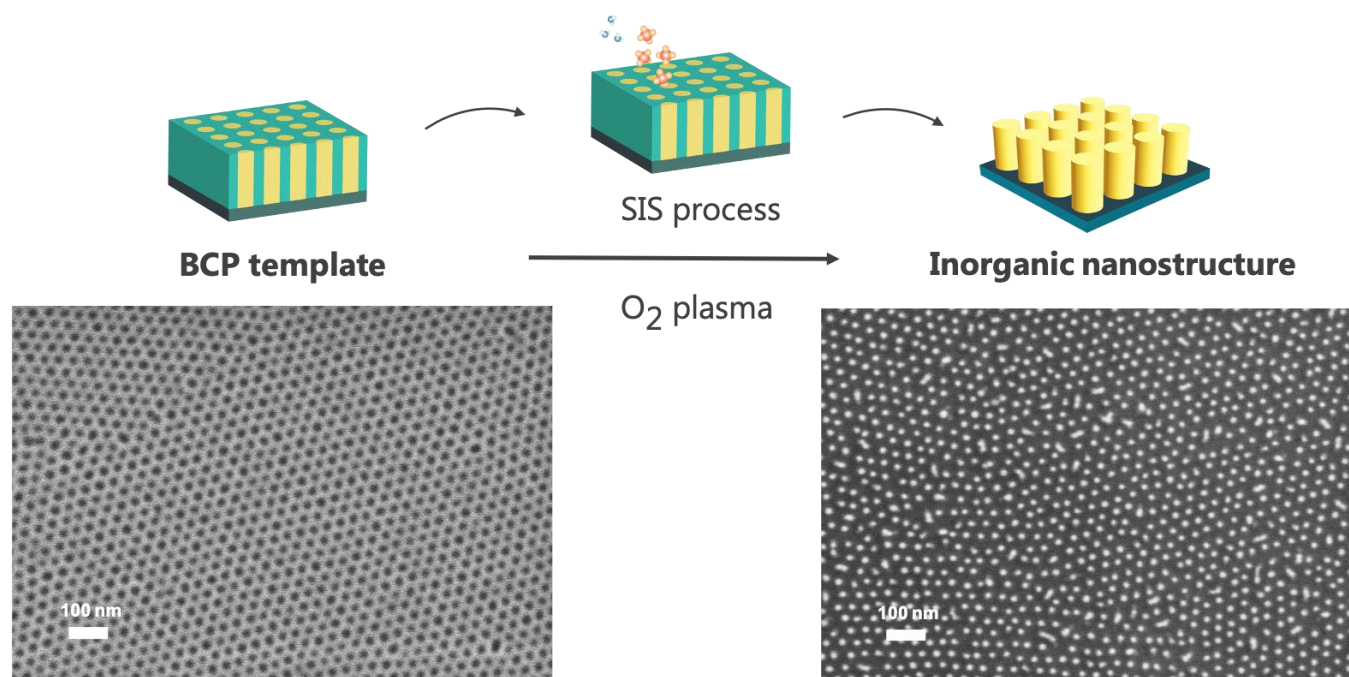
## RATIONAL DESIGN AND FABRICATION OF BLOCK COPOLYMER TEMPLATED HAFNIUM OXIDE NANOSTRUCTURE

Ruoke Cai, Tamar Segal-peretz

*Department of Chemical Engineering, Technion-Israel Institute of Technology, Haifa, Israel*

Hafnium oxide ( $\text{HfO}_2$ ) is an attractive material for optoelectronic applications and high- $\kappa$  dielectrics in semiconductor devices due to its advantageous properties- high dielectric constant, wide band gap, and high stability. However, hafnium oxide nanostructure fabrication currently relies on complex nanofabrication processes. Sequential infiltration synthesis (SIS)- a method derived from atomic layer deposition (ALD), in which vapor phase precursors diffuse into polymers and react with them to form hybrid material, can provide a simple and cost-effective alternative for these processes.

In this study, we demonstrate the formation of hafnium oxide nanostructures within block copolymers (BCPs) templates. BCP were self-assembled into highly ordered and periodic nanostructures. In SIS, selective interactions between the hafnium organometallic precursor and the polar block of the BCP resulted in selective growth within the polar block domains. Following the growth, the BCP template was removed to yield hafnium nanostructures templated by the BCP morphology. We explored the precursor-polymer interactions in various homopolymers using quartz crystal microbalance (QCM) microgravimetric measurements. This knowledge was further applied in finding a suitable BCP for templating  $\text{HfO}_2$  inorganic nanostructure.



**P-62**

## **CRYOGENIC SCANNING ELECTRON MICROSCOPY AS AN EFFECTIVE TOOL FOR NANOSTRUCTURAL STUDY OF BIOLOGICAL SYSTEMS**

**Irina Davidovich<sup>1</sup>, Ariel Koren<sup>2</sup>, Carina Levin<sup>2</sup>, Yeshayahu Talmon<sup>1</sup>**

*<sup>1</sup>Department of Chemical Engineering and the Russell Berrie Nanotechnology Institute (RBNI), Technion-Israel Institute of Technology, Haifa, Israel*

*<sup>2</sup>Pediatric Hematology Unit, Emek Medical Center in Afula, Afula, Israel*

Diseases resulting from blood cell dysfunction, like cardiovascular diseases, account for most of the mortality in modern society. Recent developments in microbiology lead to a greater understanding of cell function and structure. Techniques such as PCR, FACS, gel electrophoresis, and macromolecule blotting promote investigation of biochemical processes. However, all these techniques give numerical input, which can be interpreted by several models. It is necessary to use high-resolution (HR) imaging techniques to fully understand molecular organization within the cell and its connection to cell function and communication with its environment.

Cryo-SEM allows direct imaging of biological systems without modifying their nanostructure. The technique applicability ranges from studying the morphology of different subpopulations that may coexist in a sample, to understanding physiological processes by imaging the system at varying stages. Cryofixation with high-pressure freezing allows for maximum morphological preservation, because it captures nano-aggregates within cells at near-native conditions, while cryogenic electron microscopy provides an opportunity to study cells at high resolution as close to their native state as possible.

Here, I present an application of the cryo-SEM to analyze human blood cells. It is focused on optimization of specimen preparation procedure, and working parameters for better characterization of cell morphology, ultrastructure, and cell-cell interactions.



P-63

## COUNTING NANOPARTICLES IN GENERAL AND VIRUSES IN PARTICULAR ONE AT A TIME

**Paz Drori**<sup>1</sup>, Odelia Mouhadeb<sup>2</sup>, Gabriel Moya<sup>3</sup>, Yair Razvag<sup>1</sup>, Ron Alcalai<sup>2</sup>, Philipp Klocke<sup>3</sup>, Thorben Cordes<sup>3</sup>, Eran Zahavy<sup>2</sup>, Eitan Lerner<sup>1</sup>

<sup>1</sup>*Department of Biological Chemistry, The Hebrew University of Jerusalem, Jerusalem, Israel*

<sup>2</sup>*Department of Biochemistry and Molecular Genetics, Israel Institute for Biological Research, Ness Ziona, Israel*

<sup>3</sup>*Physical and Synthetic Biology, Ludwig-Maximilians-Universität München, München, Germany*

The SARS-CoV-2 pandemic underlined the necessity for accurate, sensitive and rapid viral diagnostics, three aspects that are commonly thought of trading off. We demonstrate the detection of single specific nanoparticles based on their correlated fluorescence signals indicating both their volumes and specific antigens. This detection scheme is achieved by probing microfluidic laminar flow of a sample of nanoparticles immersed in free dyes and with specifically dye-labeled antibodies with a dual-color 3D-printed confocal setup. First, we demonstrate the detection capabilities using nanometer-sized beads and then on two different viruses expressing the Spike protein from SARS-CoV-2: (i) rVSV- $\Delta$ G-spike, and (ii) neutralized SARS-CoV-2. Additionally, employing this detection scheme together with microfluidic hydrodynamic focusing, we count single bio-nanoparticles rapidly for viral load as low as 10<sup>4</sup> viruses/mL, which covers the a wide range of the biomedically-relevant load for viruses in general, and for SARS-CoV-2 in particular. Overall, viruses can now be counted one at a time with the presented simple to use and affordable optofluidic technology rapidly, without giving up on specificity and sensitivity, and this capability will further expand to other important bio-nanoparticles in the near future.

**P-64****MOLECULAR MOTORS ON MICROTUBULE TRACKS  
CREATED WITH NANO FOUNTAIN PEN****Orna Fridman<sup>1</sup>, Himanshu Pandey<sup>2</sup>, Larisa Gheber<sup>2</sup>, Levi A. Gheber<sup>1</sup>**<sup>1</sup>*Avram and Stella Goldstein-Goren Department of Biotechnology Engineering, Ben-Gurion University, Beer-Sheva, Israel*<sup>2</sup>*Department of Chemistry, Ben-Gurion University, Beer-Sheva, Israel*

We are exploring an approach for transport of biological cargo using motor proteins (kinesin cin-8) on their natural tracks, microtubules, between predefined stations. Using Nano Fountain Pen (NFP), we attempt to lay down microtubules between the point of origin and destination, to serve as directional tracks on which kinesin molecules will carry biological cargo.

To this end, we are patterning lines of avidin, to which biotinylated MTs are adhered. The functionality of thus immobilized MTs is demonstrated by observation of single kinesin molecules walking on the MTs. We also demonstrate alignment of MTs is via hydrodynamic drag.

Together with future refinement of alignment and polarization approaches, this method has the potential to serve as the conveyor network in miniaturized lab-on-a-chip(s).

**P-65**

## **TIME-GATED FLUORESCENCE LIFETIME IMAGING IN THE NEAR INFRARED REGIME; A COMPREHENSIVE STUDY TOWARD IN VIVO IMAGING**

**Meital Harel<sup>1</sup>, Uri Arbiv<sup>1</sup>, Rinat Ankri<sup>1</sup>**

*Physics, Ariel University, Ariel, Israel*

Fluorescence lifetime imaging (FLI) is increasingly recognized as a powerful tool for biochemical and cellular investigations, including in vivo applications. Fluorescence lifetime is an intrinsic characteristic of any fluorescent dye which, to a large extent, does not depend on excitation intensity and signal level. In particular, it allows distinguishing dyes with similar emission spectra, offering additional multiplexing capabilities. However, in vivo FLI in the visible range is complicated by the contamination by (i) tissue autofluorescence, which decreases contrast, and by (ii) light scattering and absorption in tissues, which significantly reduce fluorescence intensity and modify the temporal profile of the signal. Therefore, in order to enable deeper tissue imaging, we use the near infrared (NIR) regime, in which the tissue's scattering and autofluorescence are significantly lower. We present a time-saving Monte Carlo (MC) simulation of fluorescent photons scattering within a turbid medium, followed by phasor analyses which enabled the simple multiplexing of different targets in one frame. We then demonstrate that using the most advanced time-gated single-photon avalanche diode (SPAD) array camera, SPAD512S, provide a simple and fast method for in vivo lifetime imaging. In particular, we show how phasor dispersion increases with increasing depth, but by using an appropriate background correction, simple "cut off" method and averaging analyses we are able to multiplex two targets in one frame, from 10 mm deep within the tissue. These results showcase the possibility to perform FLI in challenging conditions, using standard, NIR fluorophores.



P-66

## SCANNING NANO-STRUCTURE ELECTRON MICROSCOPY FOR DECODING THE STRUCTURAL EVOLUTION OF META-STABLE MATERIALS

Yevgeny Rakita<sup>1,2,3</sup>, James L. Hart<sup>3</sup>, Partha P. Das<sup>4</sup>, Sina Shahrezaei<sup>5</sup>, Daniel L. Foley<sup>3</sup>,  
Suveen N. Mathaudhu<sup>5</sup>, Stavros Nicolopoulos<sup>4</sup>, Mitra L. Taheri<sup>3</sup>, Simon J. L. Billinge<sup>2</sup>

<sup>1</sup>*Materials Engineering, Ben Gurion University, Beer Sheva, Israel*

<sup>2</sup>*Department of Applied Physics and Applied Mathematics, Columbia University, New York, NY, USA*

<sup>3</sup>*Department of Materials Science and Engineering, Johns Hopkins University, Baltimore, MD, USA*

<sup>4</sup>*SPRL, NanoMEGAS, Brussels, Belgium*

<sup>5</sup>*Department of Mechanical Engineering, University of California, Riverside, Riverside, CA, USA*

In recent years, Electron Diffraction, and especially the 4D-STEM [1] is growingly becoming a routine part of structural characterizations of materials at the nano-scale. Its un-matched spatial resolution (down to sub-nm) enables the exploration of local variations within a sample, which alternatively is averaged over the entire irradiated sampled area, when explored, for example, by x-rays. As often shown in electron microscope, samples are often heterogeneous, and consequently their local properties, which then reflect on the average behaviour of the material, composite, or device. Besides morphology and composition, the local structural order can vary, especially in meta-stable systems which continuously evolve. In this study, we explore how far we can take electron diffraction when the interest is in the evolution of meta-stable materials.

We challenge ourselves with mapping the local structure in a composite of crystalline Ni and amorphous Zr-Cu-Ni-Al Bulk Metallic Glass (BMG) that was fused into a composite via hot-rolling [2]. Using a fast camera looking through the fluorescence screen, we captured diffraction patterns in a 4D-STEM modality, where we captured diffraction patterns coupled with beam precession with 3 nm step size in a Ni/BMG/Ni cross-section sample that was cut from the composite - in total 131x289 diffraction patterns (see FIGURE). Using the collected diffraction patterns and tailoring automated data reduction and analysis pipelines, such as auto-masking, azimuthal-integration, Fourier-transformation to get the electron Pair Distribution Function (ePDF) and various fittings of the PDF, we were efficiently deriving a large set of physically meaningful scalars, which we generalize as Quantities of Interest, or QoI of a Scanning Nano-structure Electron Microscopy (SNEM). [3]

By generating different QoI maps – each containing different structural information – we see in the Figure that one can extract very rich and unique structural information about the sample. For example, we see that chemical clustering may be a predeceasing (or following) step to the nucleation of nano-crystalline inclusions within the BMG. This example demonstrates the richness SNEM-based experiments can reveal, and with the assistance of automated analysis and feature detection pipelines can trace the evolution of disordered and meta-stable systems.

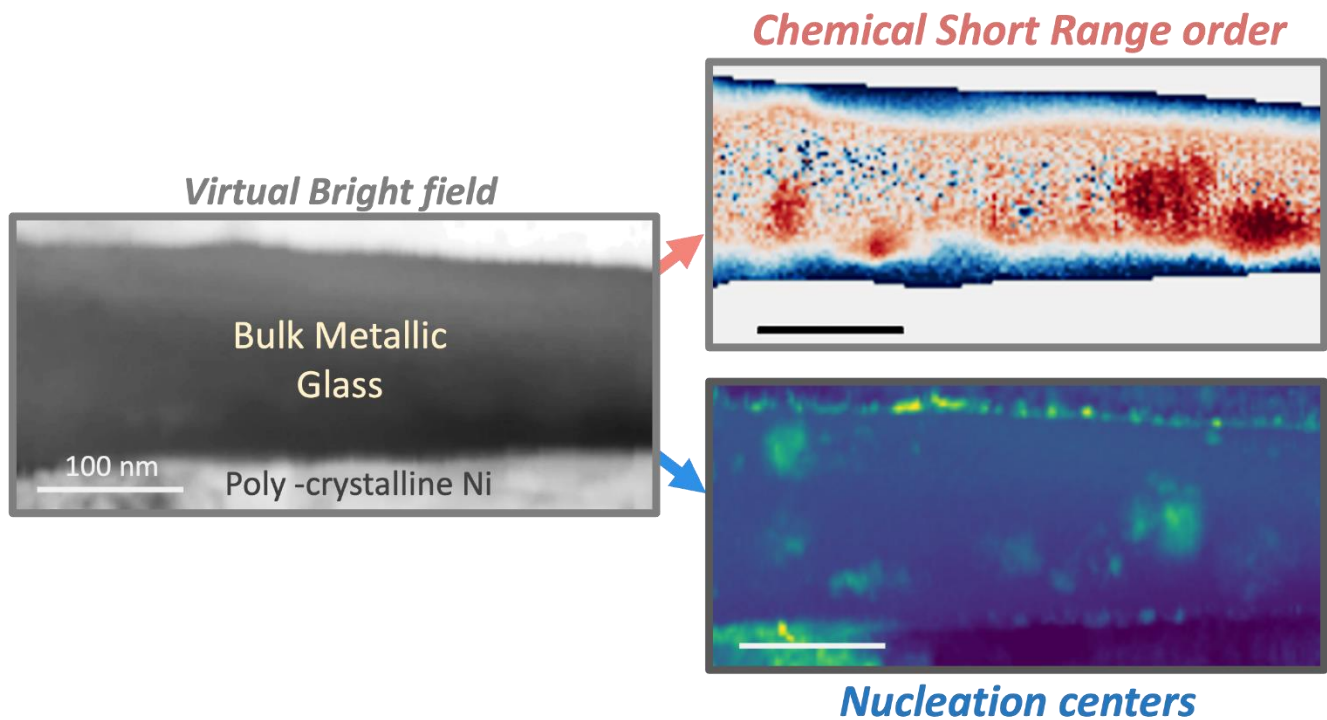


*Figure Caption:* QoI SNEM maps of the Ni/BMG/Ni structure showing: (left) a regular bright field image that emphasizes the amorphous region; (top-right) a chemical short-range order showing regions where there is a chemical ordering change (blue = ordering – increase in A-B-A-B; red = clustering – increase in A-A-A, or B-B-B clustering); (top-right) virtual dark-field mapping from a selected area of the diffraction patterns, showing (yellow-green intensity) location of nano-crystalline nuclei presence in the BMG. The scale bare in all maps is 100 nm.

References:

- [1] Xiaoke Mu, Andrey Mazilkin, Christian Sprau, Alexander Colsmann, Christian Kübel, (2019). *Microscopy*. 3554, 301
- [2] Sina Shahrezaei, Douglas C. Hofmann, Suveen N. Mathaudhu (2019). *JOM*. 71, 2
- [3] Yevgeny Rakita et. al. (2023), *Acta Materialia* 242, 118426



P-67

## **FRET-SENSITIZED ACCEPTOR EMISSION LOCALIZATION (FRETsael) – NANOMETER ACCURACY LOCALIZATION OF BIOMOLECULAR INTERACTIONS USING FLIM-FRET LASER SCANNING CONFOCAL MICROSCOPY**

**Yair Razvag<sup>1</sup>, Paz Drori<sup>1</sup>, Eitan Lerner<sup>1</sup>**

*Chemical Biology, The Hebrew University, Jerusalem, Israel*

Super-resolution light microscopy techniques shifted the diffraction-limited microscopy into nanoscopy, in which it is finally possible to observe the nanometer-scale biomolecules in the cell. Attaining the super-resolved information requires either using fluorescent dyes flickering between bright and dark states, immediate depletion of a well-defined region of dye excited states or using the knowledge of the illumination profile to track single biomolecules. We developed a technique dubbed FRET-sensitized acceptor emission localization (FRETsael), in which we gain nanometer localization accuracy of biomolecular interactions in FRET-FLIM. This is achieved by few nanometer laser scanning steps remembering the confocal illumination profile is spatially non-uniform illumination, and by finding the local extrema of parameters that report on the contribution of excitation to FRET. Using simulations, we show that the localization accuracy is 20-30 nm for all true-positive detections no matter what are the underlying experimental conditions. We also report the dynamic range in which the false discovery rate is minimal, and the true positive rate is maximal. Furthermore, we show the performance of the algorithm on a more realistic simulations of Actin-Vinculin and ER-Ribosomes pairs of interactions. Finally, we explore the performance of the FRETsael approach on cells with the nuclear pore protein Nup96 tagged with a donor GFP and with Alexa Fluor 647-labeled antibodies against GFP, as acceptors. The FRETsael imaging approach paves the way towards studying biomolecular interactions with improved spatial resolution from alternating laser excitation scanned frames in confocal microscopy without the use of blinking dyes or special optics.



P-68

## SHAPING OF ELECTRON BEAMS USING SCULPTED THIN FILMS

Dolev Roitman<sup>1</sup>, Ady Arie<sup>1</sup>

*Electrical Engineering, Tel Aviv University, Tel Aviv, Israel*

Electron-matter interactions and the wave nature of electrons allow for electron beam shaping by sculpted thin films. It can be used to develop technological applications in transmission electron microscopy (TEM) that offer increased resolution in different imaging modes and thus to improve measurement techniques. In this poster, we present preliminary results of two such applications. First, we show spherical aberration correction of field-free STEM mode in FEI Titan G2 Holo microscope by eliminating the spherical wavefront of the electron beam focused by the C3 lens. Such an application may lead to spherical aberration corrected Lorentz STEM, used for measurements of magnetic materials, which, nowadays, is impossible in many systems because even if a multipole aberration corrector is installed in them, their condenser lenses aren't strong enough to focus the beam onto it. Second, and towards the correction of chromatic aberration of STEM, we use thin film diffractive electron lenses to chromatically manipulate a focusing electron beam wavefront. Practically, we fabricated diffractive lenses which their focal lengths are dependent on the electron beam energy, changing the total focus of a TEM beam at Low Angle Diffraction (LAD) mode when they are placed at the sample holder. Due to fabrication limitations chromatic aberration correction may be impractical in the present, but this work may be a proof of concept and pave the way towards such achievements in the future.

**P-69**

## **THE LABORATORY FOR SENSING NANOMATERIALS & CONTROLLED RELEASE TECHNOLOGIES**

**Gracia Safdie<sup>1</sup>**

*Pharmacy, The Hebrew University of Jerusalem, Jerusalem, Israel*

Real-time sensing of biological processes in diseases is critical for many fields. Optical sensors enable fast, reliable, and highly sensitive detection of various states. Among many materials, the physical and optical properties of single-walled carbon nanotubes (SWCNTs) set them apart as indispensable sensors and offer unique applications in biology and medicine. Our lab is interested in engineering nanosensors for detecting diseases and monitoring biological processes. Specifically, we synthesized, characterized, and implemented the nanosensors composed of SWCNTs for in vitro and in vivo purposes. Among the various sensors, we engineered a novel sensor that tracks a specific enzymatic suicide inactivation pathway that leads to irreversible enzyme inactivation and can be further used to screen novel molecules to identify enzyme inhibitors (Yaari et al. Nano Letters, 2020). Additionally, we developed a novel platform based on an array of DNA-wrapped SWCNTs nanosensors and machine learning technology to detect multiple ovarian cancer biomarkers without using a specific binding moiety (Yaari et al., Science Advances, 2021). We are fabricating a clinical nanosensor comprising a particular antibody of biomarker conjugated to DNA-wrapped SWCNTs (Ab-SWCNTs) for early ovarian cancer detection. The nanosensors detect the three ovarian cancer biomarkers and will be tested in patients shortly. These nanosensors strengthen the utility and diversity of nanomaterial formulations in medicine.



P-70

## DEEP THREE-PHOTON IMAGING OF AN ADULT ZEBRAFISH BRAIN

David Sinefeld<sup>1,2</sup>, Dawnis M. Chow<sup>3</sup>, Kristine E. Kolkman<sup>3</sup>, Dimitre G. Ouzounov<sup>2</sup>,  
Najva Akbari<sup>2</sup>, Rose Tatarsky<sup>3</sup>, Andrew Bass<sup>3</sup>, Chris Xu<sup>2</sup>, Joseph R. Fetcho<sup>3</sup>

<sup>1</sup>*Electro-Optical Engineering and Applied Physics Dept., Jerusalem College of  
Technology, Jerusalem, Israel*

<sup>2</sup>*Department of Applied and Engineering Physics, Cornell University, Ithaca, New York,  
USA*

<sup>3</sup>*Department of Neurobiology and Behavior, Cornell University, Ithaca, New York, USA*

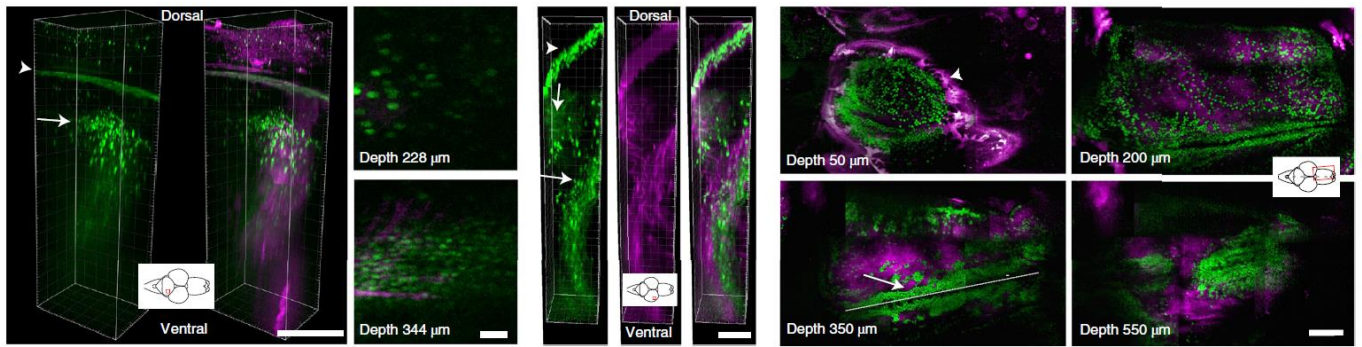
Multiphoton fluorescence microscopy (MPM) is a well-established technique for deep-tissue imaging with subcellular resolution. In fact, 2-photon laser scanning microscopy (2PM) is currently one of the main optical tools in *in vivo* animal brain imaging, which allows the visualization of a single neuron and neuronal processes in a living brain. In the last couple of years it was shown that higher order nonlinear microscopy, e.g. 3-photon fluorescence microscopy (3PM), when combined with long wavelength excitation, allows to achieve deeper imaging than 2PM [1]. This method was found to be particularly useful for volumetric animal brain imaging, because out-of-focus background generation can be further reduced due to the higher order nonlinear excitation.

The zebrafish model allowed for the first non-invasive calcium imaging in a vertebrate with both synthetic and genetically encoded calcium indicator lines, setting the stage for the burgeoning use of transparent larval fish for imaging of neurons throughout the brain of a behaving vertebrate. In contrast, opaque adult zebrafish, like other vertebrates, have proven less tractable for deep noninvasive approaches.

Here we demonstrate non-invasive long wavelength 3P imaging in adult zebrafish and reveal its power to image structure and function through the entire telencephalon, as well as deep into the optic tectum and cerebellum of intact adult fish. Large portions of the brain of an established vertebrate model are thus visible for non-invasive structural and functional studies from embryo to adult.

All zebrafish experiments were performed on adult fish, 3 to 7 months old. We used a custom made three photon (3P) imaging system that combines a femto-second pulsed laser with a repetition rate of 500K Hz at 1300 and 1700 nm, together with dispersion compensation, and scanning system and a high NA objective for imaging and collection. The collected fluorescence signal was divided to two spectral regions for fluorescence and third harmonic generation (THG). Most of the imaging was performed at 1300 nm with GCaMP6s indicators to assess both structural resolution as well as perform functional imaging. In addition, we imaged structural features at 1700 nm with glutamatergic neurons labeled with DSRed to image red light emitting fluorophores as well.

We imaged genetically labeled neurons through the zebrafish head in the cerebellum, optic tectum, and telencephalon. Our results show deep 3P non-invasive imaging of structure and/or function in major brain regions of mature adult zebrafish. In the figure below 3P imaging of the cerebellum (left) and the optic tectum of an intact zebrafish are shown [2]. In the cross section images to the right it is possible to see the 3P fluorescence signal from the neurons (in green) and the THG from the tissue structure (in purple).



1. Ouzounov, D. G., Wang, T., Wang, M., Feng, D. D., Horton, N. G., Cruz-Hernández, J. C., Xu, C. (2017). *Nat. methods*, 14(4), 388-390.
2. Chow, D. M., Sinefeld, D., Kolkman, K. E., Ouzounov, D. G., Akbari, N., Tatarsky, R., Fetcho, J. R. (2020).. *Nat. Methods*, 17(6), 605-608.



P-71

## REAL-TIME STUDY OF SURFACE-GUIDED NANOWIRE GROWTH BY IN SITU SCANNING ELECTRON MICROSCOPY

XiaoMeng Sui<sup>1</sup>, Amnon Rothman<sup>2</sup>, Kristýna Bukvišová<sup>3,4</sup>, Noya Ruth Itzhak<sup>2</sup>, Ifat Kaplan-Ashiri<sup>1</sup>, Anna Eden Kossoy<sup>1</sup>, Libor Novák<sup>5</sup>, Tomáš Šíkola<sup>3,4</sup>, Miroslav Kolíbal<sup>3,4</sup>, Ernesto Joselevich<sup>2</sup>

<sup>1</sup>*Department of Chemical Research Support, Weizmann Institute of Science, Rehovot, Israel*

<sup>2</sup>*Department of Molecular Chemistry and Materials Science, Weizmann Institute of Science, Rehovot, Israel*

<sup>3</sup>*Institute of Physical Engineering, Brno University of Technology, Brno, Czech Republic*

<sup>4</sup>*CEITEC BUT, Brno University of Technology, Brno, Czech Republic*

<sup>5</sup>*Thermo Fisher Scientific, Brno, Czech Republic*

Surface-guided growth has proven to be an efficient approach for the production of nanowire arrays with controlled orientations and their large-scale integration into electronic and optoelectronic devices. There are intensive studies on different mechanisms of guided nanowire growth. Yet, many aspects of the surface-guided growth process remain unclear due to a lack of observation in real-time. In this work, we adopt two heating systems under different environmental scanning electron microscopes (ESEMs, Quattro S and Quattro, Thermo Fisher Scientific) to observe and record the *in situ* growth of ZnSe surface-guided nanowires grow. Parameters were carefully tuned to avoid nonselective growth on the exposed substrate surfaces and other artifacts.

ZnSe surface-guided nanowires growing on periodically faceted substrates of annealed M-plane sapphire clearly show how the nanowires elongate along the substrate nano-grooves while pushing the catalytic Au nanodroplet forward at the tip of the nanowire. The *in situ* experiments allow us to study the growth mechanism in great detail, for example, to compare competing processes, and to reveal the effect of topographic discontinuities of the substrate on the growth direction. A decrease in precursor concentration as it is consumed after a long reaction time causes the nanowires to shrink back instead of grow, thus indicating that the process is reversible and takes place near equilibrium. This real-time study of surface-guided growth, enabled by *in situ* ESEM, enables a better understanding of the formation of nanostructures on surfaces.

### Reference:

1. Real-Time Study of Surface-Guided Nanowire Growth by *In Situ* Scanning Electron Microscopy A. Rothman, K. Bukvišová, N. R. Itzhak, I. Kaplan-Ashiri, A. E. Kossoy, X.M. Sui, L. Novák, T. Šíkola, M. Kolíbal, E. Joselevich, *ACS Nano* 2022, 16, 11, 18757–18766